DISSERTATION

INVESTIGATING RESISTANCE AND THE RAPID RESPONSE TO GLYPHOSATE IN GIANT RAGWEED (AMBROSIA TRIFIDA L.)

Submitted by

Christopher R. Van Horn

Graduate Degree Program in Cell and Molecular Biology

In partial fulfillment of the requirements

for the Degree of Doctor of Philosophy

Colorado State University

Fort Collins, Colorado

Fall 2016

Doctoral Committee:

Advisor: Phil Westra
Co-advisor: Anireddy Reddy

Cris Argueso
Todd Gaines
Jan Leach

ABSTRACT

INVESTIGATING RESISTANCE AND THE RAPID RESPONSE TO GLYPHOSATE IN GIANT RAGWEED (*AMBROSIA TRIFIDA* L.)

The introduction of glyphosate-resistant crops along with widespread multiple in-season applications of glyphosate as part of weed management strategies that fail to address long-term weed control have provided the perfect scenario to foster the recent boom in glyphosate-resistant weeds. In order to implement best strategies to manage glyphosate-resistant weeds, it is important to understand the mechanism of resistance. Glyphosate targets and inhibits the enzyme 5-enolpyruvylshikimate-3-phosphate synthase (EPSPS), which prevents the synthesis of aromatic amino acids. We have investigated the mechanism of glyphosate resistance using several geographically diverse giant ragweed populations. From these populations we have characterized three phenotypic responses to glyphosate treatment: susceptible (GS), resistant slow response (GR slow), and resistant rapid response (GR rapid). Glyphosate resistance in giant ragweed (*Ambrosia trifida* L.) was first discovered in 2004 and the rapid response biotype was first identified in 2008. The molecular basis for resistance and the rapid response remains unknown. Our objective is to analyze glyphosate resistance and the rapid response in giant ragweed using physiological and molecular techniques. In whole-plant dose-response experiments conducted under greenhouse conditions, the glyphosate ED_{50} values (the effective dose that reduced shoot mass 50% relative to non-treated plants) of GR rapid biotypes were 4.2- and 2.3-fold greater than the ED_{50} values of GS biotypes and GR slow biotypes were 3.3- and 3.6-fold greater than the ED_{50} values of GS biotypes. The effective concentration that increased

shikimate accumulation 50% relative to non-treated leaf tissue (EC_{50}) was 4.1- and 3.9-fold higher ($P < 0.05$) for GR rapid and GR slow biotypes, respectively, than GS biotypes based on values averaged across accessions of the same biotype. However, at high glyphosate concentrations (1,000 to 2,000 μM), shikimate accumulation in the GR biotypes was similar to or greater than the GS biotypes. *EPSPS* sequence analysis showed no nucleotide mutation at a position where mutations are known to confer resistance in multiple species. Genomic copy number analysis found no evidence of target gene amplification. Whole plant physiology experiments suggest the rapid response is carbon dependent and both Phenylalanine and Tyrosine play a role in the stimulation of the rapid response. Excised leaf discs show H_2O_2 accumulation in mature leaf tissue of the GR rapid response biotype within 30 minutes after glyphosate application. Transcriptomic analysis of GR rapid and GS giant ragweed has identified significant differentially expressed genes that may be linked to glyphosate resistance and/or the rapid response. RNA-seq data was validated through qRT-PCR analysis. Six candidate genes were analyzed using qRT-PCR, two of which were selected for further expression analysis in an F_2 population segregating for resistance. The final two candidate genes, osmotin 34 and S-adenosylmethionine synthetase 3, did not show a similar segregation pattern as seen in the F_2 individuals. The large amount of RNA-seq data collected will continue to be used to determine key marker genes that could provide further insight into the glyphosate resistance mechanism present in this species. These initial results provide a framework for the future of giant ragweed glyphosate resistance research, which becomes increasingly important as the use of glyphosate-resistant crops develops world-wide. With this research, we can continue to work toward sustainable forms of herbicide weed management.

ACKNOWLEDGEMENTS

I would like to thank all those people who have supported me and contributed to my research and my experience at Colorado State University. I would like to express my deepest gratitude to my major advisor, Phil Westra, for providing me with the opportunity to work in weed science and the guidance to excel as a scientist and grow as a person. His unbridled enthusiasm for weed science sparked my learning and creativity throughout my graduate career.

I would like to thank all members of my graduate committee for preparing me for this degree. Thank you to Anireddy Reddy and Jan Leach for providing valuable perspectives and expertise that enriched my learning and understanding. I would like to extend a special thanks to Cris Argueso and Todd Gaines for their mentorship and availability for advice at a moment's notice. The Weed Research Laboratory staff and students also deserve many thanks for always being willing to help out and offer good advice and ideas.

Thank you to Bayer CropScience for providing financial support to the project. I would like to thank Roland Beffa, Sascha Gille and the staff at Bayer CropScience, in Frankfurt, Germany for a wonderful collaboration. I am grateful to have had the experience to visit Germany and work in the welcoming and productive environment at Bayer CropScience.

Thank you to my parents and brother, mother- and father-in-law and the rest of my extended family for all the love and support you have given me. Finally, thank you to my wife (Tori) for her endless support, encouragement and unconditional love. She is the source of my strength and helps me in more ways than I can count every day of my life.

DEDICATION

I dedicate this work to my daughter, Avery.

May you always value the power and wisdom gained through continual learning.

TABLE OF CONTENTS

CHAPTER 1. INTRODUCTION

1.1 BACKGROUND

Giant Ragweed

Giant ragweed (*Ambrosia trifida* L.) is a broadleaf summer annual C_3 weed that is native to North America (Abul-Fatih *et al*., 1979; Bassett and Crompton, 1982). Though prevalent in North America, giant ragweed has been introduced into Europe, South America and Asia and is now becoming a global invasive species (Bassett and Crompton, 1982; Hansen, 1976; Washitani and Nishiyama, 1992). Giant ragweed grows in disturbed soils of riparian areas, roadside ditches, field margins, and over the last 30 years it has successfully adapted to thrive in both conventionally tilled and no-till crop production systems throughout the Midwestern United States and some areas in Canada (Abul-Fatih *et al*., 1979; Barnett *et al*., 2013; Bassett and Crompton, 1982; Baysinger and Sims, 1991; Bryson and DeFelice, 2009; Hartnett *et al*., 1987; Johnson *et al*., 2007; Norsworthy *et al*., 2011). The prolificacy of giant ragweed in agricultural systems throughout the eastern United States corn belt is partially due to its seed dormancy characteristics, allowing seedlings to emerge in early spring with germination highest between March and May, but germination can occur through July, making giant ragweed one of the most competitive and troublesome weeds in this agricultural region (Abul-Faith and Bazzaz, 1979; Ballard *et al*., 1996b; Gibson *et al*., 2005; Harrison *et al*., 2001; Loux and Berry, 1991; Schutte *et al*., 2008; Webster *et al*., 1994). This prolonged seedling emergence enables late seedlings to evade early season control efforts, making giant ragweed very difficult to manage in crop fields (Harrison *et al*., 2001; Schutte *et al*., 2008).

Giant ragweed also exhibits a high level of genetic and phenotypic diversity, with much of its success attributed to aspects of this diversity (Johnson *et al*., 2007). The effect of different selection pressures was observed on two ecotypes (distinct geographic populations) of giant ragweed, the ecotype from an agricultural field left fallow for 15 years was found to produce more dry biomass, a higher number of seeds and seed mass plant^{-1}, and have a higher reproductive allocation than the ecotype from an annually disturbed agricultural field (Hartnett *et al*., 1987). Both ecotypes were originally from the same population in a cultivated agricultural field (Hartnett *et al*., 1987). The differences observed between the two ecotypes were attributed to different selection pressures found in the two environments (Hartnett *et al*., 1987). Though annual species rarely persist in non-disturbed or fallow fields, the ability of giant ragweed to adapt and compete with perennial successional species was hypothesized to be a result of high genetic polymorphism (Hartnett *et al*., 1987).

Seeds and Germination

Seeds vary in size and morphology ranging from 20 to 80 mg in weight and 6 to 8 mm long (Bassett and Crompton, 1982). The outer involucral hull consists of one central spike surrounded by a circle of 3 to 6 marginal points (Bassett and Crompton, 1982). Within the involucre the embryo is further encased by the clear seed coat and smooth black pericarp, which further protect the embryo and regulate dormancy (Schutte *et al*., 2008). Upon dispersal from the parent plant, seeds must undergo a period of cold stratification before germination can occur. It has been reported that seeds require cold and moist soil conditions to weaken the hard involucres and reduce the levels of germination inhibiting chemicals in order to break dormancy (Ballard *et al*., 1996a). In nature this is achieved by overwintering in the soil seed bank. During this period,

there is an increase in gibberellic acid biosynthesis and abscisic acid degradation, which function to release the seed from dormancy and promote germination (Ali-Rachedi *et al*., 2004; Finch-Savage and Leubner-Metzger, 2006; Schutte *et al*., 2012).

Seeds have a high energy reserve and exhibit high dormancy, ≤ 4 years seed longevity in soil, which is beneficial in allowing seedlings to emerge and grow quickly throughout the entire growing season (Harrison *et al*., 2003). Optimal seed germination conditions were found to be between 10 to 24 °C with soil moisture content ranging between 26 and 33% and a sowing depth of 2 cm, however, seeds can germinate from depths of 16 cm (Abul-Faith and Bazzaz, 1979). A different study observed a maximum rate of emergence at 5 cm soil depth (Harrison *et al*., 2007). Different populations exhibit varying germination patterns. The germination period for an Ohio population of giant ragweed seeds was found to begin between March 25 and April 5, and end between July 24 and July 30, with a general pattern of an early flush followed by more intermittent germination over the course of the summer (Schutte *et al*., 2008). A similar pattern of germination was observed in an Illinois population of giant ragweed seed, but germination did not continue after June 1 (Stoller and Wax, 1974). This temporal pattern of emergence occurring in arable fields may be an adaptation for success selected by agricultural soil disturbance and early season weed management operations (Davis *et al*., 2013; Hartnett *et al*., 1987).

Growth and Competitive Ability

Giant ragweed is a dicot species with cotyledons appearing spatulate to oblong, which can be 1 to 1.5 cm wide by 2 to 4 cm long (Bassett and Crompton, 1982). True leaves are oppositely arranged on the stem having a rough and hairy texture (Bassett and Crompton, 1982; Frankton, 1970). The first true leaves are typically unlobed while successive leaves display a

characteristically palmately lobed phenotype, having three to five deep lobes with serrated margins (Bassett and Crompton, 1982). The early emergence and rapid growth of seedlings allows giant ragweed to suppress or eliminate surrounding plants from the community by shading and by excessive consumption of water, soil nutrients and other habitat resources (Abul-Fatih *et al*., 1979; Bassett and Crompton, 1982). The roots of giant ragweed are fibrous with a relatively short taproot (Bassett and Crompton, 1982). The large photosynthetic cotyledons and successive true leaves allow giant ragweed to grow rapidly, reaching heights of 5 m or taller, with height and biomass production dependent on the plant density of neighboring species and competition for sunlight (Abul-Fatih *et al*., 1979; Johnson *et al*., 2007). In agricultural fields giant ragweed typically grows between 0.3 to 1.5 m taller than the competing crop (Johnson *et al*., 2007). Inadequate control of giant ragweed can result in large yield losses in agronomic crops. Season long interference from giant ragweed at one plant m^{-2} in corn (*Zea mays* L.) resulted in a yield loss of 55% (Harrison *et al*., 2001). In soybean (*Glycine max* L.), one giant ragweed plant m^{-2} resulted in a yield loss of 77% (Vink *et al*., 2012a; Webster *et al*., 1994). In 2015, corn and soybean production in the United States were valued at 50 and 35 billion dollars, respectively (USDA, 2016).

Grown in monoculture at 500 plants m^{-2}, giant ragweed produced 3,058 g m^{-2} of above ground biomass (Abul-Fatih *et al*., 1979). Plants grown in higher densities produced much more above ground biomass and had a higher leaf area index compared to plants grown in lower densities (Abul-Fatih *et al*., 1979). Giant ragweed in Illinois were found to have a leaf area index of 5, reducing light reaching the ground below the plant canopy by 95%, and its radiation-use efficiency when grown in mixed communities with corn was 50% greater than when grown in monoculture (Bassett and Crompton, 1982; Gramig and Stoltenberg, 2007). Giant ragweed

responds to and utilizes resources in response to varying environmental factors, such as light, nutrients and competition. When provided with fertilizer, giant ragweed produced leaf tissue at twice the rate of non-fertilized plants, which dedicated more energy to root production during early growth stages (Abul-Fatih *et al*., 1979). Giant ragweed has also been shown to synthesize allelopathic phytochemicals that act to inhibit the growth of surrounding plants (Kong *et al*., 2007; Kong, 2010; Wang *et al*., 2005).

Reproduction

Giant ragweed is a facultative outcrossing plant that is consecutively monoecious (Bassett and Crompton, 1982). A single plant produces multiple male flowers occurring on long terminal racemes with clusters of female flowers occurring at the leaf axils of upper leaves and base of racemes (Abul-Fatih *et al*., 1979; Bassett and Crompton, 1982; Johnson *et al*., 2007). Expression of reproductive structures is dependent on phenotype and environmental factors, with plants higher in the canopy distributing resources more evenly compared to plants lower in the canopy, which may invest more resources in female structures (Abul-Fatih *et al*., 1979). A study in Illinois found shorter plants to be more likely to produce only female flowers, allocating energy for seed production opposed to both pollen and seed (Abul-Fatih *et al*., 1979). Giant ragweed is photoperiod sensitive, resulting in flowering dates occurring between July and October (Bassett and Crompton, 1982). Due to the timing difference between the production of male and female flowers, giant ragweed is reported to be self-incompatible (Johnson *et al*., 2007). It is possible to generate in-bred lines through self-pollination by isolating a single plant in a controlled environment. However, the seed production and viability dramatically decrease under these conditions and the progeny are reported to have less vigor (Bassett and Crompton,

1982). Giant ragweed relies on the wind to transfer pollen grains between plants, which promotes outcrossing leading to a high degree of genetic diversity within a population (Johnson *et al*., 2007). Another factor leading to genetic diversity is the exceptionally large amount of pollen produced by giant ragweed (Abul-Fatih *et al*., 1979). A single plant can produce over one billion pollen grains during its life span and about one to ten million pollen grains per day and can be dispersed up to a kilometer in distance (Bassett *et al*., 1978; Johnson *et al*., 2007; Raynor *et al*., 1970). It was reported that viable giant ragweed pollen was found to travel 60 m from its source (Vollenberg *et al*., 2005). This excessive pollen production contributes to seasonal allergies and it is reported that pollen from plants in the genus *Ambrosia* are responsible for more cases of hay fever than all other plant species combined (Ziska *et al*., 2011). In fact, 15 to 20% of populations in developed countries suffer from IgE-mediated atopic diseases, and the AmbV allergen from giant ragweed has been cloned and sequenced to be used as a model for studying the basic structural requirements for immune recognition of foreign protein allergens (Ghosh *et al*., 1991).

After pollination occurs, the characteristically large seeds mature on the parent plant where they are susceptible to high degrees of damage from pre-dispersal predation by birds, insects and bacteria (Harrison *et al*., 2003). With no obvious method of dispersal, mature seeds begin to drop in late summer through early fall, leaving them susceptible to further predation by earthworms, rodents, insects, bacteria and fungi (Abul-Faith and Bazzaz, 1979; Harrison *et al*., 2003; Harrison *et al*., 2001; Regnier *et al*., 2008). Due to this high rate of predation, less than one-half of all seeds produced contribute to the seed bank (Harrison *et al*., 2001; Schutte *et al*., 2008; Stoller and Wax, 1974). Without yearly addition of fresh seeds to the soil seed bank, the seed bank will be depleted by ≥ 90% after four growing seasons (Harrison *et al*., 2007). In addition to predation, approximately 10 to 20% of the total seed production is made up of

seedless fruits (Schutte *et al*., 2012). Perhaps deep germination with no emergence, high predation rates, and lack of seed viability are all adaptive factors owing to the very high number of seed production per plant (Abul-Faith and Bazzaz, 1979; Amatangelo, 1974; Harrison *et al*., 2001; Schutte *et al*., 2008; Stoller and Wax, 1974). At low densities, giant ragweed is estimated to produce approximately 4,200 to 5,100 seeds plant^{-1}, and approximately 775 to 1,465 seeds plant^{-1} at high densities (Baysinger and Sims, 1991). Grown in soybeans, a single giant ragweed plant can produce 5,100 seeds (Abul-Faith and Bazzaz, 1979; Baysinger and Sims, 1991; Harrison *et al*., 2001; Johnson *et al*., 2007).

Economic Importance

Giant ragweed has effectively adapted to thrive in agro-ecosystems and has become one of the most competitive weeds relative to other common weeds in corn and soybean cropping systems (Harrison *et al*., 2001; Johnson *et al*., 2007). Control and management of giant ragweed is challenging and poses a serious threat to crop yield potential. Crop yield loss can be estimated based on the factors of crop growth stage and row spacing, as well as weed density and height (Fickett *et al*., 2013a). A competitive index (CI) is assigned to a weed species based on the above factors and has a scale from 0 to 10, with 10 being the most competitive. A study in Wisconsin, using WeedSOFT® to calculate CI, found the CI of giant ragweed in corn and soybeans to be 8.0, the highest of any weed (Fickett *et al*., 2013a; Fickett *et al*., 2013b). In corn, season long interference of one giant ragweed plant 10 m^{-2} that emerged at the same time as the crop, reduced crop yield by 13.6% (Harrison *et al*., 2001). Corn yield loss due to giant ragweed competition was greater than that from barnyardgrass (*Echinochloa crus-galli* L.), giant foxtail (*Setaria faberi* L.), wild-proso millet (*Panicum miliaceum* L.), common lambsquarters (*Chenopodium*

album L.), redroot pigweed (*Amaranthus retroflexus* L.), and velvetleaf (*Abutilon theophrasti* Medicus), making it the most competitive weed in corn reported thus far (Harrison *et al*., 2001). It was also reported that when giant ragweed emergence was delayed by four weeks from crop emergence, its competitive ability was reduced by 4 to 8 fold (Harrison *et al*., 2001). The economic threshold for giant ragweed in corn was reported to be 0.4 plants 10 m^{-2} when weed and crop emerge together and 4.2 plants 10 m^{-2} when weeds emerge four weeks after crop emergence (Harrison *et al*., 2001). These results stress the economic importance of controlling giant ragweed for a minimum of four weeks after corn emergence in order to minimize crop yield losses.

Giant ragweed has been reported to be more competitive in soybeans than in corn. In soybeans, season long interference of one giant ragweed plant 10 m^{-2} can reduce crop yield by 50% (Johnson *et al*., 2006). The duration of this weed to crop interference is highly important in determining the extent of crop yield loss. With regard to most weeds, soybeans require a four to six week weed-free period after planting in order to protect crop yields (Johnson *et al*., 2006). However, with giant ragweed, it is necessary to have at least a ten week weed-free period to prevent significant crop yield loss (Baysinger and Sims, 1991; Johnson *et al*., 2006).

The abundance and competitive ability of giant ragweed are also dependent on nutrient management, crop rotation, and tillage system. Nitrogen (N) fertilizer is an important and expensive input in corn production, thus stressing the need for early weed control to prevent significant crop yield losses due to nitrogen accumulation by weeds. Giant ragweed at 0.5 plants m^{-2} in corn accumulated 104 kg nitrogen (N) ha^{-1} over the season (Johnson *et al*., 2007). In the same study, this season long interference resulted in corn yield loss of 19% (Johnson *et al*., 2007). A 12 year study in Wisconsin found the highest crop-weed competition between corn and

giant ragweed to be in chisel plow systems, such as moldboard plowing (Stoltenberg *et al*., 2011). This particular type of plow system distributes giant ragweed seed below the soil surface, preventing most types of predation, but does not distribute the seed deep enough to hinder germination and emergence, thus placing the seed in an ideal location for preservation in the weed seedbank (Stoltenberg *et al*., 2011). These studies show that giant ragweed is of economic importance and its control and proper management must occur for crop yields to be maintained at acceptable levels.

Weed Management

Weed management is an essential part of all cropping systems and left uncontrolled, weeds compete with crops for sunlight, water, and nutrients. Growers must effectively manage weeds in agro-ecosystems to minimize crop yield losses that occur as a result of competition with weeds. For a farmer, reduced crop yield means less profit. Weed populations in a field are relatively constant from year to year, giving growers a knowledge of the weeds expected and allowing them to develop a targeted management plan based on the type of crop and past weed communities (LeBaron, 1991). In general, crops are most vulnerable during the early growth stages and will often be outcompeted by early germinating weeds present at or around the time of crop emergence (Hall *et al*., 1992). Harvesting operations may be affected by weeds, such that they hinder machinery and block the ability to adequately harvest the crop (Webster and Sosnoskie, 2010). Weeds also serve as harbors for insects and diseases, which may infest future crops (Johnson *et al*., 2006).

An effective and economical weed management approach is imperative in order to achieve adequate levels of weed suppression. Successful weed management tactics include an

integrative approach using a number of available tools and techniques including cultural, mechanical, biological and chemical control methods as well as a knowledge of the weed communities and crop production system (Swanton and Weise, 1991). It is important to avoid the use of a single weed control tactic, especially with regard to herbicides. Weed exclusion strategies such as hand removal, animal control, tilling and mowing, burning and biological control methods were developed long before herbicides and currently serve as effective means of weed management (Hay, 1974; Peterson, 1967). However, these methods of weed management are more costly to the grower than herbicides and are often labor intensive or detrimental to the soil, resulting in soil erosion, reduced soil organic matter, and less productive croplands (Hay, 1974). The introduction of herbicides allowed farmers to move away from previous weed exclusion tactics and incorporate chemicals as the sole means of weed management (Segobye, 2013). Chemical weed control has proven to be highly effective by selectively killing weeds in crops and is much cheaper than mechanical methods of weed management, thus maximizing grower profits (Caseley *et al*., 2013; Shaner *et al*., 2013).

Herbicide Development and Use

In the early twentieth century, non-selective chemical control of weeds consisted of inorganic salts, such as iron sulfate, sulfuric acid and copper salts (Monaco *et al*., 2002; Robins *et al*., 1952). The modern era of selective herbicides began in 1947 with the discovery of two synthetic auxins, 2,4-dichlorophenoxyacetic acid (2,4-D) and 2-methyl-4-chlorophenoxyacetic acid (MCPA), which were registered and released onto the market to control dicot plants (Peterson, 1967; Rao, 2000; Troyer, 2001). These synthetic plant growth regulators provided growers with a highly efficient means of weed control and thus represented a significant

breakthrough in the arena of chemical weed management. The success of 2,4-D and MCPA led to future research and development of herbicides with different modes of action (Segobye, 2013). By 1962, growers had access to approximately 6000 formulations of 100 different selective and broad spectrum herbicides (Peterson, 1967). The use of herbicides became an integral part of weed management in modern high-input cropping systems, especially with increased cultivated land and the adoption of no-till cropping systems (Holt and Lebaron, 1990; Segobye, 2013). Reduced tillage promotes soil conservation and is beneficial to cropping systems because of increased water infiltration, improved soil moisture, reduced soil erosion and herbicide loss, and reduced sandblasting of young seedlings due to wind erosion (Potter *et al*., 2004; Webster and Sosnoskie, 2010; Wilcut *et al*., 1993). Herbicides also led to a reduction in labor and time needed for effective weed control, allowing growers to farm more acreage and adopt more advanced agronomic practices, resulting in higher yields and profits (Holt and Lebaron, 1990).

In 1974, the compound glyphosate [N-(phosphonomethyl) glycine] was combined with an isopropylamine salt and released as a post-emergence herbicide, having broad spectrum control over both C_3 and C_4 monocot and dicot annual and perennial plants (Thompson, 2012). Glyphosate quickly became a desirable herbicide not only for its efficacy in weed control, but because of its low toxicological effects on the environment; it targets a pathway only found in plants and microbes, binds tightly to the soil and is unlikely to run off into ground water (Dill, 2005; Duke and Powles, 2008; Giesy *et al*., 2000; Kovach *et al*., 1992; Thompson, 2012; Williams *et al*., 2000). The ease and effectiveness of glyphosate, along with the development of glyphosate-resistant (GR) crops, led to the success and worldwide used of the herbicide (Baylis, 2000; Duke and Powles, 2008). The widespread use of herbicides in developed countries has

contributed to significant food security through the control of weeds that would otherwise significantly reduce crop yields (LeBaron, 1991; Segobye, 2013).

Glyphosate

Glyphosate was originally invented in 1950 at the Swiss pharmaceutical company, Cilag, by Dr. Henri Martin, but was sold to other companies because it showed no biological activity (Dill *et al*., 2010; Franz *et al*., 1997; Green, 2014). In the 1960s, Monsanto's Inorganic Division synthesized over 100 related aminomethylphosphonic acid (AMPA) analogs in an attempt to develop potential water softening agents (Dill *et al*., 2010). Dr. Phil Hamm found two of these compounds to have slight herbicidal activity on perennial weeds, but not enough to be commercially viable as an herbicide (Dill *et al*., 2010). Dr. Hamm asked Dr. John Franz, a Monsanto chemist, to improve the herbicidal efficacy of these two compounds (Dill *et al*., 2010). Dr. Franz discovered glyphosate by synthesizing metabolites of these compounds, and in May 1970, the Monsanto developed herbicide, glyphosate, was synthesized and later introduced to the market as Roundup® herbicide in 1974 (Dill *et al*., 2010; Duke and Powles, 2008; Powles and Preston, 2006). Glyphosate was extremely successful and has now become the most widely used herbicide in the world (Powles and Yu, 2010).

Glyphosate has a wide range of uses as a post-emergence, non-selective herbicide with the ability to control almost all annual, herbaceous and most woody perennial weeds in crops and non-agricultural areas (Duke and Powles, 2008). Prior to the commercialization of GR crops, glyphosate was used in agriculture for weed control in intercrop rows and around perennial trees and vines (Powles and Preston, 2006). Glyphosate will enter a plant through the aerial, typically chlorophyll-containing, parts as it does not readily penetrate mature woody stems or bark

(Segobye, 2013). The use of glyphosate has increased dramatically with the introduction of GR soybean and canola in 1996, followed by cotton in 1997 and maize in 1999 (Owen and Zelaya, 2005). These GR crops allowed for the POST in-crop application of glyphosate at high rates and at multiple times during the growing season without injuring the crop (Owen and Zelaya, 2005). Glyphosate must be foliar-applied because the herbicide has no residual soil activity (Dill *et al*., 2010). Glyphosate is very readily bound to soil particles and metabolized by soil microorganisms to produce ammonia, inorganic phosphate, and carbon dioxide, thus making the herbicide unavailable for root uptake (Dill *et al*., 2010; Monaco *et al*., 2002; Segobye, 2013). This immobility in the soil prevents glyphosate from causing unexpected damage elsewhere in the environment after application to the soil (Monaco *et al*., 2002). Additionally, glyphosate targets a key enzyme only found in plants and some microorganims such as bacteria, making it non-toxic to fish, birds, insects and humans (Shaner, 2009).

Glyphosate is a phosphonomethyl derivative of the amino acid glycine and is comprised of one basic amino function and three ionisable acidic sites (Bromilow and Chamberlain, 2000; Dill *et al*., 2010; Green, 2014). It can react both as a base or as an acid, allowing it to be dissolved in dilute aqueous bases or strong aqueous acids to produce anionic or cationic salts, respectively (Dill *et al*., 2010; Green, 2014). The most common formulation of glyphosate is in the form of a soluble monobasic salt (isopropylamine, sodium, potassium, trimethyl-sulfonium or ammonium) in concentrated water solutions (Dill *et al*., 2010; Green, 2014). The chemical properties of glyphosate allow for its rapid translocation from treated plant foliage, to roots, rhizomes and actively growing apical meristems (Grossbard and Atkinson, 1985; Segobye, 2013).

Cell Uptake and Translocation

Though not fully understood, there appear to be two mechanisms of glyphosate uptake into plant cells (Shaner, 2009). At low concentrations, glyphosate uptake occurred against a concentration gradient suggesting an active phosphate transporter, while at high concentrations it passes through the plasma membrane via passive diffusion (Denis and Delrot, 1993; Hetherington *et al*., 1998; Morin *et al*., 1997; Shaner, 2009). It is also unknown exactly how glyphosate enters the phloem (Shaner, 2009; Shaner *et al*., 2012). Glyphosate likely enters the phloem lumen through the cell symplasm either by mass diffusion into the mesophyll cells then through plasmodesmata, or it may be actively taken into the mesophyll or companion cells via a phosphate transporter described above (Shaner, 2009; Shaner *et al*., 2012). Glyphosate is mobile in both the apoplast and the symplast due to its unique zwitterionic characteristics (Bromilow and Chamberlain, 2000; Dewey and Appleby, 1983; Franz *et al*., 1997; Gottrup *et al*., 1976; Gougler and Geiger, 1981; Harvey *et al*., 1985; Jachetta *et al*., 1986; Shaner, 2009). Removal of either the basic or one of the three acidic functional groups reduces its ability to move in the plant (Bromilow and Chamberlain, 2000; Shaner, 2009). Glyphosate is translocated through the phloem following sucrose movement from source leaves to sink tissues such as roots, meristems and flowers, where its target enzyme is most highly expressed (Gougler and Geiger, 1981; McAllister and Haderlie, 1985; Shaner, 2009; Weaver and Herrmann, 1997).

Mode of Action

After contact with foliage, glyphosate is absorbed through the mesophyll cells and is moved into the phloem tissues through passive and active transport (Gougler and Geiger, 1981; Segobye, 2013; Shaner, 2009; Thompson, 2012). Once inside the phloem, glyphosate follows

sucrose movement into the metabolic sinks where it specifically targets and inhibits the enzyme 5-enolpyruvylshikimate 3-phosphate synthase (EPSPS), which catalyzes a key step in the shikimate pathway (Amrhein *et al*., 1980; Gougler and Geiger, 1981; McAllister and Haderlie, 1985; Shaner, 2009). The shikimate pathway involves seven enzymatic reactions that primarily produce chorismate, which is used to produce the aromatic amino acids Phenylalanine, Tyrosine and Tryptophan as well as quinones and indoles, which are precursors to a host of secondary metabolites (Herrmann, 1995; Jensen, 1986; Weaver and Herrmann, 1997) (Figure 1.1).

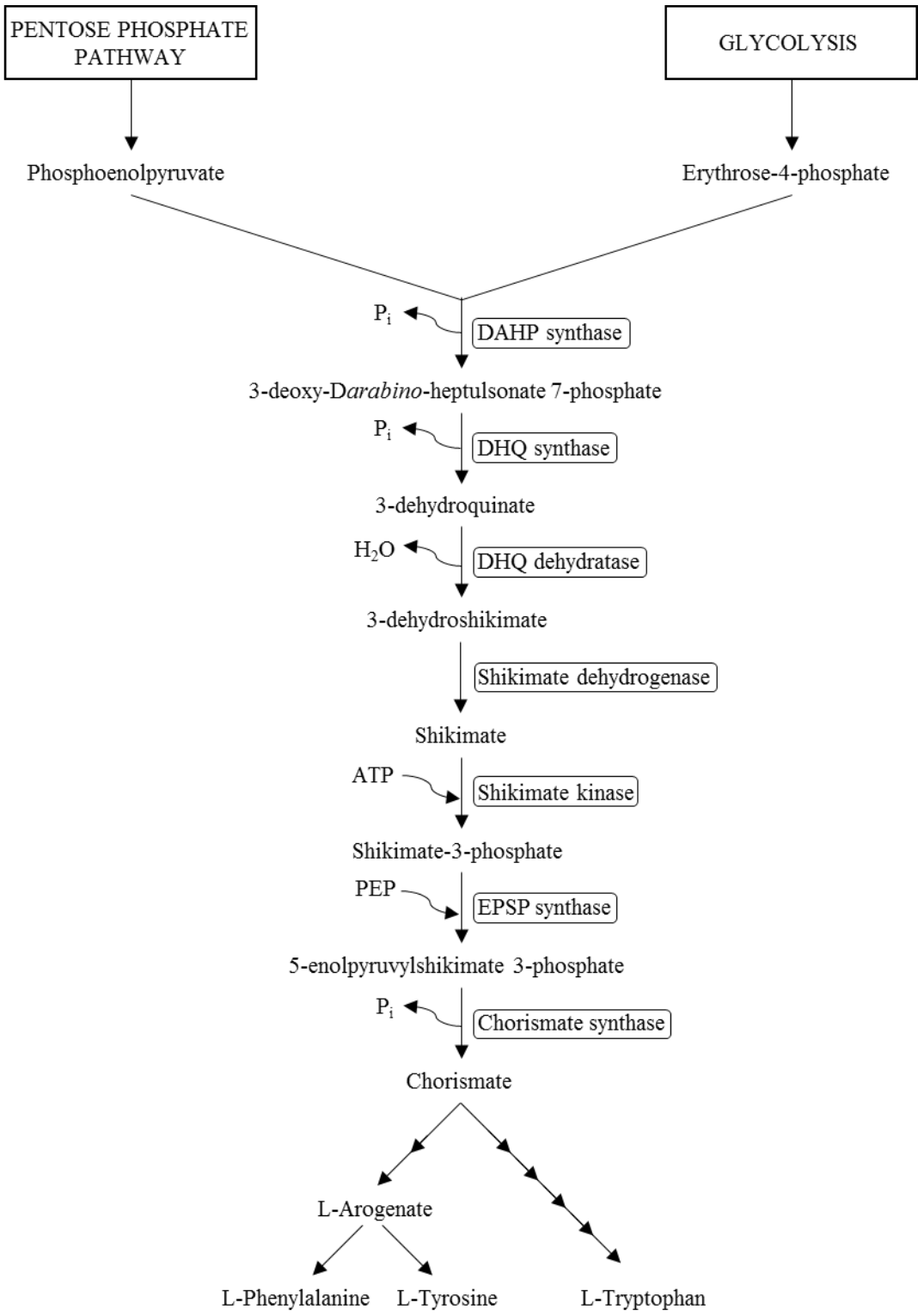

Figure 1.1. Schematic of the shikimate pathway.

The first step of the shikimate pathway involves the condensation of phosphoenolpyruvate (PEP) and erythrose-4-phosphate (E4P) from the pentose phosphate cycle to produce 3-deoxy-D*arabino*-heptulsonate 7-phosphate (DAHP) (Herrmann and Weaver, 1999). DAHP is converted to 3-dehydroquinate (DHQ) by DHQ synthase in the second step of the shikimate pathway (Herrmann and Weaver, 1999). The third step of the shikimate pathway is the dehydration of DHQ to produce dehydroshikimate (DHS), catalyzed by DHQ dehydratase (Herrmann and Weaver, 1999). The fourth step of the shikimate pathway is the reduction of DHS to shikimate, catalyzed by shikimate dehydrogenase (Herrmann and Weaver, 1999). The fifth step of the shikimate pathway is the phosphorylation of shikimate to shikimate-3-phosphate (S3P), catalyzed by shikimate kinase. Step six of the shikimate pathway produces 5-enolpyruvylshikimate 3-phosphate (EPSP) from the reversible condensation of PEP and S3P, catalyzed by EPSPS (Herrmann and Weaver, 1999; Stallings *et al*., 1991). EPSPS is an ideal herbicide target site because it plays a key role in the physiology of a plant and is only found in plants and microorganisms (Amrhein *et al*., 1980). With respect to PEP, glyphosate acts as a competitive inhibitor, while glyphosate acts as an uncompetitive inhibitor with respect to S3P (Boocock and Coggins, 1983; Stallings *et al*., 1991; Steinrücken and Amrhein, 1980). When glyphosate enters the plastids it competes with PEP for the binding site on EPSPS, halting the pathway and causing an accumulation of shikimate (Amrhein *et al*., 1980; Geiger *et al*., 1986; Jensen, 1986; Rubin *et al*., 1982; Steinrücken and Amrhein, 1980). Glyphosate does not bind efficiently to the free EPSPS enzyme, but needs the substrate S3P to first bind EPSPS, allowing glyphosate to form a ternary complex with EPSPS and S3P, thus becoming a competitive inhibitor to PEP (Boocock and Coggins, 1983; Franz *et al*., 1997; Schönbrunn *et al*., 2001). EPSPS is nuclear encoded and translocated into the plastid where the shikimic acid pathway is

located (Della-Cioppa *et al*., 1986; Green, 2014; Weaver and Herrmann, 1997). Glyphosate inhibits both the mature EPSPS in the plastid and the importation of the EPSPS precursor into the plastid (della-Cioppa and Kishore, 1988; Green, 2014).

The seventh and final step of the shikimate pathway is catalyzed by chorismate synthase, which converts EPSP to chorismate (Herrmann and Weaver, 1999). One of the post-chorismate intermediates for Phenylalanine and Tyrosine is L-arogenate, which provides negative feedback to the DAHP synthase-Mn (Gaines *et al*., 1982; Jensen, 1986). The regulation of DAHP synthase-Mn by L-arogenate is known as sequential feedback inhibition (Jensen, 1986) (Figure 1.2). This sequential feedback inhibition is regulated by a number of events that lead to elevated levels of L-arogenate, which include feedback inhibition of anthranilate synthase by L-Tryptophan, inhibition of arogenate dehydrogenase by L-Tyrosine, inhibition of arogenate dehydratase by L-Phenylalanine, and allosteric activation of chorismate mutase by L-Tryptophan (Jensen, 1986). All of these circuits of feedback control lead to an accumulation of L-arogenate, which then triggers the inhibition of DAHP synthase-Mn resulting in a shutdown of the shikimate pathway at the first step (Jensen, 1986). Therefore, when glyphosate inhibits EPSPS at the sixth step of the shikimate pathway, the formation of chorismate is inhibited, resulting in an absence of L-arogenate and a lack of negative feedback on DAHP synthase, which controls the carbon flow into the shikimate pathway (Amrhein *et al*., 1980; Holländer and Amrhein, 1980; Jensen, 1986). This inhibition by glyphosate results in the accumulation of shikimate in the tissues and a carbon shortage for other pathways (Jensen, 1986).

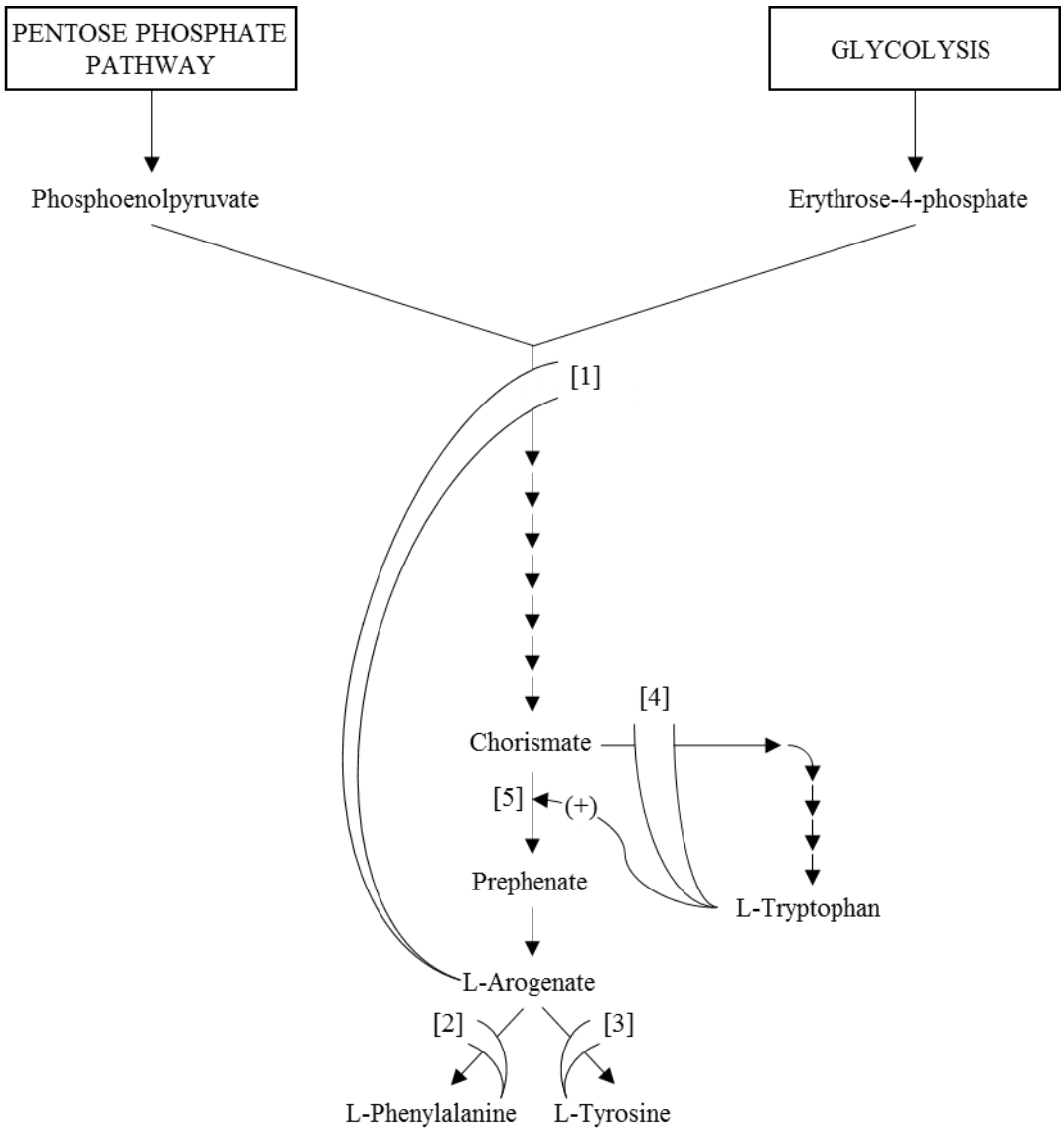

Figure 1.2. Model for sequential feedback inhibition of aromatic amino acid biosynthesis in the plastids. Individual enzymes are indicated by numbers in brackets. Under conditions of end product excess, L-arogenate accumulates owing to the combined feedback inhibitions of DAHP synthase [1], arogenate dehydratase [2], arogenate dehydrogenase [3], anthranilate synthase [4], and the allosteric activation (denoted by + symbol) of chorismate mutase [5] by Tryptophan.

There are two theories as to how the inhibition of EPSPS leads to plant death. One theory assumes death occurs through insufficient aromatic amino acid production from an inhibited shikimate pathway (Duke and Powles, 2008). Another theory suggests an increased carbon flow to the shikimate pathway when it is deregulated by the inhibition of EPSPS causing a drain on the rest of the plant (Duke and Powles, 2008; Siehl, 1997; Siehl *et al*., 2007). Of the six enzymes in the shikimate pathway, EPSPS is the only enzyme sensitive to glyphosate, allowing upstream reactions to continue to take place in the presence of glyphosate. Precursors including PEP, E4P, and ATP are continually sent into the deregulated shikimate pathway, which alters the carbon and energy balance between the chloroplast and cytosol. Therefore, glyphosate indirectly disrupts carbon metabolism (Jensen, 1986).

Erythrose-4-phosphate (E4P) is required for the generation of ribulose-1,5-bisphosphate (RuBP), which plays a key role in carbon fixation within the Calvin Cycle. Approximately eight hours after glyphosate treatment of sugar beets, RuBP levels drop to about 20% of those of the control plants, lowering the rate of carbon assimilation and starch accumulation (Geiger *et al*., 1986; Servaites *et al*., 1987). The lower levels of RuBP lead to an over-reduction of the photosynthetic electron transport chain and a decrease in photosynthetic efficiency (Crawford *et al*., 2000; Katoh *et al*., 2006). The Calvin Cycle is also indirectly disrupted by glyphosate due to the lack of ATP required for enzymatic reactions within the Calvin Cycle (Buchanan *et al*., 2000). Regardless of how plant death occurs after glyphosate treatment, the primary mode of action of glyphosate is the inhibition of EPSPS.

Herbicide Resistance

The Weed Science Society of America (WSSA) and the International Survey of Herbicide-Resistant Weeds defines herbicide-resistance as "the inherited ability of a plant to survive and reproduce following exposure to a dose of herbicide normally lethal to wild type" and "the evolved capacity of a previously herbicide-susceptible weed population to withstand a herbicide and complete its life cycle when the herbicide is used at its normal rate in an agricultural situation", respectively (Heap, 2005). In order to be classified as herbicide-resistant a weed must fulfill these definitions, as well as demonstrate a practical field impact and have unbiased data confirming the resistance to be heritable and naturally occurring, not the result of artificial or deliberate selection (Heap, 2005). As early as 1954, observations were made describing apparent reduction of sensitivity to herbicides (Abel, 1954; Appleby, 2005). The first confirmed case of high level herbicide resistance was reported in 1970 when common groundsel (*Senecio vulgaris* L.) showed resistance to simazine and atrazine after yearly application of both herbicides for ten consecutive years (Appleby, 2005; Ryan, 1970). Following the confirmation of herbicide-resistant common groundsel, many other weed species were confirmed to be resistant to the triazines (Appleby, 2005). Resistance to other herbicide chemical groups soon followed. As of 2016, there are 249 species of herbicide-resistant weeds having evolved resistance to 159 different herbicides (Heap, 2016).

Herbicide resistance alleles occur at low frequencies in natural populations without the selection pressure imposed by herbicide application, which suggests a fitness penalty associated with the resistance trait (Jasieniuk *et al*., 1996; Preston and Powles, 2002; Purrington, 2000). Fitness is the ability of a genotype to produce viable offspring relative to all other genotypes in a population and any trait impeding an individual's ability to contribute to the gene pool is known

as a fitness penalty (Preston *et al*., 2009). The occurrence, persistence, and spread of herbicide resistance alleles is impacted by the initial frequency of resistance alleles, heritability, reproduction, gene dispersal method, gene mutation rate, fitness and the environment (Jasieniuk *et al*., 1996; Roush *et al*., 1990). Another factor contributing to the evolution of herbicide resistant weeds is the intense selection pressure created by the reliance on one herbicide mode of action (Wilson *et al*., 2007). When selection pressure for herbicide resistance is no longer being imposed, it is thought that the frequency of the resistance trait in a population would decrease over time (Jasieniuk *et al*., 1996). If the herbicide resistance trait is associated with a large fitness penalty, then the frequency of resistant phenotypes will decrease in years when alternate herbicide modes of action or other resistance management tactics are used (Jasieniuk *et al*., 1996; Preston *et al*., 2009).

Evidence for a fitness penalty resulting from herbicide resistance is dependent on the weed species and the mechanism of resistance (Glettner and Stoltenberg, 2015). Mutations in herbicide target enzymes may alter the normal plant function and metabolism, while increased production of enzymes conferring herbicide resistance may require additional energy, thus reducing the amount of energy allocated to growth and reproduction in the absence of the herbicide (Vila-Aiub *et al*., 2009). It is also possible the herbicide resistance allele has pleiotropic effects such that the resistant phenotype may become less attractive to pollinators or more susceptible to diseases (Salzmann *et al*., 2008; Vila-Aiub *et al*., 2009). Rigid ryegrass (*Lolium rigidum* Gaudin) resistance to glyphosate was found to be associated with a fitness penalty, such that in the absence of glyphosate selection pressure, the proportion of resistant plants declined after three growing seasons (Preston *et al*., 2009). In another study, glyphosate-resistant (GR) and -susceptible (GS) phenotypes of rigid ryegrass from a single population in

Australia had similar biomass production but the seeds produced from resistant plants had a greater mass than from susceptible plants (Pedersen *et al*., 2007). However, the susceptible plants produced a greater number of seeds than the resistant plants at low levels of crop competition (Pedersen *et al*., 2007). GR horseweed (*Conyza canadensis* L.) individuals were shown to be more competitive than GS individuals when grown at high densities and low soil moisture (Shrestha *et al*., 2010). Giant ragweed with the GR rapid response trait from Indiana displayed early, rapid growth in the absence of glyphosate, flowered earlier, but produced 25% less seed than a GS biotype (Brabham *et al*., 2011). Other studies comparing the growth, competitive ability, and reproductive output of GR and GS biotypes of horseweed, palmer amaranth (*Amaranthus palmeri* L.) and common lambsquarter (*Chenopodium album* L.) have found minor to no fitness costs to resistance (Davis *et al*., 2009; Giacomini *et al*., 2014; Vila-Aiub *et al*., 2009; Westhoven *et al*., 2008). Fitness studies comparing weed populations can be difficult to conduct in order to draw clear conclusions due to high degrees of heterogeneity within populations. It is important to have similar genetic backgrounds or multiple biotypes with the same mechanism of resistance to reduce the likelihood that genotypic differences or additional loci are causing any observed fitness penalties (Bergelson and Purrington, 1996; Cousens *et al*., 1997; Jasieniuk *et al*., 1996).

Glyphosate-Resistant Weeds

Glyphosate has become the world's largest selling and most widely used herbicide because of its broad spectrum applications, excellent toxicological and environmental profiles, and little to no competition with similar herbicide classes due to the fact that glyphosate is the only herbicide that targets EPSPS (Baylis, 2000; Dill, 2005; Duke and Powles, 2008). Some

scientists thought it would be highly unlikely for plants to develop resistance to glyphosate because of its unique biochemical inhibition of EPSPS and the fact that it acts on an essential pathway and alterations to this pathway would be detrimental to plant growth (Bradshaw *et al*., 1997; Padgette *et al*., 1991). Glyphosate was used extensively for more than 20 years with no reports of weeds evolving resistance under field situations (Bradshaw *et al*., 1997; Holt *et al*., 1993; Powles and Preston, 2006). The introduction of GR crops have led to changes in herbicide use patterns with glyphosate commonly used as the sole means of weed control (Reddy *et al*., 2010). GR crop technology was first introduced in 1996 in soybean (*Glycine max* L.) and canola (*Brassica campestris* L.), followed by cotton (*Gossypium hirsutum* L.) in 1997 and corn (*Zea mays* L.) in 1998 (Powles and Duke, 2010). The profound efficacy of the GR crop/glyphosate combination led to the rapid adoption of GR crops because it reduced the cost of weed control and fuel inputs, improved soil conservation through widespread adoption of no-tillage soil management, and since glyphosate is a systemic non-selective herbicide, almost all weed species could be controlled in GR crops with one or two appropriately-timed post-emergent applications of glyphosate, while maintaining crop safety (Dill *et al*., 2010; Feng *et al*., 2010; Powles and Duke, 2010). However, this system led to the over-dependence on glyphosate, which led to growers making multiple in-season applications and applications at the wrong weed growth stage, thus creating a strong selection pressure for resistance (Baylis, 2000; Dill, 2005; Dill *et al*., 2010; Duke and Powles, 2008; Powles, 2008).

The first reported GR weed was a biotype of rigid ryegrass (*Lolium rigidum* L.) in 1996, discovered in an orchard in New South Wales, Australia where glyphosate had been applied for 15 years at rates between 720 to 1440 g·a.e.·ha^{-1} two to three times a year (Powles *et al*., 1998). Glyphosate resistance was later reported in 1997 in a biotype of goosegrass (*Eleusine indica* L.

Gaertn.) from Malaysia (Lee and Ngim, 2000). The first reported case of glyphosate resistance in a GR cropping system was the dicot weed, horseweed (*Conyza canadensis* L. Cronq.) found in a GR soybean field in Delaware, United States (VanGessel, 2001). To date, there are 35 species resistant to glyphosate belonging to the Amaranthaceae, Asteraceae, Brassicaceae, Chenopodiaceae, Plantaginaceae, Poaceae and Rubiaceae families in 27 countries around the world (Heap, 2016).

Mechanisms of Glyphosate Resistance

There are several types of evolved resistance mechanisms to many different herbicides, but the known resistance mechanisms for glyphosate exceed those described for any other herbicide (Sammons and Gaines, 2014). Mechanisms conferring resistance to glyphosate in weeds include target site mutation, increased EPSPS production, reduced translocation, reduced foliar uptake, vacuolar sequestration and increased metabolism (Baerson *et al*., 2002; de Carvalho *et al*., 2012; Dinelli *et al*., 2006; Ge *et al*., 2010; Lorraine-Colwill *et al*., 2002; Michitte *et al*., 2007; Ng *et al*., 2004; Sammons and Gaines, 2014; Yu *et al*., 2007). The evolution of novel mechanisms in which weeds have developed resistance to glyphosate and understanding the molecular basis for these resistance mechanisms are of particular interest. Currently the mechanism of glyphosate resistance in giant ragweed is unknown.

Target Site Mutation

Target site resistance can be defined as "resistance that is provided by gene mutation conferring a change to a target site enzyme such that the herbicide no longer effectively inhibits the normal enzyme function" (Green, 2014; Powles and Preston, 2006). A target site mutation

will typically be a nucleotide substitution within a specific coding region resulting in a different amino acid that may confer a structural change in the target enzyme (Powles and Preston, 2006). These changes prevent the herbicide from inhibiting the target enzyme by altering the herbicide binding affinity, thus conferring resistance (Powles and Preston, 2006).

Glyphosate target site resistance was first reported in goosegrass (*Eleusine indica* (L.) Gaertn.) from Malaysia (Lee and Ngim, 2000). Four single nucleotide polymorphisms were identified from cDNA sequence, two of which resulted in amino acid substitutions in the EPSPS enzyme (Baerson *et al*., 2002). Of the two non-synonymous mutations, the Pro_{381}Leu substitution resulted in a nonconservative change of Pro for the hydrophobic Leu residue which did not contribute significantly to the resistance (Baerson *et al*., 2002). However, the Pro_{106}Ser substitution resulted in a polar, helix-destabilizing residue of the Ser in the place of the nonpolar residue from the Pro, which did contribute significantly to the resistance (Baerson *et al*., 2002). This substitution was of particular significance because it corresponds with the same substitution found in the GR EPSPS enzyme from *Salmonella typhimurium* (*aroA*), which is determined as the genetic basis for glyphosate resistance (Baerson *et al*., 2002; Comai *et al*., 1983; Stalker *et al*., 1985). The Pro_{106}Ser substitution in goosegrass conferred a resistance index of 8- to 12-fold and the same mutation was later found in rigid ryegrass from Australia conferring a 2- to 3-fold resistance and recently found in the dicotyledonous species tall waterhemp (*Amaranthus tuburculatus* L.) (Baerson *et al*., 2002; Bell *et al*., 2013; Bostamam *et al*., 2012; Nandula *et al*., 2013).

Three other point mutations at position 106 were found to also confer resistance to glyphosate. One coded for a Pro_{106}Thr substitution found in goosegrass and rigid ryegrass, while the other two coded for a Pro_{106}Ala and a Pro_{106}Leu substitution found in rigid ryegrass

(Bostamam *et al*., 2012; Jasieniuk *et al*., 2008; Kaundun *et al*., 2011; Ng *et al*., 2004; Wakelin and Preston, 2006; Yu *et al*., 2007). Interestingly, a previous study identified the $Pro_{106}Leu$ substitution in a GR rice (*Oryza sativa* L.) mutant EPSPS that was selected through a directed evolution approach (Zhou *et al*., 2006). All four amino acid substitutions at site 106 confer glyphosate target site resistance due to the cyclic nature of proline (Yu *et al*., 2007). When proline forms a peptide bond in an α-helix or a β-sheet, it does not have the hydrogen bond to stabilize it due to conformational constraints caused by its pyrrolidine side group (Berg *et al*., 2002; Ng *et al*., 2003; Yu *et al*., 2007). Proline at site 106 in EPSPS is in an α-helix and the lack of the hydrogen bond with proline results in a slight bend in the α-helix structure (Yu *et al*., 2007; Zhou *et al*., 2006). Therefore, any amino acid substitution at this site will change the conformation of the α-helix, altering the structure and function of EPSPS, ultimately affecting the binding of glyphosate (Ng *et al*., 2003; Yu *et al*., 2007; Zhou *et al*., 2006).

It was hypothesized that plants would not develop target site resistance because a mutation resulting in a conformational change in EPSPS would not only have lower binding affinity to glyphosate but may also have reduced binding affinity for PEP, the substrate, resulting in a fitness cost (Bradshaw *et al*., 1997). This reduced affinity for PEP was shown through a cloned petunia (*Petunia* × *atkinsiana* D. Don ex Loudon [*axillaris* × *integrifolia*]) enzyme that conveyed resistance due to the substitution of $Pro_{106}Ser$ (Padgette *et al*., 1991). Using the Michaelis-Menten model of enzyme kinetics, where the Michaelis constant $K_{m(app)}$ represents the apparent affinity of the substrate and the inhibitory constant $K_{i(app)}$ represents the apparent affinity of the inhibitor, the ratio K_i / K_m is considered to be a selectivity factor for PEP over glyphosate binding (Johnson and Goody, 2011; Michaelis and Menten, 1913; Sammons and Gaines, 2014). The $K_{i(app)}$ for glyphosate in the wild-type petunia was 0.4 μM and was increased

to 3 μM in the mutant containing the Pro_{106}Ser mutation, while the $K_{m(app)}$ for PEP went from 5 to 44 μM with the introduction of the Pro_{106}Ser mutation, resulting in a K_i/ K_m ratio change from 0.08 in wild type to 0.07 in the mutant (Padgette *et al*., 1991; Sammons and Gaines, 2014). These results show an equally reduced affinity for glyphosate and PEP. Subsequent research with goosegrass showed a wild-type K_i/ K_m ratio of 0.013 and a Pro_{106}Ser mutant ratio of 0.12, a 9.2-fold increase (Baerson *et al*., 2002; Sammons and Gaines, 2014). This loss of substrate affinity was less severe than reported in petunia. Despite a slight increase in $K_{m(app)}$ for PEP, the goosegrass EPSPS Pro_{106}Ser mutation maintains adequate PEP affinity for survival while conferring glyphosate resistance in the field (Baerson *et al*., 2002; Sammons and Gaines, 2014).

Despite the fitness cost associated with a less efficient EPSPS, the Pro_{106} mutation has evolved in many GR species, which demonstrates the evolutionary process by which mutations can accumulate to confer resistance when selection pressure is persistent (Sammons and Gaines, 2014). Recently, a naturally evolved Thr_{102}Ile mutation has been found in combination with the Pro_{106}Ser mutation in goosegrass that confers a >180-fold resistance to glyphosate compared to the wild type and a >32-fold resistance compared to the previously known Pro_{106}Ser mutants (Jalaludin *et al*., 2013; Sammons and Gaines, 2014; Yu *et al*., 2015). This Thr_{102}Ile+Pro_{106}Ser (TIPS) mutant is the only example of a double EPSPS mutation to evolve naturally in a wild population (Sammons and Gaines, 2014; Yu *et al*., 2015). In corn, the TIPS mutation was shown to increase the $K_{i(app)}$ of glyphosate from the 0.5 μM in the wild-type to 58 μM, while the $K_{m(app)}$ of PEP decreased from 27 μM in the wild-type to 10.6 μM in the mutant, suggesting the Thr_{102}Ile mutation occurred after the Pro_{106}Ser mutation due to its significant reduction in PEP K_m (Sammons and Gaines, 2014). The sequential evolution of the TIPS mutation is a dramatic example of evolution in action due to intense herbicide selection pressure (Yu *et al*., 2015).

Increased EPSPS Production

Another mechanism conferring glyphosate resistance is an increase in EPSPS production, which can occur either by overexpression or gene amplification (Pline-Srnic, 2006). EPSPS overexpression has not been found to occur naturally in weeds, while EPSPS gene amplification has been reported in GR palmer amaranth (*Amaranthus palmeri* S. Wats.) and in Italian ryegrass (*Lolium multiflorum* Lam.) (Gaines *et al*., 2010; Salas *et al*., 2012). EPSPS overexpression due to an increased rate of transcription has only been documented in cultured cells of GR rock harlequin (*Corydalis sempersirens* L. Pers.) (Pline-Srnic, 2006; Smart *et al*., 1985). EPSPS levels were determined through immunoblot assays and the increased rate of EPSPS synthesis was determined through *in vivo* pulse-labeling with [^{35}S] methionine (Smart *et al*., 1985). Despite exhibiting a 40-fold increase in EPSPS activity, these cultured cells also accumulated high levels of shikimic acid, the dephosphorylated substrate of the enzyme when exposed to glyphosate (Smart *et al*., 1985). The EPSPS from these GR untreated cultured cells showed identical physical, kinetic and immunological properties as the EPSPS from GS untreated cultured cells (Smart *et al*., 1985). Due to no evidence of EPSPS gene amplification and the conserved enzyme sensitivity to glyphosate, resistance in this cultured cell line was attributed to an increased rate of transcription and turnover of EPSPS (Pline-Srnic, 2006; Smart *et al*., 1985). No other plant or cell line has been reported having this glyphosate resistance mechanism (Pline-Srnic, 2006).

Gene amplification as a glyphosate resistance mechanism was first documented in tissue culture of wild carrot (*Daucus carota* L.) (Nafziger *et al*., 1984; Pline-Srnic, 2006). This cultured cell line exhibited a 12-fold increase in EPSPS activity and contained a glyphosate-sensitive EPSPS, however, genome analysis found a 4- to 25-fold increase in the number of copies of *EPSPS*, along with one inverted repeat of the EPSPS gene (Nafziger *et al*., 1984; Pline-Srnic,

2006; Suh *et al*., 1993). Similar results were later found in a cultured petunia (*Catharanthus roseus* (L.) G. Don.) cell line having a 10- to 20-fold increase in genomic copies of EPSPS and a 20-fold increase in the EPSPS activity (Pline-Srnic, 2006; Steinrucken *et al*., 1986). The first report of glyphosate resistance due to gene amplification in a naturally occurring plant population was found in palmer amaranth from Georgia in 2009 (Gaines *et al*., 2010). These plants had a 6- to 8-fold increase in resistance to glyphosate, showed no differences in absorption or translocation of the herbicide compared to GS plants and no shikimate accumulation was detected in the resistant leaf tissue (Culpepper *et al*., 2006; Gaines *et al*., 2010). The EPSPS gene was found to be duplicated 5-fold to over 160-fold in the genomes of GR plants compared to the genomes of GS plants (Gaines *et al*., 2010). EPSPS gene expression and protein levels were positively correlated with the genomic copy number using quantitative RT-PCR on cDNA and immunoblot assays (Gaines *et al*., 2010). Continued analysis correlated glyphosate resistance with increases in genomic copy number of *EPSPS*, expression of the *EPSPS* transcript, EPSPS protein level and EPSPS enzymatic activity (Gaines *et al*., 2011). This mechanism of EPSPS gene amplification was also found to confer a 7- to 13-fold resistance to glyphosate in a population of Italian ryegrass in Arkansas (Salas *et al*., 2012). Resistant plants were found to contain up to 25 copies of *EPSPS*, with a 6-fold increase in EPSPS activity compared to GS plants (Salas *et al*., 2012). EPSPS gene amplification shows a positive correlation with the gene copy number and the resistance factor to glyphosate, thus demonstrating another evolutionary adaptation to the selective pressure from excessive glyphosate use (Sammons and Gaines, 2014).

Reduced Absorption and Translocation

Reduced glyphosate absorption and translocation mechanisms are commonly found to occur in tandem. Reduced spray retention and absorption of glyphosate have been reported to play a role in resistance but have never been described as the sole mechanism of glyphosate resistance (Green, 2014). A GR Italian ryegrass population was observed having a thicker cuticle and more textured leaf surface in comparison to a susceptible population (Michitte *et al*., 2004). The composition of the epicuticular wax of GR plants was found to contain 5% more polar compounds (alcohols and aldehydes) than GS plants (Guimarães *et al*., 2009). This GR population also showed altered herbicide translocation to the tip of the treated leaf (Michitte *et al*., 2007). Recently, reduced absorption of glyphosate was reported in sourgrass (*Digitaia insularis* L.), where the resistant biotype absorbed at least 12% less glyphosate than the susceptible biotype at 12 hours after treatment, however there was no difference in absorption at 72 hours after treatment (de Carvalho *et al*., 2012). Along with reduced absorption, reduced translocation, metabolism and gene mutation also contributed to resistance to glyphosate in this biotype of sourgrass (de Carvalho *et al*., 2012).

Reduced translocation of glyphosate has been found to be a sole mechanism of resistance in rigid ryegrass, where resistant plants were found to accumulate 50% of applied glyphosate in the leaf tips, resulting in a 10-fold level of resistance (Lorraine-Colwill *et al*., 2002; Powles *et al*., 1998; Wakelin *et al*., 2004). GS populations accumulated the majority of glyphosate in the roots and shoot meristem tissues (Lorraine-Colwill *et al*., 2002). These findings led to the theory of a cellular glyphosate pump that would retain glyphosate in the apoplastic space and prevent it from entering neighboring cells to pass into phloem tissue (Lorraine-Colwill *et al*., 2002). Some populations of rigid ryegrass in South Australia have both a target site mutation along with the

reduced glyphosate translocation mechanism (Bostamam *et al*., 2012). These populations containing both mechanisms of resistance exhibited 5.6-fold to greater than 10-fold resistance compared to a 2-fold resistance in populations containing the target site mutation alone and a 4-fold resistance in populations containing the reduced translocation mechanism alone (Bostamam *et al*., 2012). Thus, reduced translocation can confer a high level of glyphosate resistance, but having both mechanisms of resistance in a population can contribute to a greater level of resistance.

Reduced translocation to the root and shoot meristem tissue has also been described in GR horseweed (Feng *et al*., 2004). Autoradiography of [^{14}C]-glyphosate-treated plants revealed that glyphosate remained localized to the treated leaf in resistant plants and phloem loading and export were delayed compared to GS plants (Feng *et al*., 2004). The shikimate to glyphosate ratio was much lower in the GR plants relative to the GS plants, however shikimate did accumulate in GR plants, indicating a sensitive EPSPS (Feng *et al*., 2004; Mueller *et al*., 2003). These results suggest glyphosate may be partially excluded from the plastids in GR plants, which would result in reduced inhibition of EPSPS (Feng *et al*., 2004). This type of resistance is the result of a single-locus dominate or semi-dominant nuclear encoded gene (Halfhill *et al*., 2007; Lorraine-Colwill *et al*., 2002; Wakelin *et al*., 2004). It is speculated that a tonoplast localized glyphosate transporter is up-regulated or only present in resistant biotypes, however the detailed mechanism and the transporter involved have not yet been described (Basu *et al*., 2004; Shaner, 2009; Yuan *et al*., 2007).

Rapid Vacuolar Sequestration

Rapid sequestration of glyphosate to the vacuole as a mechanism of resistance has been reported in GR horseweed and GR *Lolium spp.* (Ge *et al*., 2010; Ge *et al*., 2012). This mechanism is thought to work via the preferential movement of glyphosate from the cytosol to the vacuole in GR tissue but not in GS tissue (Ge *et al*., 2010). Therefore, glyphosate in the cytoplasmic pool is available for translocation to sink tissues, whereas glyphosate sequestered within the vacuole is effectively removed from the phloem-accessible pool of glyphosate (Ge *et al*., 2010). ^{31}P nuclear magnetic resonance (NMR) was used to determine the fractionation of glyphosate pools in the cytoplasm and vacuole from both source and sink tissue (Ge *et al*., 2010; Ge *et al*., 2012). In GR horseweed, the vacuoles of source tissues contained greater than 85% of the glyphosate pool compared to approximately 15% in GS plants (Ge *et al*., 2010). The majority of the glyphosate pool in sink tissues of GR plants was found in the vacuoles, whereas all of the glyphosate pool in sink tissues of GS plants was found in the cytoplasm (Ge *et al*., 2010). Glyphosate uptake into the vacuole was also more rapid in the GR plants compared to the GS plants (Ge *et al*., 2010).

Similar results were found in ryegrass populations from around the world, however, GS lines showed no measurable sequestration (Ge *et al*., 2012). In ryegrass lines showing a higher level of glyphosate resistance, a larger fraction of the glyphosate pool was sequestered into the vacuole compared to moderately resistant ryegrass lines (Ge *et al*., 2012). Sequestration was also more rapid in the highly resistant lines compared to the moderately resistant lines (Ge *et al*., 2012). This correlation between vacuolar sequestration and level of resistance suggests the major role of vacuolar sequestration in the resistance mechanism (Ge *et al*., 2012). Interestingly, vacuolar sequestration was suppressed in GR horseweed when plants were cold acclimated and

treated with glyphosate at low temperatures (~12 °C), effectively making the plants GS (Ge *et al*., 2011). This suppression was reversible if plants were exposed to warmer conditions (Ge *et al*., 2011). These results support vacuolar sequestration being the primary mechanism of resistance.

The results seen in horseweed and ryegrass are similar to results in *Arabidopsis* demonstrating an ABC transporter system to pump a xenobiotic into the vacuole and shield the cell from the normally toxic effects of the antibiotic (Ge *et al*., 2010). Therefore, it is strongly suggested that a tonoplast membrane pump is being overexpressed or upregulated in GR tissues, thus sequestering glyphosate to the vacuole and effectively shielding the chloroplast EPSPS from glyphosate (Ge *et al*., 2010). The idea of a transport protein being overexpressed or upregulated is supported by the functional ability to move glyphosate into the tonoplast in GS horseweed, while this process is dramatically improved in GR horseweed (Ge *et al*., 2010).

Metabolism

The breakdown of glyphosate into non-toxic metabolites is rare in plants and many scientists have considered soil microbes to be the only organisms capable of significantly degrading glyphosate (Duke, 2010). There have been a few reports of glyphosate metabolism in weeds, but prior to 2011, no one has found enhanced detoxification of glyphosate to be involved in glyphosate resistance (de Carvalho *et al*., 2012; Duke, 2010; Duke *et al*., 2003; Putnam, 1976; Sandberg *et al*., 1980; Simarmata *et al*., 2003; Wyrill III and Burnside, 1976). Glyphosate metabolism in soil occurs either by a C-P lyase making sarcosine and inorganic phosphate or by a GOX enzyme that degrades glyphosate to AMPA and glyoxylate (Duke, 2010). Transgenic GR canola was designed to have an inserted *gox247* gene for metabolism resistance along with an

inserted *cp4 epsps* gene for target site resistance (Green, 2009). No transgenic GR crops rely solely on metabolism as a means for resistance (Duke, 2010). Metabolism based resistance to glyphosate is not often suspected in GR weeds because both of these glyphosate metabolism pathways do not occur naturally in plants (Duke, 2010; Green, 2014).

Significant glyphosate metabolism was reported in sourgrass in 2012, but this was not the sole mechanism of resistance to glyphosate (de Carvalho *et al*., 2012). Other glyphosate resistance mechanisms found in this biotype include gene mutation and altered absorption and translocation (de Carvalho *et al*., 2012). Reversed-polarity capillary electrophoresis was used to determine the concentration of glyphosate and its metabolites (de Carvalho *et al*., 2012). In the resistant biotype, 25 to 59% of glyphosate, in relation to its metabolites, was detected at 48 hours after treatment (HAT) and <10% was detected at 168 HAT (de Carvalho *et al*., 2012). In the sensitive biotype, >90% of glyphosate was detected at 48 HAT and 80% at 168 HAT (de Carvalho *et al*., 2012). Up to 96 HAT, 37-64% of AMPA and 15-32% of glyoxylate and low levels of sarcosine were detected in the GR biotype, while no metabolites were found in the GS biotype (de Carvalho *et al*., 2012). At 168 HAT, AMPA and glyoxylate were detected in the GS biotype, indicating that a more rapid glyphosate degradation occurred in the GR biotype (de Carvalho *et al*., 2012). Despite the significant difference in glyphosate metabolism at 168 HAT, it is unclear if this metabolism would be sufficient or rapid enough to confer resistance to glyphosate, because of the other glyphosate resistance mechanisms present in this biotype (Green, 2014).

Giant Ragweed Response to Glyphosate

Glyphosate-susceptible (GS) giant ragweed plants treated with glyphosate begin to show herbicide injury symptoms about seven days after treatment (DAT) (Thompson, 2012). The apical meristem tissues become chlorotic, and by 21 DAT the above ground tissues are mostly necrotic with very little green tissue remaining (Hoss *et al*., 2003; Singh and Shaner, 1998). By 28 DAT, almost all of the above ground plant tissue is dead with no signs of new growth or budding. Whereas, glyphosate-resistant (GR) giant ragweed biotypes respond to glyphosate treatment in one of two ways. One GR biotype, referred to as GR slow response, shows minimal visible injury in the first two weeks after glyphosate treatment, with some slight chlorosis and necrosis. However, the growth of this GR biotype is slowed or halted during the first two weeks after treatment, then around three weeks after treatment the plants continue to grow as if untreated. This response suggests a target site mutation or amplification of the EPSPS gene, that would either prevent glyphosate from binding the EPSPS enzyme or causes an overproduction of the enzyme which allows the shikimic acid pathway to produce chorismate after treatment with glyphosate (Thompson, 2012). This type of glyphosate resistance in giant ragweed was first confirmed in Ohio in 2004 (Heap, 2016; Stachler *et al*., 2006; Stachler, 2008; Vink *et al*., 2012b). Populations with the slow response biotype have a resistance index of about 4, which suggests that the glyphosate resistance mechanism is caused by a target site mutation (Green *et al*., 2011; Nandula, 2010). Suggested mechanisms of resistance in giant ragweed are based on similar responses described in other weed species because the exact mechanisms causing glyphosate resistance in giant ragweed have not yet been described (Thompson, 2012).

The other GR biotype, described as GR rapid response, shows an extremely rapid response to glyphosate in which the larger, mature leaves become necrotic within hours after

treatment, while the meristematic tissue remains unaffected by this rapid tissue death (Robertson, 2010). By 24 HAT, the mature tissue is completely necrotic and desiccated and the plant will drop these affected leaves within one week after treatment. The plant survives through continued growth from the apical meristem and new growth from axillary shoots. At 24 to 48 HAT, the plant looks as if it were controlled by glyphosate, showing almost 90% tissue death, but by four weeks after treatment the plant has put on new growth and appears as if it were untreated (Van Horn and Westra, 2014). This response suggests that the biotype has an altered translocation mechanism, with the glyphosate either being quarantined to the mature tissue or actively pumped into these mature tissues to prevent EPSPS disruption in the meristematic tissues (Thompson, 2012). This type of glyphosate resistance in giant ragweed was first confirmed in Ontario in 2008 (Green, 2014; Sikkema *et al*., 2009). Populations with the rapid response biotype have a resistance index of about 6.5, which may suggest that the biotype has a reduced translocation mechanism of resistance (Green *et al*., 2011; Nandula, 2010). One study using a GR rapid response population from Ontario, Canada, found at 24 HAT, [^{14}C]-glyphosate was shown to increase in the larger mature leaves and decrease in the apical meristem in comparison to GS plants (Lespérance *et al*., 2016).

Recent microscopy studies of the GR rapid response show an organized cell death similar to autophagy or apoptosis in mammalian systems (Lespérance *et al*., 2016). The cell first recycles the cell contents and shrinks the inner membrane before collapsing in on itself (Lespérance *et al*., 2016). This type of programmed cell death (PCD) is unique to the GR rapid response biotype. The GS biotype also shows tissue death, but only about one to two weeks after glyphosate treatment. The same microscopy studies showed this cell death to be unorganized and chaotic, similar to a total cellular breakdown resulting in necrosis (Lespérance *et al*., 2016). In

this process, it appears the integrity of the cell wall was lost and the plasma membrane burst, releasing the cell contents into the extracellular space (Lespérance *et al*., 2016). This cell death occurred in all tissue types of the GS biotype one to two weeks after glyphosate treatment, whereas the controlled cell death in the GR rapid response biotype that occurs within hours after glyphosate treatment only occurs in mature leaf tissue (Lespérance *et al*., 2016). The molecular mechanism causing this rapid cell death response to glyphosate is unknown.

Programmed Cell Death: Autophagy, Necrosis and The Hypersensitive-Response

It is hypothesized that the GR rapid response to glyphosate is a defense mechanism in which the plant is attempting to quarantine glyphosate away from young actively growing tissue to prevent EPSPS inhibition at these sites (Robertson, 2010). Transmission electron microscopy showed differences in cellular morphology between GR and GS plants during cell death (Lespérance *et al*., 2016). The GR rapid response within 24 hours after glyphosate application resembles a plant hyper-sensitive response (HR) to a pathogen, while the GS cell death one to two weeks after glyphosate application resembles a disorganized necrosis (Lespérance *et al*., 2016).

HR, a type of PCD, is a plant immune response that can be recognized as the rapid and localized death of plant cells at the site of pathogen infection (Lam *et al*., 2001). HR regulates the extent of cell death to limit the spread of pathogen growth while preventing runaway cell death, whereas the GR rapid response induced by glyphosate causes cell death in all mature leaf tissue throughout the plant. Interestingly, when a single drop of 26.4 mM glyphosate is placed on one leaf of a GR rapid response giant ragweed plant, cell death will occur in every mature leaf on that plant within 24 hours (Van Horn and Westra, 2014). The same response was seen regardless

of glyphosate droplet application. Whether a drop of glyphosate was placed on the top most meristematic tissue, or the lowest true leaf, the rapid cell death was seen only in mature leaf tissue 24 HAT (Van Horn and Westra, 2014). Despite the difference concerning the spread of cell death, the GR rapid response to glyphosate shares many similarities to HR. The term hypersensitive, relating to defense, was first introduced by Stakman (1915), describing the rapid and localized plant cell death induced by rust fungi in rust-resistant plants (Heath, 2000; Stakman, 1915). Over a century later, HR is considered a landmark of successful pathogen recognition during plant-microbe interactions, yet we still do not fully understand the molecular mechanism behind this form of PCD (Zurbriggen *et al*., 2010).

We do know that the complexity of plant defense responses requires a large amount of energy, specifically from carbohydrate metabolic processes such as glycolysis, the pentose phosphate pathway and the TCA cycle. Pathogens and elicitors induce the expression of genes involved in these pathways that affect downstream responses such as the expression of pathogenesis-related (PR) genes, generation of hydrogen peroxide (H_2O_2), accumulation of salicylic acid (SA), jasmonic acid (JA) and ethylene, and the initiation of HR (Rojas *et al*., 2014). It is also known that several genes involved in amino acid biosynthesis are upregulated after pathogen recognition and it is likely these amino acids play a role in plant defense (Rojas *et al*., 2014).

After initial recognition of a pathogen, which can be a highly variable system depending on the plant host and the specific pathogen strain, one of the earliest features of HR is an efflux of potassium ions out of the cell and an influx of protons and calcium ions (Balagué *et al*., 2003; Mur, 2007). These ions not only alter the ionic homeostasis in the cytosol, but may be crucial signaling molecules in the events leading to HR cell death by initiating the generation of reactive

oxygen species (ROS) (Lam *et al*., 2001). The first observation of ROS preceding HR was made by Doke (1983), wherein superoxide production occurred prior to HR elicited by *P. infestans* on potato tubers and TMV in tobacco (Doke, 1983). Other forms of ROS include hydroxyl radical, hydrogen peroxide and singlet oxygen. It is important to note that some aspects of HR proceed unaffected and cell death may be enhanced or delayed even when ROS are completely removed via mutation, transgenic or pharmacological approaches (Zurbriggen *et al*., 2010). For example, it is known that the accumulation of some amino acids trigger resistance responses against pathogens independent of the generation of ROS or SA (Rojas *et al*., 2014). There are multiple sources of ROS including the chloroplast, plasma membrane oxidases, and the mitochondria. The initial source of ROS generated during HR come from the chloroplasts due to over-reduction of the photosynthetic electron transport chain and excess excitation energy in the thylakoids (Zurbriggen *et al*., 2010). This photo-production of ROS occurs when photon intensity is in excess of that required for CO^2 fixation (Asada, 2006; Mur *et al*., 2008). It has been shown that plants left in the dark during pathogen attack do not accumulate ROS in plastids and cell death was considerably delayed, implicating the effect light can have on the speed at which cell death occurs (Liu *et al*., 2007).

During HR, ROS production continues in the apoplast via nicotinamide adenine dinucleotide phosphate (NADPH) oxidases (Mur, 2007). NADPH oxidases, encoded by the *Rboh* family, embedded in the plasma membrane are responsible for extracellular ROS, which could serve as diffusible signaling molecules (Zurbriggen *et al*., 2010). Two other chemical signals generated in response to oxidative stress include nitric oxide (NO) and SA. NO has been shown to act with ROS in eliciting HR (Mur, 2007). SA inhibits the mitochondrial respiratory chain by disrupting ATP synthesis and electron flow through the respiratory transport chain, thus leading

to ROS generation in the mitochondria (Xie and Chen, 2000). If SA levels are reduced during HR, the rate of cell death is delayed, which could allow a pathogen to escape the quarantining effects of HR cell death (Mur, 2007). Another mechanism by which to delay HR is through ROS detoxification by enzyme scavengers such as superoxide dismutase, catalase, glutathione peroxidase and ascorbate peroxidase. It has been shown that tobacco plants with reduced levels of ascorbate peroxidase were hyper-reactive to challenge by avirulent bacteria (Mittler *et al*., 1999; Mur *et al*., 2008). It is important to note that many of these signaling molecules associated with HR are also effective initiators of resistance in the absence of HR cell death (Grün *et al*., 2006; Mittler, 2002; Ryals *et al*., 1996). This could imply that HR is a secondary response to pathogen resistance, due to the fact that these resistance signals also disrupt mitochondrial function. Although, HR is most likely a useful response because it has been maintained throughout plant evolution (Mur *et al*., 2008). Interest in HR from an agricultural perspective has mostly been focused on how it is triggered. The gene-for-gene model describing the interaction between a plant resistance gene with a single pathogen-encoded avirulence gene product has typically been accepted (Mur, 2007). However, we have since gained a deeper understanding into the complexity of HR and its relation to resistance. There are many ways to initiate the vastly interconnected signaling cascades that lead to HR and it is very possible that we have discovered yet another trigger for HR in the GR rapid response to glyphosate phenotype in giant ragweed.

Another type of PCD is autophagy (also known as macroautophagy) (Michaeli *et al*., 2015; Reggiori and Klionsky, 2013). Autophagy is a major cellular degradation pathway that recycles damaged or unwanted cell materials under conditions of stress or during specific developmental processes (Liu and Bassham, 2012; Michaeli *et al*., 2015). Autophagy was first described in yeast (*Saccharomyces cerevisiae*) and autophagy-related (*ATG*) genes have been

found in all eukaryotes, suggesting this process has been widely conserved through evolution (Liu and Bassham, 2012; Michaeli *et al*., 2015; Pérez-Pérez *et al*., 2012; Tsukada and Ohsumi, 1993). Autophagy is typically associated with developmental processes, but has been shown to be a general response to a variety of abiotic stresses, most commonly induced under drought or salt stress (Bassham, 2007; Liu and Bassham, 2012). In conditions lacking amino acids, yeast and Dictyostelium undergo autophagy as a means of survival through the degradation of proteins (van Doorn and Woltering, 2005). Both ROS and autophagy play important roles in signaling and cellular adaptation to stress (Pérez-Pérez *et al*., 2012). The autophagy process has been shown to be involved in plant responses to oxidative stress and abscisic acid (Liu and Bassham, 2012). Studies using *Arabidopsis* mutants showed autophagy-defective RNAi-*AtATG18a* plants to be more sensitive to H_2O_2 treatment and accumulate higher levels of oxidized proteins, while the wild type was able to degrade harmful ROS through the autophagy pathway (Liu and Bassham, 2012; Xiong *et al*., 2007a; Xiong *et al*., 2007b). The autophagy pathway was also shown to degrade AtTSPO, which is an ABA-induced protein (Liu and Bassham, 2012; Vanhee *et al*., 2010). These results implicate the autophagy pathway serving a prosurvival role under plant abiotic stress.

During biotic pathogen infection, autophagy also serves a prosurvival role by preventing pathogen spread and run away cell death (Liu and Bassham, 2012). Autophagy-defective *Arabidopsis* mutants showed a hypersensitive-response to *Botrytis cinerea* and *Alternaria brassiciola*, in which necrosis spread to healthy tissue and distal leaves, while wild type plants contained the pathogen infection (Lai *et al*., 2011; Lenz *et al*., 2011). Similar results were seen in autophagy knock-down and knock-out *Arabidopsis* mutants infected with *Pseudomonas syringae* pv. *Tomato* (*Pst*) DC3000, where the HR-PCD escapes from the infected area and spreads to

adjacent healthy tissues (Liu and Bassham, 2012; Patel and Dinesh-Kumar, 2008; Yoshimoto *et al*., 2009). These results suggest that autophagy functions to restrict HR in plants (Liu and Bassham, 2012).

There is another form of programmed cell death known as non-lysosomal PCD, or necrosis (van Doorn and Woltering, 2005). During necrosis, the cell membranes become destabilized by inhibition of some major biosynthetic pathway or other unknown mechanism (van Doorn and Woltering, 2005). Necrosis appears disorganized compared to autophagy. The cellular morphology of GS giant ragweed plants at one to two weeks after glyphosate application appear to follow this necrosis cell death pattern while the GR rapid response plants within 24 hours after glyphosate application follow the description of autophagy, in which the cell degrades or mobilizes its constituents before death (Lespérance *et al*., 2016; van Doorn and Woltering, 2005). Autophagy occurs much slower than HR, because it is typically associated with a developmental process or response to abiotic stress such as drought or salt stress, while HR is typically associated with biotic stress, such as fungi, bacteria or viruses. The pattern of cell death in the GR rapid response giant ragweed occurs simultaneously throughout all mature leaf tissue and does not appear as a spreading cell death originating from a single location. This response shares similar aspects of HR and autophagy, but at this time there is not enough information to classify it to a specific type of PCD. For that reason, we will continue to refer to this response as the GR rapid response to glyphosate.

1.2 PURPOSE AND SCOPE OF THIS WORK

The intense selection pressure created by continued glyphosate use over the past 30 years has provided a scenario in which genetically diverse weeds have evolved multiple resistance mechanisms to the herbicide. There are currently more known resistance mechanisms to glyphosate than to any other herbicide (Sammons and Gaines, 2014). The known mechanisms of resistance to glyphosate include target-site mutation, target-site gene duplication, active vacuole sequestration, limited cellular uptake and an undefined rapid tissue death response (Sammons and Gaines, 2014). The study of glyphosate resistance mechanisms has led to fascinating insights into plant genetic and evolutionary processes, from which new technologies and ideas were developed. Understanding the molecular basis for glyphosate resistance and the GR rapid response in giant ragweed will increase our fundamental knowledge of plant responses to glyphosate and may lead to the identification of a mechanism of resistance regulated by previously unknown molecular interactions. Investigations into this unique resistance response will lead to applications in biotechnology related to herbicide resistance and programmed cell death, as well as the development of novel solutions for weed control.

Towards these goals, the research described here focuses on two main areas: the mechanism of glyphosate resistance and the molecular basis for the rapid response to glyphosate. In chapter two, the research focuses on understanding the physiology of the rapid resistance response to glyphosate through glyphosate applications under various experimental conditions and inputs of exogenous compounds. Molecular analysis of the target gene includes sequencing at a position where mutations are known to confer resistance in multiple species and gene copy number analysis. In chapter three, a *de novo* transcriptome was developed and used as a

reference for RNA-seq analysis of giant ragweed response to glyphosate treatment. Differential gene expression analysis was used to identify candidate genes that may have a role in stimulation or regulation of resistance and/or the rapid response to glyphosate. RNA-Seq results were validated using qRT-PCR and initial testing of candidate genes on an F_2 population of giant ragweed segregating for the resistance trait was performed. The methods and results of this research provide a framework from which continued analyses of candidate genes will continue.

For the foreseeable future, herbicides will remain important tools for global weed management. In the past 25 years, weed resistance to current herbicides has greatly increased, thereby increasing the complexity of weed management decisions. After many years of no discoveries of new herbicide modes of action, global weed management now relies on a limited number of older herbicides for use in major food crops. The future requires the discovery and development of new herbicide modes of action such as may be uncovered through the research laid out in this PhD thesis on the novel biochemical response of giant ragweed to glyphosate.

CHAPTER 2. PHYSIOLOGICAL AND MOLECULAR ANALYSIS OF RESISTANCE AND THE RAPID RESPONSE TO GLYPHOSATE IN GIANT RAGWEED

2.1 INTRODUCTION

Glyphosate is an extremely valuable herbicide in both glyphosate-resistant (GR) and non-glyphosate-resistant cropping systems because of its cost effectiveness, efficacy in weed control, and low environmental impact (Baylis, 2000; Dill, 2005; Duke and Powles, 2008; Powles and Preston, 2006; Shaner, 2009). The unique chemical properties of glyphosate allow for its rapid translocation from treated plant foliage, to roots and actively growing apical meristems (Grossbard and Atkinson, 1985; Segobye, 2013). The primary target of glyphosate is the enzyme 5-enolpyruvylshikimate 3-phosphate synthase (EPSPS), which catalyzes a key step in the shikimic acid pathway (Amrhein *et al*., 1980; Gougler and Geiger, 1981; McAllister and Haderlie, 1985; Shaner, 2009). Glyphosate competes with the substrate phosphoenolpyruvate (PEP) for binding to EPSPS after the PEP binding site is generated by a conformational change in EPSPS induced by shikimate-3-phosphate binding (Schönbrunn *et al*., 2001). Inhibition by glyphosate not only halts the pathway preventing the production of chorismate and the three aromatic amino acids, but also prevents regulation of the pathway (Boocock and Coggins, 1983; Franz *et al*., 1997; Jensen, 1986; Schönbrunn *et al*., 2001). This inhibition ultimately leads to an accumulation of shikimate and a carbon shortage for other plant pathways (Amrhein *et al*., 1980; Holländer and Amrhein, 1980; Jensen, 1986). Today, at least 35 species of weeds have evolved resistance to glyphosate (Heap, 2016).

Giant ragweed (*Ambrosia trifida* L.) is a summer annual weed that has effectively adapted to thrive in agricultural fields and has become one of the most competitive weeds

relative to other common weeds in corn and soybean cropping systems (Harrison *et al*., 2001; Johnson *et al*., 2007). Over the past decade, giant ragweed has become an increasing concern in economically important crops throughout the Midwest United States and southwestern Ontario due to the evolution and prevalence of GR biotypes. The occurrence of GR giant ragweed has made eradication of this weed species an even greater challenge. Glyphosate resistance in giant ragweed was first discovered in 2004 (Stachler *et al*., 2006) and the rapid response biotype was first identified in 2008 (Sikkema *et al*., 2009). The exact mechanisms of glyphosate resistance in giant ragweed have not been identified, but target site mutations (Powles and Preston, 2006; Wakelin and Preston, 2006), target gene amplification (Gaines *et al*., 2010), and altered translocation possibly due to vacuolar sequestration (Feng *et al*., 2004; Ge *et al*., 2010; Shaner, 2009; Wakelin *et al*., 2004) have been described in GR goosegrass (*Eleusine indica* L.), tall waterhemp (*Amaranthus tuburculatus* L.), rigid ryegrass (*Lolium rigidum* L.), Palmer amaranth (*Amaranthus palmeri* L.), Italian ryegrass (*Lolium multiflorum* L.), and horseweed (*Conyza Canadensis* L.).

There are two distinct phenotypes of GR giant ragweed following treatment: a rapid response and a slow response (Robertson, 2010). During the rapid response, the mature leaves either develop a chlorotic water-soaking appearance throughout the entire leaf or chlorotic spots spread across the leaf within four hours after treatment (HAT). By 24 HAT, these mature leaves all display similar leaf curling and total tissue death. The plant will eventually drop these dead leaves within one to two weeks after treatment (WAT). Young leaf tissues located at apical and axillary meristems are unaffected and show no response to glyphosate. The plant survives through continued growth from the axillary and apical meristems. By four WAT, the rapid response biotype appears similar to untreated control plants. This rapid response to glyphosate

has not been previously observed in any other species. During the slow response, growth will slow for the first two weeks after treatment. Young meristematic tissue becomes chlorotic one WAT. Minimal tissue damage develops slowly within one to two WAT in mature leaves, but does not cause whole leaf death. By four WAT, the slow response biotype continues to grow normally, but appears shorter with minimal signs of tissue damage compared to untreated control plants. Glyphosate-susceptible (GS) biotypes do not show a rapid response. GS plants develop chlorosis one to two WAT, which slowly transitions to total tissue death in all above ground plant tissues by four WAT.

The objective of this research is to characterize the unique GR rapid response phenotype in giant ragweed through physiological and molecular analysis in order to further develop strategies to overcome resistance in this weed species. Through observation we believe the GR rapid response biotype is immediately responding to glyphosate treatment by senescing and dropping mature leaves in an attempt to prevent glyphosate translocation to actively growing tissues. Ultimately, results from this project will increase our fundamental knowledge of plant responses to glyphosate and lead to better weed management and sustainability of herbicide resistance technologies in crops derived through biotechnology. The need for understanding the mechanism of glyphosate resistance and the rapid response in giant ragweed is extremely important for many reasons including the sustainability of glyphosate use, potential applications in biotechnology relating to resistance and programmed cell death, and developing novel solutions for weed control.

2.2 MATERIALS AND METHODS

Seed Sources, Germination, Planting, and Growth.

Giant ragweed seeds were collected from field sites and shipped to CSU by collaborators. Seed sources are outlined in Table 2.1. Seed samples were cleaned in an air-column separator and stored dry at 10 °C until conditioning for experiments. For conditioning, seeds were planted in moist commercial potting media (Fafard Custom Mix, Sun Gro Horticulture, 770 Silver Street, Agawam, MA 01001) in plastic Magenta® boxes where they would undergo cold stratification for 4-8 weeks to break dormancy. Adequate moisture is necessary to soften the outer structures surrounding the embryo (Appendix 1). Planted seeds were moved between 10 °C to 25 °C for one week at each temperature resulting in a large number of seeds germinating simultaneously (Appendix 2). Once germinated, seedlings were transplanted to 2 L pots containing potting mix. Plants were fertilized once with 30 g 14-14-14 (N, P_2O_5, and K_2O) Osmocote® at the time of transplantation. Plants were grown in a greenhouse (25/20 °C day/night, 14-h photoperiod). Plants for seed production were grown to maturity and individually bagged, using micro-perforated bags, once male flower development was observed (Appendix 3). Pollination bags were 12 x 34 inches with a pore size of 0.75 millimeters. Self-pollinated individuals would produce seed that was collected and stored dry at 10 °C until needed for experiments (Appendix 4).

Glyphosate Dose Response.

The responses of GR rapid, GR slow and GS biotypes, using accessions, 2, 3, 5, 11, 12, and 15, to glyphosate were determined in two single run experiments conducted at the Colorado

State University Weed Lab greenhouse. Seeds and plants were prepared as described above. Individual plants from each population were arranged in a completely randomized design until time of spray. A rate titration experiment using glyphosate (Roundup WeatherMAX; Monsanto Company, 800 N. Lindburgh Blvd., St. Louis, MO 63167) plus 2% (w/v) ammonium sulfate (AMS) was conducted on 3- to 4-node giant ragweed individuals at heights between 10- and 15-cm tall. Glyphosate rates evaluated include 0.21, 0.42, 0.84, 1.68, 3.36, and 6.72 $kg \cdot ae \cdot ha^{-1}$. A control that was treated with AMS only was included. Experiments were arranged in a completely randomized design with six replications of each glyphosate treatment. Each replication consisted of a single individual. Glyphosate treatments were applied in a commercial chamber track sprayer equipped with an 8002EVS single even flat-fan nozzle (TeeJet, Spraying Systems Co., Wheaton, IL) calibrated to deliver 187 $L \cdot ha^{-1}$ spray solution at the level of the plant canopy. After treatment, individuals were re-randomized twice weekly on the greenhouse bench to reduce effects of spatial variation in the microenvironment. At 28 days after treatment (DAT), survival was determined and all above ground plant material was cut at soil level, placed in individual paper bags and dried at 60 °C until constant mass, and weighed.

Percent survival and above ground dry-mass (measured as percentage of the untreated) data were subjected to a nonlinear regression using the function 'drm' (Price *et al*., 2012) in package 'drc' (Ritz and Streibig, 2005) in R Statistical Language software (R Development Core Team 2013; R Foundation for Statistical Computing, Wien, Austria). Dose response curves were plotted and presented using GraphPad Prism 6® statistical software (GraphPad Software, Inc., 7825 Fay Avenue, Suite 230, La Jolla, CA 92037). Regression parameters were estimated using the following three-parameter log-logistic equation, with the lower limit being zero:

$$Y = d/1 + \exp[b(\log x - \log e)]$$

where b is the relative slope of the curve at e, d is the upper asymptote, and e is the inflection point, equal to the ED_{50} or LD_{50} (Knezevic *et al*., 2007). ED_{50} is the effective dose of glyphosate that decreased shoot biomass 50% relative to non-treated plants and LD_{50} is the lethal dose of glyphosate that decreased survival 50% relative to non-treated plants. The parameter e was statistically compared between accessions using the *t*-test in 'drm'. Differences in other dose-response model parameter estimates were determined by 95% confidence intervals. During the time course of the dose response experiment, observational ratings for tissue necrosis were made and graphed using GraphPad Prism 6® statistical software.

Shikimate Accumulation Assay.

An experiment investigating the glyphosate resistance phenotype using the shikimate assay developed by Shaner *et al*. (2005) was conducted at the Colorado State University Weed Lab facility. Seeds and plants were prepared as described above. GR rapid, GR slow and GS giant ragweed individuals from accessions 1-18 at heights of 10- to 15-cm tall were used in this experiment. Three replicate leaf discs measuring 4 mm were taken from each individual. Three biological replicate individuals were used from each accession. Five glyphosate doses were used, including 100, 250, 500, 1000, and 2000 μM as well as a no glyphosate control. Leaf discs were taken from untreated individuals and placed into 96-well microtiter plates (Corning Costar 96-Well Clear-Bottom Polystyrene Microplate; Corning Inc., Tower 2, 4th Floor, 900 Chelmsford St., Lowell, MA 01851) containing 10 mM $(NH_4)3PO_4$, 0.1% (v:v) surfactant (Tween 80; Sigma-Aldrich, 3050 Spruce Street, St. Louis, MO 63103), and glyphosate. Following incubation in light (130 μmol photons m^{-1} s^{-1}) at room temperature for 16 h, samples were frozen at -20 °C then thawed at 60 °C to rupture plant cells. After the addition of 25 μL 1.25 N HCl, samples

were incubated at 60 °C for 15 min. Twenty-five µL from each well was transferred to a new 96-well microtiter plate and 100 µL of a solution consisting of 0.0025 g mL^{-1} periodic acid and 0.0025 g mL^{-1} sodium meta-periodate was added. Following incubation of the samples at room temperature for 90 min, 100 µL of a solution of 0.6 N NaOH and 0.22 M Na_2SO_3 was added, and optical density (OD) readings were made using a spectrophotometer with a high-throughput 96-well plate reader (SynergyTM 2 Multi-Mode Microplate Reader; BioTek, 100 Tigan Street, Winooski, VT 05404). A standard shikimate concentration curve was generated to facilitate the conversion of optical density to µg shikimate mL^{-1} in test wells (Shaner *et al*., 2005). Shikimate concentrations were subjected to linear regression against spectrophotometer absorbance readings at 380 nm. The resulting equation was used to report shikimate concentrations as µg shikimate mL^{-1} solution. Replicate wells were averaged and standard deviation calculated. By subtracting wells with 0 µM glyphosate from those with glyphosate doses, shikimate accumulation after glyphosate treatment above background could be reported as Δ µg shikimate mL^{-1}.

Shikimate accumulation data were averaged across biotypes to be reported as GR rapid response, GR slow response and GS. Data were subjected to nonlinear regression using the function 'drm' (Price *et al*., 2012) in package 'drc' (Ritz and Streibig, 2005) in R Statistical Language software. Dose response curves were plotted and presented using GraphPad Prism 6® statistical software.

EPSPS Sequence Analysis.

Experiments investigating possible nucleotide mutations in the glyphosate target site of *EPSPS* were conducted at the Colorado State University Weed Lab facility. Seeds and plants

were prepared as described above. Young tissue from untreated GR rapid, GR slow and GS giant ragweed was collected. Tissue was collected from one individual from each of the following accessions, 1-15 and 17-19. The glyphosate resistance or susceptibility of these accessions was determined after tissue collection by glyphosate applied to each individual at 0.84 $kg \cdot ae \cdot ha^{-1}$. Genomic DNA was extracted using the DNeasy Plant Mini kit (QIAGEN, Valencia, CA, USA). The quantity and quality of the DNA was determined by a NanoDrop spectrophotometer and A260/280 ratios. A 197 base pair amplicon of *EPSPS* containing the Pro106 codon was amplified using PCR. Reaction mixtures and primers were as follows: 10 µL EmeraldAmp PCR Master Mix®, gDNA to a final concentration of 600 pg/µL, forward primer (AtF1 5'-ACATGCTTGGGGCTCTAAGAA-3') and reverse primer (AtR1 5'-TTGAATTACCACCAGCAGCGGT-3') to final concentrations of 0.25 µM each, and water to bring the reaction mixture to 20 µL. Cycle conditions were as follows: 95 °C for 2 min, 30 cycles of 95 °C for 30 s, 56 °C for 30 s, and 72 °C for 1 min, then 72 °C for 5 min. PCR products were separated by gel electrophoresis and extracted using the Gel Extraction kit from QIAGEN. Once purified, the DNA amplicon was sequenced by Sanger sequencing at the Colorado State University Proteomics and Metabolomics Facility using the same primers from the PCR amplification. The sequence data was analyzed and aligned using CLC Genomics Workbench software (CLC Bio-Qiagen, Aarhus, Denmark, http://www.clcbio.com/index.php).

EPSPS Copy Number Analysis.

Experiments investigating the *EPSPS* copy number in GR rapid, GR slow and GS giant ragweed using qPCR were conducted at the Colorado State University Weed Lab facility. Seeds and plants were prepared as described above. Tissue was collected from one individual from

each of the following accessions, 1-13, 15, 17 and 18. The glyphosate resistance or susceptibility of these accessions was determined after tissue collection by glyphosate applied to each individual at 0.84 kg·ae·ha^{-1}. Genomic DNA was extracted and analyzed as described above. Only DNA samples with low protein contamination (260/280 ratio of ≥ 1.8) and low salts/phenol contamination (260/230 ratio of ≥ 2.0) were used for qPCR. For the qPCR assay, DNA was diluted to 2 ng/µL in highly purified water. Using BioRad SsoAdvanced™ SYBR® Green Supermix, and following the supplied protocol, qPCR reactions were set up containing 2.5 µL gDNA template, 1x BioRad SsoAdvanced™ SYBR® Green Supermix (containing Sso7d fusion polymerase, dNTPs, SYBR Green I dye, $MgCl_2$, and stabilizers) and 0.25 µM each of forward and reverse primers for a final reaction volume of 12.5 µL.

Primer efficiency curves were created for each primer set using a 1/10x dilution series of genomic DNA from a resistant plant from accession 3. Efficiency values were calculated for each primer set using the equation $E = -1+ 10^{(-1/m)}$, where *m* is the slope (http://www.genomics.agilent.com/biocalculators/calcSlopeEfficiency.jsp). The *EPSPS* primers (AtF1: 5'-ACATGCTTGGGGCTCTAAGAA-3' and AtR1: 5'-TTGAATTACCACCAGCAGCGGT-3') had an efficiency of 95.8% and the *IDH* primers (IDH_F: 5'- GCTTTGCATTGTCATCCAACTT-3' and IDH_R: 5'-TGGTTCTCTTGGATTGATGACC-3') had an efficiency of 96.9%. Isocitrate dehydrogenase (IDH) was used as a reference gene because it is known to occur at one locus in the genome (TAIR, 2016)(TAIR, 2016). These efficiencies were very similar and thus directly comparable in subsequent calculations (Gaines *et al*., 2010).

The genomic DNA templates were run with each primer set in triplicate in 12.5 µL reactions on a 96-well plate. Duplicate plates were repeated as an additional technical

replication. Amplification was performed using the BioRad CFX96 Touch™ Real-Time PCR Detection System with the following thermoprofile: 15 minutes at 95 °C, 40 cycles of 95 °C for 30 seconds and 60 °C for 1 minute, and finally a melt curve analysis to check for primer-dimers. No-template reaction mixes, consisting of 10 µL of Master Mix (1x BioRad SsoAdvanced™ SYBR® Green Supermix and 250 nM primers) and 2.5 µL of water, served as the negative controls for this procedure. No primer-dimers and no amplification products were seen in the melt-curve analysis and the controls, respectively.

Threshold cycles (*C*t) were calculated and relative copy number was determined by the BioRad CFX Manager™ software using the normalized gene expression (ΔΔ*C*t) analysis (BioRad Laboratories, 1000 Alfred Nobel Drive, Hercules, California 94547, USA) (Livak and Schmittgen, 2001). The *IDH* gene was used as a reference gene present in the genome at a copy number of one. *EPSPS* copy number was estimated by finding Δ*C*t = (*C*t, IDH - *C*t, EPSPS). Increase in *EPSPS* copy number was expressed as ΔΔ*C*t. Six technical replications were averaged for each biological replicate. Data were subjected to an ANOVA using R Statistical Language software. A relative copy number graph was created using GraphPad Prism 6® statistical software.

Effect of Light and Dark with and Without Exogenous Sucrose Via Roots.

The responses of GR rapid and GS biotypes, using accessions, 15 and 11 respectively, to glyphosate under light and dark conditions were determined in three separate experiments conducted at the Colorado State University Weed Lab facility. Seeds and plants were prepared as described above. Three replicate giant ragweed individuals at heights between 10- and 15-cm tall were used for each treatment. Twelve individuals from each accession were removed from the

greenhouse and placed in the dark environment, which was a growth chamber at 75% humidity, 22 °C day/18 °C night, with no light, 24 hours before glyphosate treatment. The remaining 24 giant ragweed individuals were kept in the light environment, which was the greenhouse at the conditions described above. At the time of treatment, all individuals were removed from the soil and the roots were washed with tap water to remove excess potting soil. Twelve individuals from each accession were placed in H_2O and the other twelve individuals were placed in a 2% sucrose solution, submerging the roots in solution. Immediately following the root treatment, a foliar application was made with AMS alone or glyphosate at 0.84 $kg \cdot ae \cdot ha^{-1}$ plus AMS. After treatment, the giant ragweed individuals from the dark environment were immediately placed back into the dark growth chamber and the giant ragweed individuals from the light environment were placed back into the greenhouse. Twenty-four hours after treatment, all 48 individuals were photographed and visually assessed for tissue damage. Experiments were repeated in time and data pooled for statistical analysis. Data were subjected to ANOVA and Tukey HSD multiple comparisons of means using R Statistical Language software. Percent necrosis at 24 HAT was graphed using GraphPad Prism 6® statistical software.

Effect of Exogenous Aromatic Amino Acids Via Roots.

Two separate experiments investigating the role of Tyrosine, Phenylalanine and Tryptophan (the aromatic amino acids downstream of EPSPS in the shikimate pathway) in relation to the GR rapid response were conducted at the Colorado State University Weed Lab facility. Seeds and plants were prepared as described above. GR rapid and GS giant ragweed individuals from accessions 3 and 11 respectively, at heights between 10- to 15-cm tall were used in these experiments. Ten minutes prior to glyphosate treatment, individuals were removed

from pots and the roots were washed with water to remove excess potting soil. Washed roots were placed into flasks containing 200 mL of one of six treatment solutions. The six root treatment solutions were 10 mM Phenylalanine, 10 mM Tyrosine, 10 mM Tryptophan, 5 mM Phenylalanine + 5 mM Tyrosine, 5 mM Phenylalanine + 5 mM Tryptophan, 5 mM Tyrosine + 5 mM Tryptophan, or H_2O. Twenty-one individuals from each accession were used in total to ensure three replicates for each root treatment. Within 20 minutes of being placed into the treatment solutions, all individuals were treated with a foliar application of glyphosate at 0.84 $kg \cdot ae \cdot ha^{-1}$. After glyphosate application, all treatments were placed in the greenhouse and visual ratings for tissue necrosis were made at 24 HAT. Experiments were repeated in time and data pooled for statistical analysis using GraphPad Prism 6® statistical software.

Dose Response of Exogenous Phenylalanine and Tyrosine Via Roots.

Two separate experiments investigating the dose dependent role of Phenylalanine and Tyrosine (two aromatic amino acids downstream of EPSPS in the shikimate pathway) in relation to the GR rapid response were conducted at the Colorado State University Weed Lab facility. Seeds and plants were prepared as described above. GR rapid response giant ragweed individuals from accession 3, at heights between 10- to 15-cm tall were used in these experiments. Ten minutes prior to glyphosate treatment, individuals were removed from pots and the roots were washed with water to remove excess potting soil. Washed roots were placed into flasks containing 200 mL of one of four treatment solutions. The four root treatment solutions were 0.5 mM Phenylalanine + 0.5 mM Tyrosine, 5 mM Phenylalanine + 5 mM Tyrosine, 50 mM Phenylalanine + 50 mM Tyrosine or H_2O. Twenty-four individuals were used in total to ensure three replicates for each root treatment and untreated controls. Within 15 minutes of being placed

into the treatment solutions, 12 individuals were treated with a foliar application of glyphosate at 0.84 kg·ae·ha^{-1}. The other 12 individuals were not treated with glyphosate to observe the effects of the amino acid root treatment. After glyphosate application, all treatments were placed in the greenhouse and visual ratings for tissue necrosis were made at 24 HAT. Experiments were repeated in time and data pooled for statistical analysis using GraphPad Prism 6® statistical software.

Effect of Exogenous Phenylalanine and Tyrosine Via Shoots.

Three separate experiments investigating the role of Phenylalanine and Tyrosine (two aromatic amino acids downstream of EPSPS in the shikimate pathway) in relation to the GR rapid response were conducted at the Colorado State University Weed Lab facility. Seeds and plants were prepared as described above. Three GR rapid response giant ragweed individuals at heights between 60- to 80-cm tall were used in these experiments to ensure individuals had at least twelve axillary shoots with both young and mature leaf tissue on each shoot. Ten minutes prior to glyphosate treatment, axillary side shoots consisting of at least two mature leaves and young meristematic tissue were cut from one parent plant and immediately placed into a 15 mL test tube containing one of four treatment solutions. The four cut shoot treatment solutions were 10 mM Phenylalanine, 10 mM Tyrosine, 5 mM Phenylalanine + 5 mM Tyrosine, or H_2O. All cuts were made underwater and cut shoots were transferred to the treatment solutions entirely underwater to avoid cavitation in the transpiration stream. From a single individual, twelve cut shoots were made allowing for three replicates of each treatment solution. Within ten minutes of being placed into the treatment solutions, all cut shoots and the remaining donor plant were treated with a foliar application of glyphosate at 0.84 kg·ae·ha^{-1}. After glyphosate application, all

treatments were placed in the greenhouse and visual ratings for tissue necrosis were made at 24 HAT. See Appendix 5 for an example of a cut shoot in 13.2 mM glyphosate immediately after (A) and 24 hours after (B) shoot glyphosate treatment. Experiments were repeated in time and data pooled for statistical analysis using GraphPad Prism 6® statistical software.

Leaf Disc Assay for Hydrogen Peroxide Accumulation.

Experiments investigating the accumulation of hydrogen peroxide in the mature tissues of GR rapid response giant ragweed following glyphosate application were conducted at the Colorado State University Weed Lab facility. Seeds and plants were prepared as described above. A single individual each of GR rapid and GS, accessions 3 and 11 respectively, giant ragweed at heights between 15- to 20-cm tall were treated with glyphosate at 0.84 $kg \cdot ae \cdot ha^{-1}$. Immediately before glyphosate treatment and at 15, 30, 45 minutes and 1, 2, 3, 6, 9, 12, 24, and 48 hours after treatment with glyphosate, 15 mm leaf discs were taken from mature leaf tissue and meristem tissue from each plant using a metal hole puncher. Leaf discs were vacuum infiltrated with 3,3'-Diaminobenzidine-Hydrochloric acid (DAB-HCl) (1 mg/mL), pH 3.8 (Sigma, MO, USA; D-8001) using a 20 mL syringe. Once infiltrated with DAB, leaf discs were floated in DAB solution at room temperature over-night. After incubation, leaf discs were decolorized by boiling in 100% ethanol for ten minutes to remove chlorophyll before being photographed and visually examined for the presence of hydrogen peroxide. Brown precipitates form at the sites of hydrogen peroxide accumulation (Thordal-Christensen *et al.*, 1997). Data collected represents visual detection of hydrogen peroxide accumulation by the presence of brown precipitates on treated leaf discs at different harvest times after treatment.

2.3 RESULTS AND DISCUSSION

Glyphosate Dose Response.

Overall, the response to glyphosate of GR accessions was clearly different from that of GS accessions based on survival and dry biomass (Figures 2.1-2.5). The best-fit dose-response model for accessions 2, 3, 5, 11, 12 and 15 of GR rapid, GR slow and GS giant ragweed was a three-parameter log logistic model (Tables 2.2 and 2.3). The ED_{50} value of the GR rapid accession 3 (1.2 ± 0.1 kg·ae·ha^{-1}) and the GR slow accession 12 (0.9 ± 0.08 kg·ae·ha^{-1}) were 4.2-fold greater (P = 0.0001) and 3.3-fold greater (P = 0.0001), respectively, than for the GS accession 11 (0.3 ± 0.01 kg·ae·ha^{-1}) based on Student's t-tests (Figure 2.1, Table 2.2). The ED_{50} value of the GR rapid accession 15 (0.8 ± 0.07 kg·ae·ha^{-1}) and the GR slow accession 2 (1.3 ± 0.11 kg·ae·ha^{-1}) were 2.3-fold greater (P = 0.0001) and 3.6-fold greater (P = 0.0001), respectively, than for the GS accession 5 (0.4 ± 0.02 kg·ae·ha^{-1}) based on Student's t-tests (Figure 2.3, Table 2.3). Similar to our results, Norsworthy *et al*. (2011) found GR slow response biotypes from Arkansas to have ED_{50} values of 0.8 and 1.2 kg·ae·ha^{-1}, which were 3.5- to 7.2-fold greater than GS biotypes from Arkansas. GR slow response and GS giant ragweed in Wisconsin were found to have ED_{50} values of 0.9 and 0.1 kg·ae·ha^{-1}, respectively, and an R/S ratio of 6.5 (Glettner, 2013). Stachler (2008) reported R/S ratios between 2.1 and 6.1 comparing GR slow response and GS giant ragweed from Indiana and Ohio. In Ontario, ED_{50} values for GR rapid response giant ragweed were 6.1- to 6.9-fold greater than ED_{50} values for GS giant ragweed (Green, 2014).

Glyphosate had a greater effect on reducing biomass than on survival. For GR accessions 3 and 12, survival was impacted starting at doses above of 6.0 kg·ae·ha^{-1}, while biomass was

reduced from doses as low as 0.91 kg·ae·ha^{-1} (Figures 2.1 and 2.2). For GR accessions 15 and 2, survival was impacted at doses of 3.87 and 5.94 kg·ae·ha^{-1}, respectively, while biomass was reduced from doses as low as 0.82 kg·ae·ha^{-1} (Figures 2.3 and 2.4). A similar but less dramatic response was seen for the GS accessions. This explains the higher LD_{50} compared to ED_{50} as well as the steeper slope for the survival dose response curves compared to the biomass dose response curves. Despite the differences in phenotypic response to glyphosate, both the GR rapid response and GR slow response biotypes showed no significant difference with regard to the effect of glyphosate dose on either biomass or survival.

The development of tissue death as a result of glyphosate treatment at 0.84 kg·ae·ha^{-1}, can be seen in Figure 2.5. This figure highlights the dramatic resistant rapid response within the first 48 hours after glyphosate treatment as well as the development of new tissue in this biotype over time. The GS biotype shows the progression of tissue death over time typically seen after glyphosate application.

Shikimate Accumulation Assay.

Shikimate accumulation in leaf tissue was less for the GR biotypes than for the GS biotypes at glyphosate concentrations ranging up to 500 µM (Figure 2.6). In vivo shikimate bioassays showed differential shikimate accumulation between GR and GS accessions consistent with the level of resistance demonstrated at the whole-plant level. The EC_{50} values for GR rapid (631.3 ± 19.1 µM) and GR slow (600.1 ± 25.3 µM) accessions were 4.1- and 3.9-fold greater ($P = 0.00001$) and ($P = 0.00001$) than for the GS accessions (154.2 ± 5.3 µM) based on Student's t-tests (Table 2.4). However, the differential accumulation of shikimate between GR and GS accessions decreased as glyphosate concentration increased. At 1,000 to 2,000 µM glyphosate,

shikimate accumulation in the GR accessions were similar to or greater than the GS accessions (Table 2.4, Figure 2.6), indicating that the EPSPS target site in the GR accessions is inhibited by glyphosate at these high doses. Other dose-response model parameters did not differ between GR and GS accessions based on 95% confidence intervals. These results suggest that the mechanism of resistance may be overcome at higher glyphosate concentrations, and that the EPSPS target site in the GR giant ragweed accessions is sensitive to glyphosate. Similar to our results, Glettner (2013) found that shikimate accumulation in a GR slow response giant ragweed biotype from Wisconsin was 4.6-fold less than in a GS biotype. Norsworthy *et al*. (2010) also found that a GR slow response giant ragweed biotype from Tennessee was 3.3-fold less than in a GS biotype. They concluded that resistance was not conferred by an insensitive target site and may be due to reduced translocation, although this was not confirmed. Similar patterns of shikimate accumulation have been reported in Italian ryegrass from Mississippi (Nandula *et al*., 2008) and Oregon (Perez-Jones *et al*., 2005), and in horseweed from Arkansas, Delaware, and Mississippi (Koger *et al*., 2005). These results found higher levels of shikimate accumulation in GS individuals at lower glyphosate doses, but shikimate accumulation did not differ between GR and GS individuals at higher glyphosate doses. These results indicate the target site was sensitive in GR individuals and that resistance was not conferred by an altered target site.

EPSPS Sequence Analysis.

The conserved region of *EPSPS* containing the Pro106 amino acid was sequenced from one individual each of 7 GR rapid, 7 GR slow and 5 GS accessions. Alignment of the sequences from the 19 individuals showed that the previously-reported Pro106 target site mutation responsible for glyphosate resistance was absent in the GR individuals (Table 2.5). Nandula *et*

al. (2015) found similar results, with no target site resistance reported in a GR population from Mississippi. Although the full EPSPS gene was not sequenced, these results indicate that a mechanism other than a point mutation in this conserved region of *EPSPS* is responsible for glyphosate resistance in the GR giant ragweed accessions analyzed in this experiment.

EPSPS Copy Number Analysis.

EPSPS relative copy number estimates of accessions 2-13, 15, 17 and 18 obtained by qPCR, and measured against an internal reference gene, *IDH*, showed no significant change between GR and GS biotypes (P = 0.71) (Figure 2.7). The EPSPS gene is present in the genome at a copy of approximately one relative to the IDH gene in all GR and GS accessions analyzed. Slight variability in copy number at this level is due to error and sensitivity of qPCR. *EPSPS* copy number has been reported as high as 180 copies in GR *Amaranthus palmeri* (Giacomini, 2015) and 8 copies in GR *Kochia scoparia* (Wiersma *et al*., 2014). Contrary to these other species, all individuals tested across 15 giant ragweed accessions had < 2 copies of the *EPSPS* gene. These results indicate that a mechanism other than target gene amplification is responsible for glyphosate resistance in the GR giant ragweed accessions analyzed in this experiment.

Effect of Light and Dark with and Without Exogenous Sucrose Via Roots.

Light is an important factor in the stimulation of most plant functions and responses. From previous experiments, we found light to be a necessary factor in the GR rapid response due to a lack of the rapid response seen in glyphosate-treated individuals placed in a dark environment after treatment (Appendix 6). However, the data presented in Figure 2.8 show that the GR rapid response is not dependent on light specifically but rather it is a carbon dependent

response. When 24 h dark adapted GR rapid giant ragweed individuals were fed a 2% sucrose solution via roots prior to glyphosate treatment then returned to the dark environment after a foliar glyphosate application at 0.84 kg·ae·ha^{-1}, they showed a statistically similar degree of rapid tissue death at 24 HAT compared to GR rapid glyphosate-treated individuals in a light environment, based on 95% confidence intervals (P = 0.28) (Table 2.6). The glyphosate-untreated and GS treatment groups showed zero tissue necrosis at 24 HAT and were not statistically different from one another and thus were excluded from the graph in Figure 2.8. The experiment by treatment interactions were not significant for percent necrosis, such that data from repeated experiments were pooled for analysis.

These results confirm the GR rapid response to be a carbon dependent process, not reliant on light activation, but it is unclear if the response is specific to carbon or the energy released from glycolysis. It was recently shown in plants that sucrose modulates cell death by inducing UDP-glucose pyrophosphorylase 1 (UGP1) (Chivasa *et al*., 2013). In *UGP1* knockout mutants of *Arabidopsis*, sucrose-dependent cell death is abolished (Chivasa *et al*., 2013). In animal cells, addition of glucose reduces cell death induced by Phenylalanine and Tyrosine restriction (Fu *et al*., 2010). The lack of these two amino acids seems to reduce glucose consumption through increased phosphorylation of glycogen synthase kinase 3 (GSK3), which in turn impacts mitochondrial metabolism or their integrity, leading to cell death (Fu *et al*., 2010). However, in this case sucrose (a source for glucose) promotes cell death. There is still much to learn about the complex interplay between glyphosate, the shikimate pathway and glucose metabolism related to this unique rapid tissue death response.

Effect of Exogenous Phenylalanine and Tyrosine on the GR Rapid Response.

Both Phenylalanine and Tyrosine play a role in the sequential feedback inhibition of L-arogenate in the shikimate pathway (Jensen, 1986). It is thought that the deregulation of the shikimate pathway caused by glyphosate inhibition of EPSPS results in an increased carbon flow into the shikimate pathway causing a drain on the rest of the plant (Duke and Powles, 2008; Siehl, 1997; Siehl *et al*., 2007). Our experiments with these aromatic amino acids suggest their involvement in the GR rapid response as well. When GR rapid giant ragweed individuals were fed a combination of exogenous Phenylalanine and Tyrosine at concentrations ≥ 10 mM prior to foliar glyphosate treatment, individuals did not show the expected rapid response leading to tissue death. These treated plants supplied with Phenylalanine and Tyrosine showed little to mild signs of rapid tissue death (Figure 2.9). At extremely high concentrations of Phenylalanine and Tyrosine, GR rapid individuals showed essentially no signs of the rapid tissue death response after glyphosate treatment (Figure 2.10).

Variability in the response seen at lower concentrations of Phenylalanine and Tyrosine may be due in part to the amount of amino acids getting into the plant. We did not measure amino acid concentration inside the plant and therefore do not know exactly how much of the amino acid solution entered the plant. Biological replicates from these root treatment experiments may differ in their ability to take up the supplied amino acids. Despite the observed variability at lower concentrations, the results clearly show a significant difference between the combination of Phenylalanine and Tyrosine in comparison to other amino acids and combinations with Tryptophan (Figure 2.9). The reduced effect of glyphosate to elicit the rapid response in the presence of Phenylalanine and Tyrosine was further supported by similar experiments feeding the amino acid combination directly into the transpiration stream opposed to

crossing the root barrier. These results again showed a significant difference between the combination of Phenylalanine and Tyrosine in comparison to the amino acids alone and the untreated control (Figure 2.11). A number of individuals fed Phenylalanine and Tyrosine via roots having been treated with glyphosate and showed little to no rapid response were subsequently removed from the amino acid solution, roots washed, and placed into H_2O and sprayed a second time with glyphosate 48 hours later. Interestingly, these plants did show the expected rapid response to glyphosate (data not shown), indicating their inherent ability to display the rapid response to glyphosate under normal treatment conditions.

These results clearly indicate Phenylalanine and Tyrosine as having a role in the rapid response to glyphosate, but it is not clear whether this is directly due to the amino acids themselves or a downstream product or precursor to Phenylalanine and Tyrosine. A previous study reports similar findings regarding the synergistic effect of Phenylalanine and Tyrosine on the reversal of growth inhibition by glyphosate (Gresshoff, 1979). Experiments in bacterium, alga, plant cell cultures and whole plant roots found that Phenylalanine and Tyrosine always acted synergistically to reverse or prevent herbicide action, while other amino acids or aromatic precursors had no significant effect (Gresshoff, 1979). In plants and some animal cells, low levels of Phenylalanine and Tyrosine promote necrosis/cell death, while exogenous supply of these amino acids suppresses cell death (Fu *et al*., 2010). It is unknown if sucrose and these amino acids have opposing effects and it is possible that they are functioning through different mechanisms entirely. To test this, additional experiments need to be done to see if the sucrose induced cell death in the dark can be rescued by Phenylalanine and Tyrosine. A metabolome analysis in glyphosate-treated GR rapid giant ragweed in the presence and absence of Phenylalanine and Tyrosine should address this aspect.

Leaf Disc Assay for Hydrogen Peroxide Accumulation.

Previously, the earliest signs of tissue necrosis seen in the mature leaves of glyphosate-treated GR rapid response giant ragweed individuals were visually observed by 6 HAT (data not shown). By staining treated leaf discs with DAB, we were able to see the effects of glyphosate treatment much sooner than expected. Within 30 minutes after glyphosate treatment, hydrogen peroxide reactive oxygen species begin to accumulate in the mature tissues of GR rapid response giant ragweed (indicated by the dark brown particulates), but not in the younger meristematic tissue (Figure 2.12 A and B). These results support the rapid cell death observed in mature leaves of GR rapid response giant ragweed after glyphosate treatment as well as provide further insight into the physiological mechanism of the resistant rapid response.

Further experiments testing for presence of hydrogen peroxide in regards to the previously examined roles of sucrose and Phenylalanine and Tyrosine need to be done. Results from such experiments might provide clues about the relationship between effects of sucrose and these amino acids on cell death induced upon glyphosate treatment. The lack of Phenylalanine and Tyrosine may be impacting the phenylpropanoid pathway and production of flavonoids, since these amino acids serve as precursors for pathways that produce these. Some of these are known to function as antioxidants and protect cells from cell death due to excessive production of free radicals, such as H_2O_2 as seen in the GR rapid response to glyphosate. This hypothesis would support the mechanism of glyphosate inhibition of EPSPS in the GR rapid biotype, as well as suggest a rapid transcriptional response to this inhibition not seen in the GS biotype.

Implications.

Glyphosate resistance is a serious issue for growers in the Midwest U.S. and southern Ontario and these results report on the occurrence of glyphosate resistance in multiple giant ragweed accessions from this agriculturally important region. Reduced translocation of glyphosate has been reported in some biotypes, but does not clearly explain the level of resistance seen in GR giant ragweed (Green, 2014; Lespérance *et al*., 2016; Nandula *et al*., 2015). A recent review on the state of the knowledge on glyphosate resistance mechanisms observed very little data reporting the basis for resistance in GR giant ragweed and noted that the mechanism for resistance remains unclear (Sammons and Gaines, 2014). The research reported here will provide further insight into the glyphosate resistance mechanism(s) present in giant ragweed from a wide range of geographic locations.

The absence of a target-site mutation and target gene amplification indicate glyphosate resistance is due to another mechanism. A novel mechanism of resistance to glyphosate related to a rapid cell death response would open an exciting new area of research in plant abiotic interactions. It is possible that the rapid response to glyphosate is due to a combination of resistance mechanisms working together to produce higher resistance levels. It is common for species to accumulate multiple mechanisms of resistance, particularly in cross-pollinating species (Sammons and Gaines, 2014). The rapid onset of cell death after glyphosate treatment as seen by the formation of destructive hydrogen peroxide within 30 minutes, may act in coordination with an altered translocation mechanism present in the GR rapid response biotype.

The timing of the GR rapid response and onset of cell death along with the accumulation of shikimate and effect of added Phenylalanine and Tyrosine suggests at least some glyphosate is reaching its target enzyme in the chloroplasts, altering the shikimate pathway and stimulating the

immediate cell death response. From these results, we hypothesize that the inhibition caused by glyphosate is indirectly stimulating genes or transcriptional factors that lead to the regulation of a number of stress response and/or cell death related pathways in the GR rapid response biotype (Padmanabhan KR, 2016). Continued research will be able to use the results presented here to aid in the development of new hypothesis driven goals specific to the unique resistant rapid response.

2.4 TABLES

Table 2.1. Giant ragweed accessions at Colorado State University. Seed collection sites, locations and collaborators who provided the collected seed samples. Biotype based on phenotypic response to 0.84 kg·ae·ha^{-1} glyphosate.

Accession	Source	Collection Site	Biotype	Collaborator
1	Ontario, CAN	McGuire	GR slow response	Peter Sikkema
2	Ontario, CAN	Orton	GR slow response	Peter Sikkema
3	Ontario, CAN	Leamington	GR rapid response	Peter Sikkema
4	Ontario, CAN	South Windsor	GR rapid response	Peter Sikkema
5	Ontario, CAN	Ridgetown wood-lot	GS	Peter Sikkema
6	Ontario, CAN	Windsor airport	GR rapid response	Peter Sikkema
7	Ontario, CAN	Dover ditch-bank	GS	Peter Sikkema
8	Ontario, CAN	Belle River	GR rapid response	Peter Sikkema
9	Ontario, CAN	Dean Martin	GR slow response	Peter Sikkema
10	Ontario, CAN	Pelee Island	GR rapid response	Peter Sikkema
11	Wisconsin, USA	Rock County	GS	Dave Stoltenberg
12	Wisconsin, USA	Rock County	GR slow response	Dave Stoltenberg
13	Ohio, USA	Ohio	GS	Steve Weller
14	Ohio, USA	Ohio	GR slow response	Steve Weller
15	Ohio, USA	Ohio	GR rapid response	Steve Weller
16	Indiana, USA	Noble County	GR rapid response	Steve Weller
17	Ohio, USA	Dark County	GS	Steve Weller
18	Tennessee, USA	Tennessee	GR slow response	Larry Steckel
19	Missouri, USA	Missouri	GR slow response	Kevin Bradley
20	Kansas, USA	Topeka	GR slow response	Kassim Al-Khatib
21	Nebraska, USA	David City	GR slow response	Stevan Knezevic
22	Minnesota, USA	Olmsted County	GR rapid response	Fritz Breitenbach

Table 2.2. Dry shoot mass for accessions 3, 12 and 11 representing GR rapid, GR slow and GS biotypes, respectively, 28 d after treatment with glyphosate doses ranging up to 6.72 kg·ae·ha^{-1}, including a non-treated check. All treatments included 2% (w/v) ammonium sulfate. Standard errors are shown in parentheses. Dose-response is shown in Figure 2.1.

Biotype	Accession	Dose-response model parameter [a]			ED_{50} R:S	P value ED_{50} R:S [b]
		b	*d*	*e*		
		g dry shoot biomass plant^{-1} (as a % of mean control)			kg·ae·ha^{-1}	
GR rapid	3	1.31 (0.12) a[c]	100.21 (3.2) a	1.15 (0.1) a	4.19	0.0001
GR slow	12	1.26 (0.12) a	99.21 (3.3) a	0.91 (0.08) a	3.34	0.0001
GS	11	2.05 (0.29) a	100.53 (3.51) a	0.27 (0.01) b		

[a] *b* = relative slope around *e*; *c* = lower asymptote; *d* = upper asymptote; *e* = ED_{50}, effective dose of glyphosate that decreased biomass accumulation by 50% relative to non-treated plants.
[b] P-value determined by a Student's t-test.
[c] Estimates followed by the same letter within a column do not differ at the 5% level of significance as determined by 95% confidence intervals.

Table 2.3. Dry shoot mass for accessions 15, 2 and 5 representing GR rapid, GR slow and GS biotypes, respectively, 28 d after treatment with glyphosate doses ranging up to 6.72 kg·ae·ha^{-1}, including a non-treated check. All treatments included 2% (w/v) ammonium sulfate. Standard errors are shown in parentheses. Dose-response is shown in Figure 2.3.

Biotype	Accession	Dose-response model parameter [a]			ED_{50} R:S	P value ED_{50} R:S [b]
		b	*d*	*e*		
		g dry shoot biomass plant^{-1} (as a % of mean control)			kg·ae·ha^{-1}	
GR rapid	15	1.36 (0.13) a[c]	100.41 (0.14) a	0.82 (0.07) a	2.34	0.0001
GR slow	2	1.40 (0.14) a	101.66 (3.29) a	1.25 (0.11) a	3.56	0.0001
GS	5	1.73 (0.22) a	101.31 (3.73) a	0.35 (0.02) b		

[a] *b* = relative slope around *e*; *c* = lower asymptote; *d* = upper asymptote; *e* = ED_{50}, effective dose of glyphosate that decreased biomass accumulation by 50% relative to non-treated plants.
[b] P-value determined by a Student's t-test.
[c] Estimates followed by the same letter within a column do not differ at the 5% level of significance as determined by 95% confidence intervals.

Table 2.4. Shikimate concentration in leaf tissue averaged across biotype of GR rapid, GR slow and GS giant ragweed accessions 1-15, 17 and 18 after treatment with glyphosate concentrations ranging from 0 to 2,000 µM. Standard errors are shown in parentheses. Dose response is shown in Figure 2.6.

Biotype	Accessions	Dose-response model parameter [a]			EC_{50} R:S	P value EC_{50} R:S [b]
		b	*d*	*e*		
		—— µg shikimate mL^{-1} ——		µM glyphosate		
GR rapid	3, 4, 6, 8, 10, 15	-6.39 (0.73) a[c]	69.56 (1.2) a	631.25 (19.06) a	4.09	0.0001
GR slow	1, 2, 9, 12, 14, 18	-7.49 (1.63) a	70.34 (1.18) a	600.12 (25.32) a	3.89	0.0001
GS	5, 7, 11, 13, 17	-2.17 (0.13) a	72.62 (0.96) a	154.16 (5.27) b		

[a] *b* = relative slope around *e*; *c* = lower asymptote; *d* = upper asymptote; *e* = ED_{50}, effective concentration of glyphosate that increased shikimate accumulation by 50% relative to non-treated plant tissue.
[b] P-value determined by a Student's t-test.
[c] Estimates followed by the same letter within a column do not differ at the 5% level of significance as determined by 95% confidence intervals.

Table 2.5. Multiple sequence alignment of *EPSPS* active site from GR rapid, GR slow and GS giant ragweed accessions aligned to *Amaranthus palmeri EPSPS*. Second row: EPSPS protein coding sequence. Third row: *EPSPS* reference sequence from *Amaranthus palmeri* (AMAPA), to which all *Ambrosia trifida* (AMBTR) sequences were aligned. Fourth row: *EPSPS* sequence from giant ragweed RNA-seq reference (REF) transcriptome generated from accession 3. Subsequent rows: *EPSPS* sequence from 18 giant ragweed individuals generated from gDNA amplified by PCR and sequenced by Sanger sequencing. Primer sequences used were AtF1- 5' ACATGCTTGGGGCTCTAAGAA 3' and AtR1- 5' TTGAATTACCACCAGCAGCGGT 3' (Nandula *et al*., 2015).

Source	Accession	EPSPS Target Site Sequence					
		G	T	A	M	R	P
AMAPA		GGA	ACA	GCG	ATG	CGC	CCA
AMBTR_REF	3	GGA	ACT	GCT	ATG	CGC	CCT
AMBTR	1	GGA	ACT	GCT	ATG	CGC	CCT
AMBTR	2	GGA	ACT	GCT	ATG	CGC	CCT
AMBTR	3	GGA	ACT	GCT	ATG	CGC	CCT
AMBTR	4	GGA	ACT	GCT	ATG	CGC	CCT
AMBTR	5	GGA	ACT	GCT	ATG	CGC	CCT
AMBTR	6	GGA	ACT	GCT	ATG	CGC	CCT
AMBTR	7	GGA	ACT	GCT	ATG	CGC	CCT
AMBTR	8	GGA	ACT	GCT	ATG	CGC	CCT
AMBTR	9	GGA	ACT	GCT	ATG	CGC	CCT
AMBTR	10	GGA	ACT	GCT	ATG	CGC	CCT
AMBTR	11	GGA	ACT	GCT	ATG	CGC	CCT
AMBTR	12	GGA	ACT	GCT	ATG	CGC	CCT
AMBTR	13	GGA	ACT	GCT	ATG	CGC	CCT
AMBTR	14	GGA	ACT	GCT	ATG	CGC	CCT
AMBTR	15	GGA	ACT	GCT	ATG	CGC	CCT
AMBTR	17	GGA	ACT	GCT	ATG	CGC	CCT
AMBTR	18	GGA	ACT	GCT	ATG	CGC	CCT
AMBTR	19	GGA	ACT	GCT	ATG	CGC	CCT

Table 2.6. Effect of light and dark environment with or without exogenous sucrose via roots on the resistant rapid response. GR rapid and GS giant ragweed accessions 15 and 11, respectively, were subjected to either a light or dark environment with washed roots placed into either H_2O or 2% sucrose, before treatment with glyphosate at doses of 0.0 and 0.84 kg·ae·ha^{-1}. All treatments included 2% (w/v) ammonium sulfate. Glyphosate-untreated and GS treatment groups data not shown. Standard errors of the mean are shown in parentheses. Percent necrosis is shown in Figure 2.8. Treatment groups are assigned the following letters: (A) GR rapid in H_2O and light, (B) GR rapid in sucrose and light, (C) GR rapid in H_2O and dark, (D) GR rapid in sucrose and dark.

Group-Group Comparison	Mean Difference	P value [a]
A-B	< 0.0001 (5.75)	>0.9999 a [c]
A-C	84.67 (5.75)	< 0.0001 b
A-D	13 (5.75)	0.28 a
B-C	84.67 (5.75)	< 0.0001 b
B-D	13 (5.75)	0.28 a
C-D	-71.67 (5.75)	< 0.0001 b

[a] P-value determined by a Tukey multiple comparisons of means test.
[c] Estimates followed by the same letter within a column do not differ at the 5% level of significance as determined by 95% confidence intervals.

2.5 FIGURES

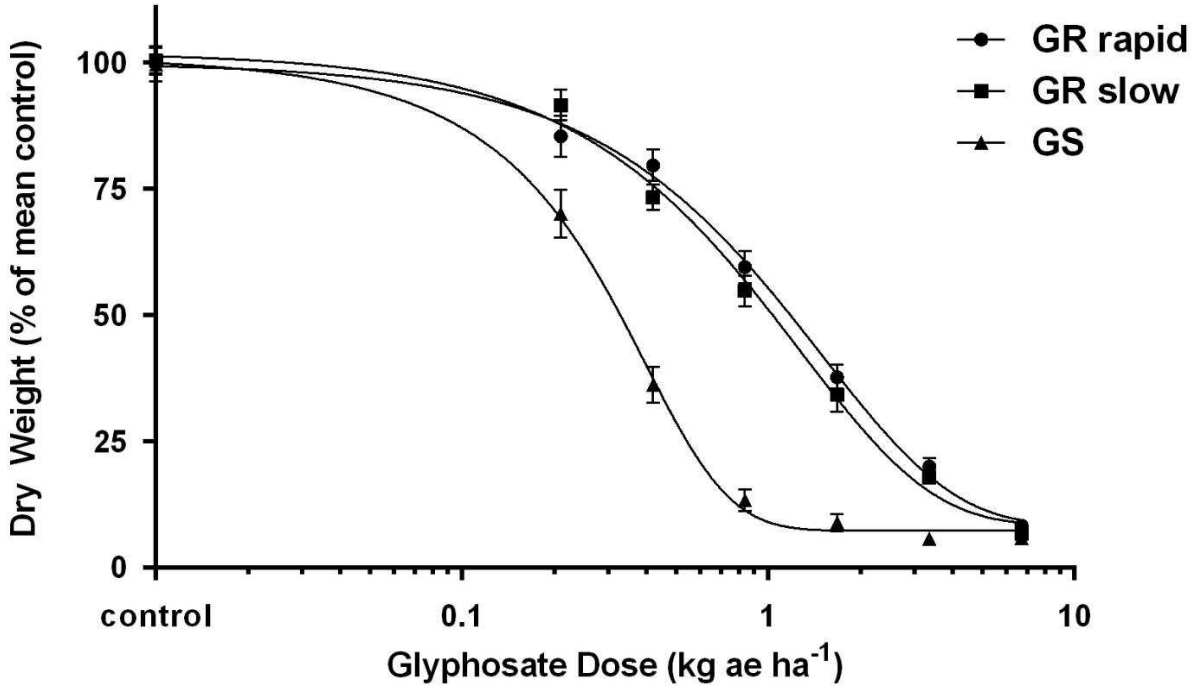

Figure 2.1. Effect of glyphosate on the above ground dry biomass at 28 DAT of giant ragweed accessions 3, 12 and 11, representing biotypes GR rapid, GR slow and GS, respectively. Dry weights are presented as a percentage of the untreated control. Each point represents the average of six technical replicates. Vertical error bars represent standard error of the mean. Dose response curves were generated by non-linear regression using a log-logistic model with the following equations: $Y = 100.21/ 1+ \exp[1.31(\log(x) – \log(1.15))]$ and $Y = 99.21/ 1+ \exp[1.26(\log(x) – \log(0.91))]$ and $Y = 100.53/ 1+ \exp[2.05(\log(x) – \log(0.27))]$ for accessions 3, 12 and 11, respectively; where Y is the dry weight (% of mean control) and x is the glyphosate dose. Dose response model parameter values are shown in Table 2.2.

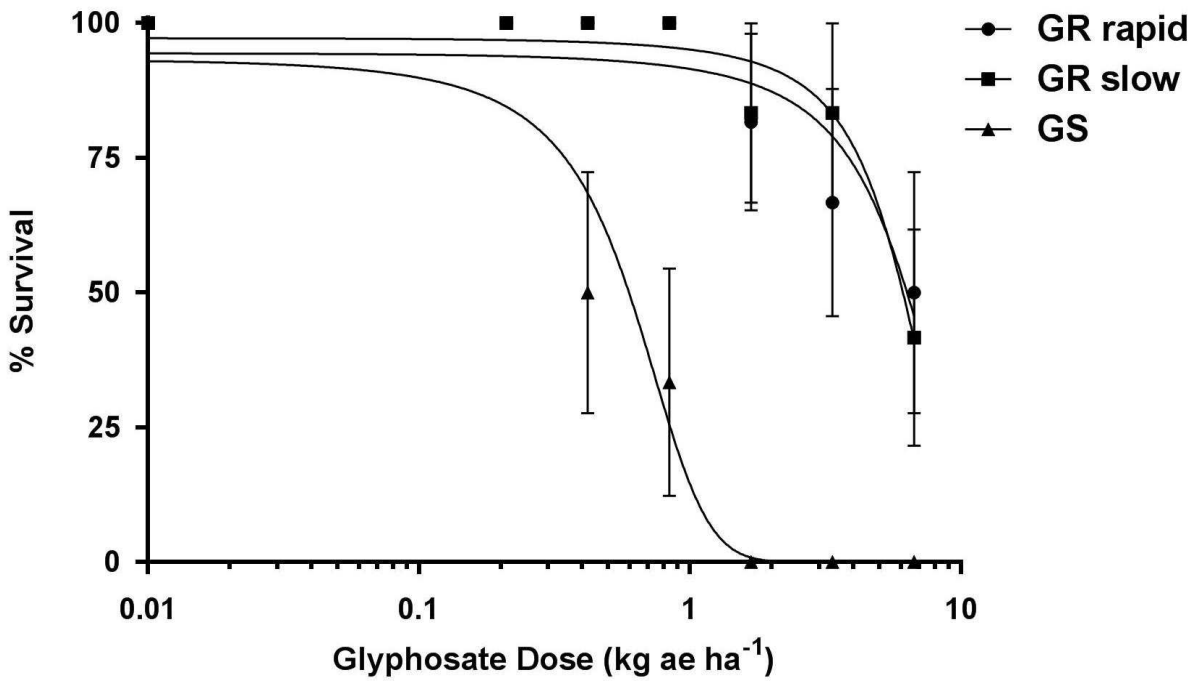

Figure 2.2. Effect of glyphosate on the survival of giant ragweed accessions 3, 12 and 11, representing biotypes GR rapid, GR slow and GS, respectively. Each point represents the average of six technical replicates. Vertical error bars represent standard error of the mean. Dose response curves were generated by non-linear regression using a log-logistic model with the following equations: $Y = 102.35/ 1+ \exp[1.26(\log(x) – \log(6.07))]$ and $Y = 98.9/ 1+ \exp[2.22(\log(x) – \log(6.02))]$ and $Y = 104.19/ 1+ \exp[2.26(\log(x) – \log(0.48))]$ for accessions 3, 12 and 11, respectively; where Y is the survival and x is the glyphosate dose. Both GR biotypes showed 100% survival at glyphosate doses of 0.84 kg·ae·ha^{-1} and below.

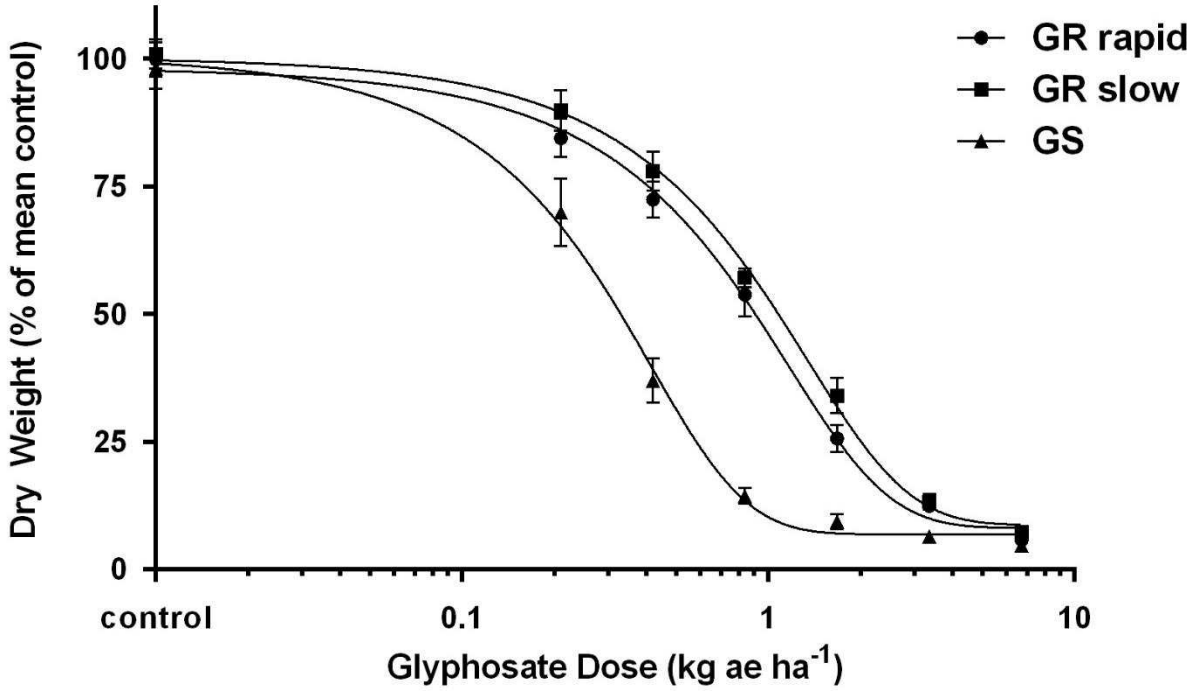

Figure 2.3. Effect of glyphosate on the above ground dry biomass at 28 DAT of giant ragweed accessions 15, 2 and 5, representing biotypes GR rapid, GR slow and GS, respectively. Dry weights are presented as a percentage of the untreated control. Each point represents the average of six technical replicates. Vertical error bars represent standard error of the mean. Dose response curves were generated by non-linear regression using a log-logistic model with the following equations: $Y = 100.41/ 1+ \exp[1.36(\log(x) – \log(0.82))]$ and $Y = 101.66/ 1+ \exp[1.4(\log(x) – \log(1.25))]$ and $Y = 101.31/ 1+ \exp[1.73(\log(x) – \log(0.35))]$ for accessions 15, 2 and 5, respectively; where Y is the dry weight (% of mean control) and x is the glyphosate dose. Dose response model parameter values are shown in Table 2.3.

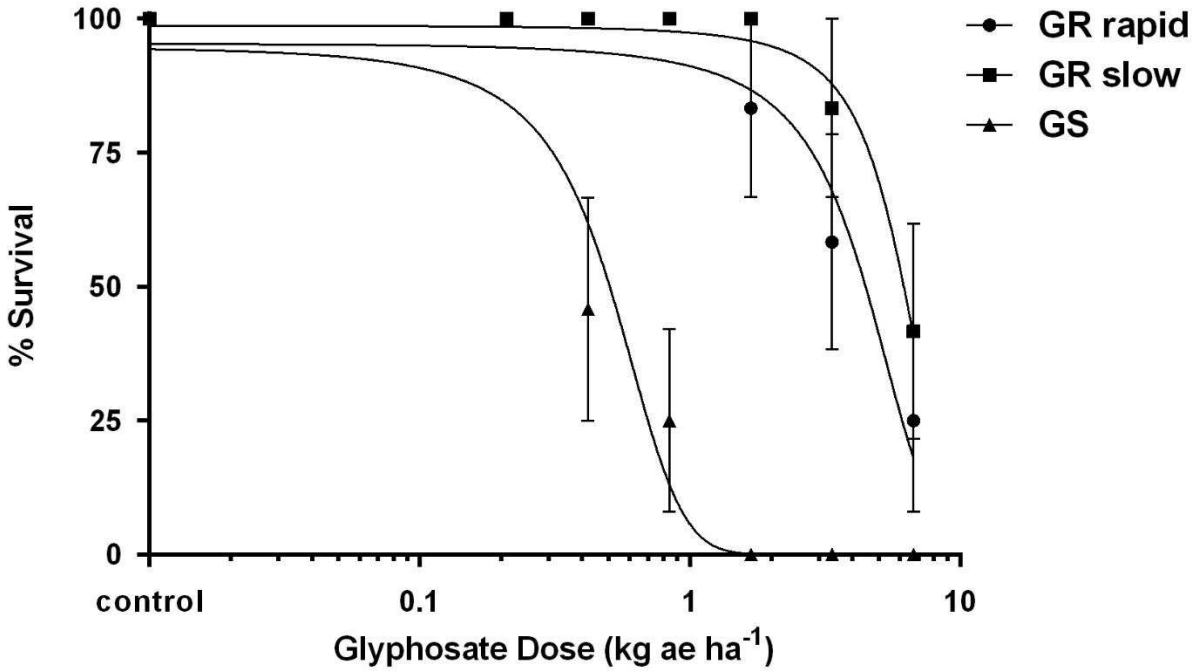

Figure 2.4. Effect of glyphosate on the survival of giant ragweed accessions 15, 2 and 5, representing biotypes GR rapid, GR slow and GS, respectively. Each point represents the average of six technical replicates. Vertical error bars represent standard error of the mean. Dose response curves were generated by non-linear regression using a log-logistic model with the following equations: $Y = 101.05/ 1+ \exp[2.02(\log(x) – \log(3.87))]$ and $Y = 100.47/ 1+ \exp[2.87(\log(x) – \log(5.94))]$ and $Y = 103.55/ 1+ \exp[4.43(\log(x) – \log(0.36))]$ for accessions 15, 2 and 5, respectively; where Y is the survival and x is the glyphosate dose. Both GR biotypes showed 100% survival at glyphosate doses of 0.84 kg· ae· ha^{-1} and below.

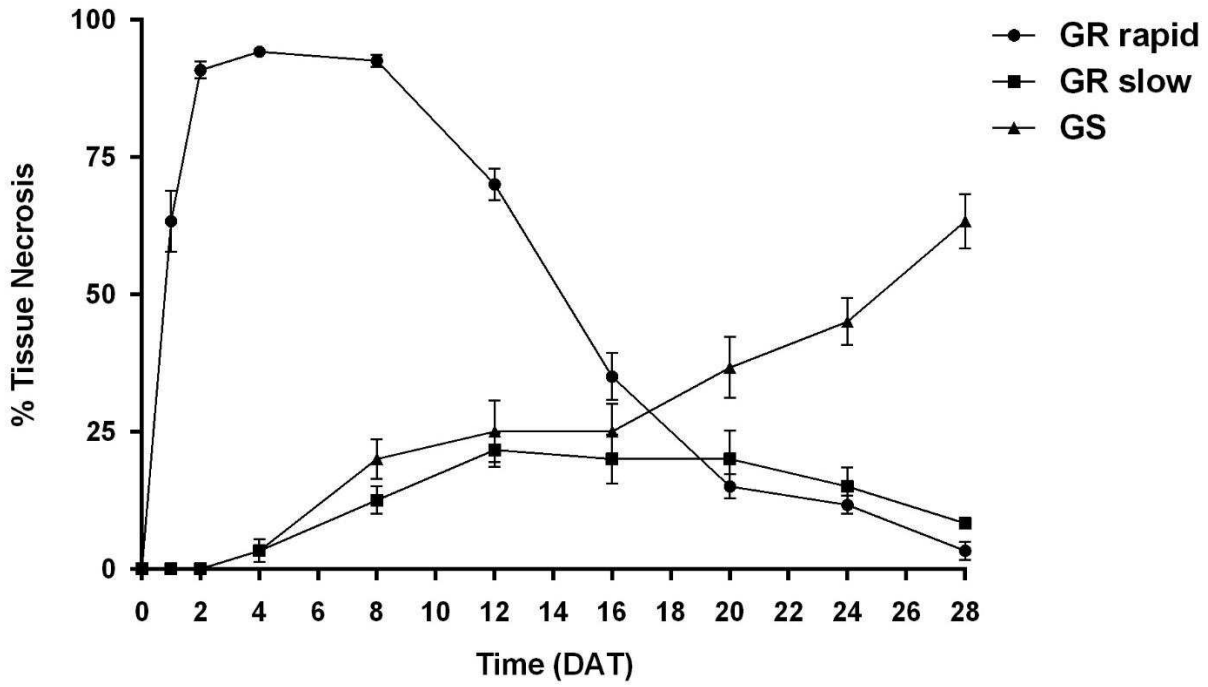

Figure 2.5. Visual rating of percent tissue necrosis after glyphosate treatment over time of GR rapid, GR slow and GS giant ragweed. Vertical bars represent standard error of the mean. Data were pooled from two repeat experiments for graphical analysis, where n = 12 for each biotype.

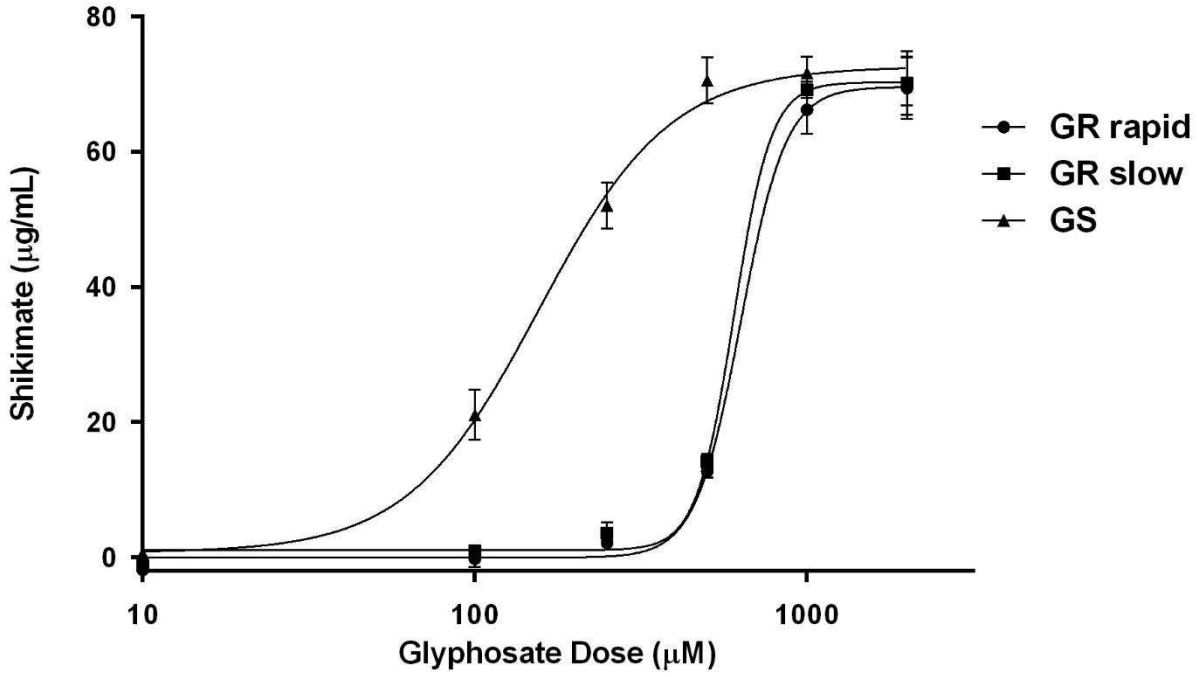

Figure 2.6. Effect of glyphosate dose on shikimate accumulation of GR rapid, GR slow and GS giant ragweed accessions at glyphosate concentrations ranging from 0 to 2000 µM after 16 h incubation under continuous light. Shikimate accumulation data were averaged across biotypes to be reported as GR rapid response (n = 6), GR slow response (n = 7) and GS (n = 5). Vertical bars represent standard error of the mean. Data were pooled from two repeat experiments for analysis, where n = 9 for each accession. Dose response model parameter values are shown in Table 2.4.

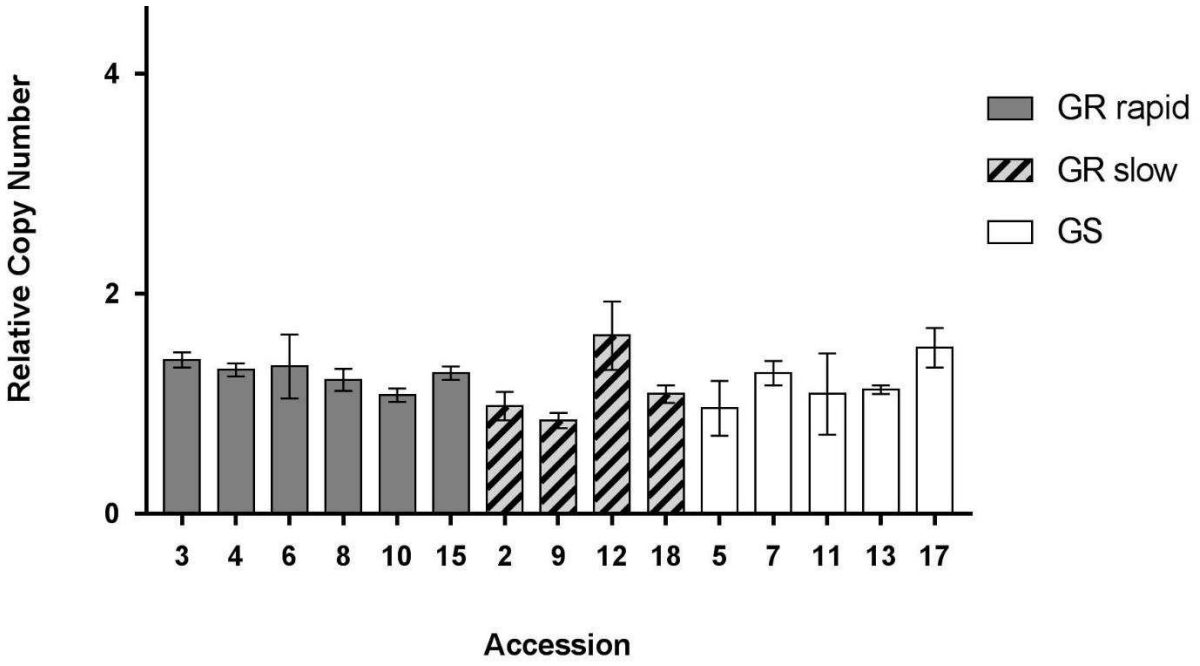

Figure 2.7. All *EPSPS* copy number estimates were obtained by quantitative polymerase chain reaction (qPCR), measured against a low-copy internal reference gene (isocitrate dehydrogenase, *IDH*), at a copy of one. Vertical bars represent standard error of the mean. Relative copy number data from one individual and six technical replicates were averaged from each accession.

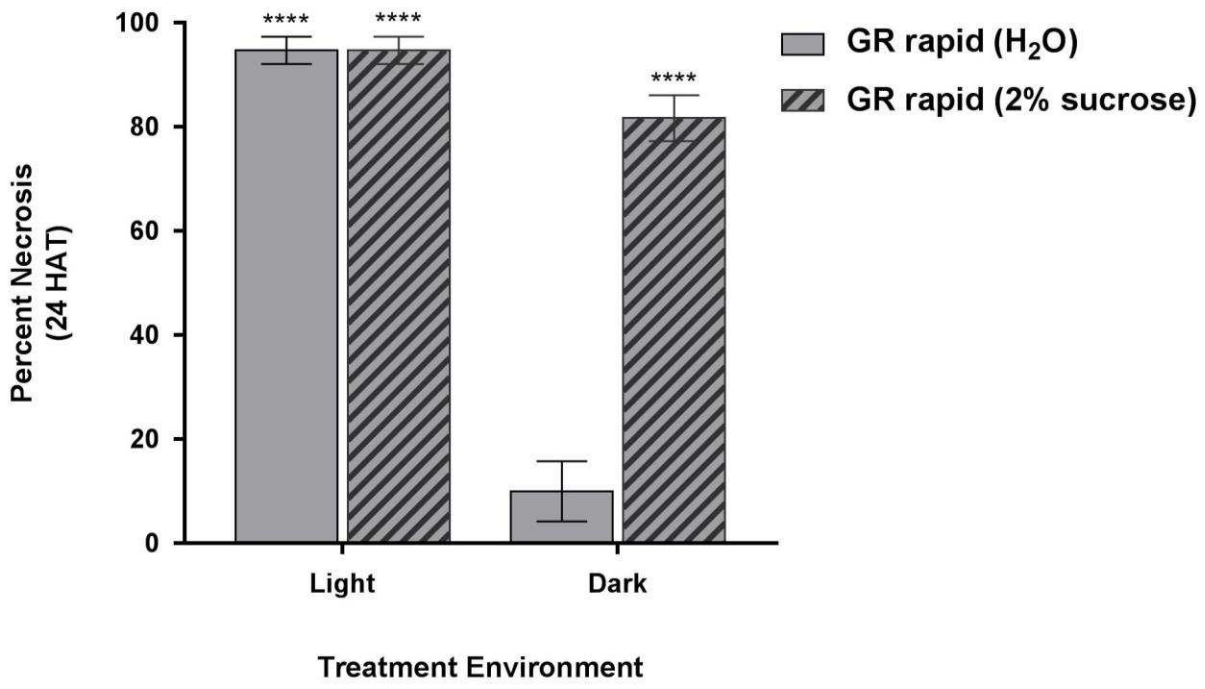

Figure 2.8. Percent tissue necrosis at 24 HAT. GR rapid and GS plant roots were washed and placed in water or 2% sucrose prior to glyphosate treatment. Plants were also subjected to light or dark environments after glyphosate foliar application at 0.84 kg·ae·ha^{-1}. Only GR rapid response treatment groups are represented in this graph as all other treatment groups showed zero tissue necrosis and were not statistically different from one another. Vertical bars represent standard error of the mean. Significance code of '****' represents a P value of ≤ 0.0001. Significance represents comparison to untreated controls of each treatment group (not shown). Data were pooled from repeat experiments (n = 3).

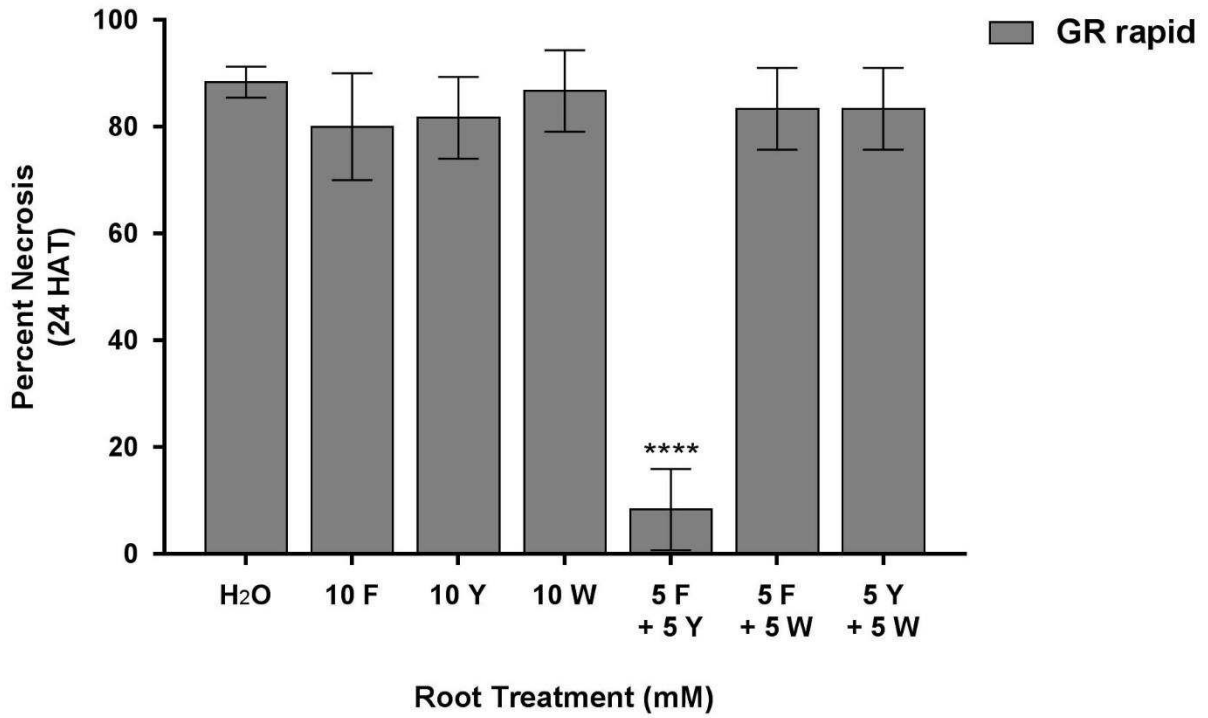

Figure 2.9. Percent tissue necrosis at 24 HAT. GR rapid and GS plant roots were washed and placed into solutions containing different combinations of Phenylalanine (F), Tyrosine (Y) or Tryptophan (W). Only the GR rapid biotype data was graphed due to a lack of necrosis in GS. Vertical bars represent standard error of the mean. Significance code of '****' represents a P value of ≤ 0.0001. Significance represents comparison to the untreated control (H_2O). Data were pooled from repeat experiments for analysis (n = 3).

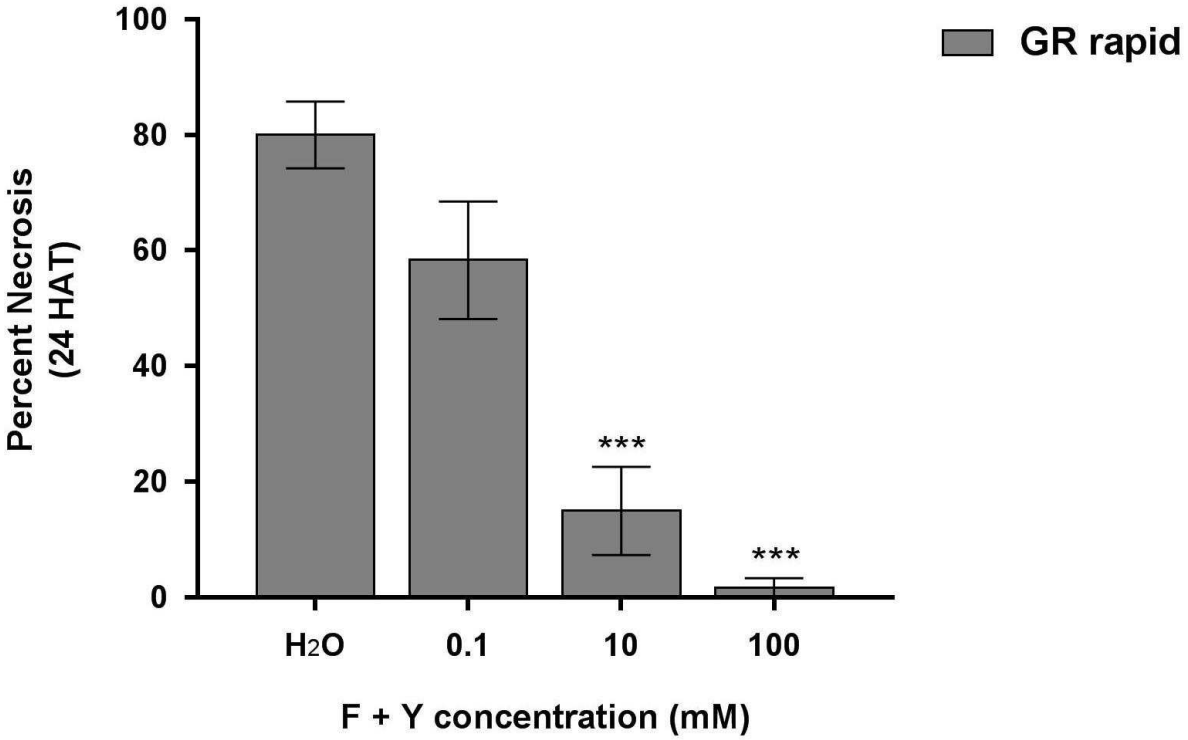

Figure 2.10. Percent tissue necrosis at 24 HAT. GR rapid response plant roots were washed and placed into solutions containing different concentrations of Phenylalanine (F) + Tyrosine (Y). Vertical bars represent standard error of the mean. Significance code of '***' represents a P value of ≤ 0.001. Significance represents comparison to the untreated control (H_2O). Data were pooled from repeat experiments for analysis (n = 3).

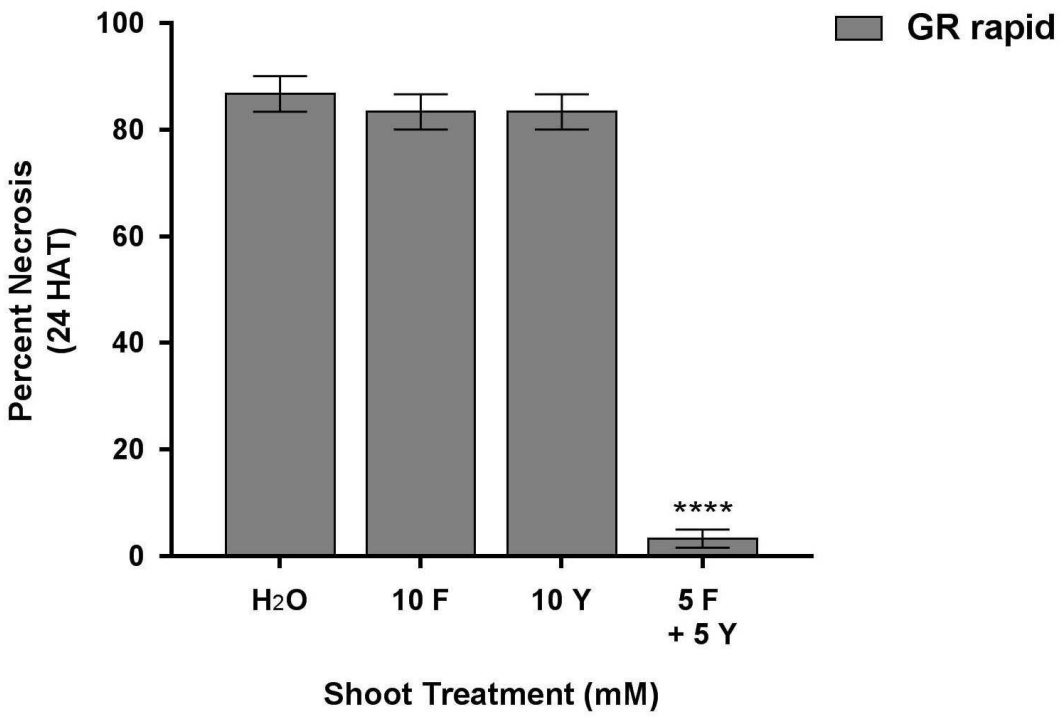

Figure 2.11. Percent tissue necrosis at 24 HAT. GR rapid response plant shoots were cut and placed into solutions containing Phenylalanine (F), Tyrosine (Y), or both F and Y. Significance code of '****' represents a P value of ≤ 0.0001. Significance represents comparison to the untreated control (H_2O). Vertical bars represent standard error of the mean. Data were pooled from repeat experiments for analysis (n = 3).

A.

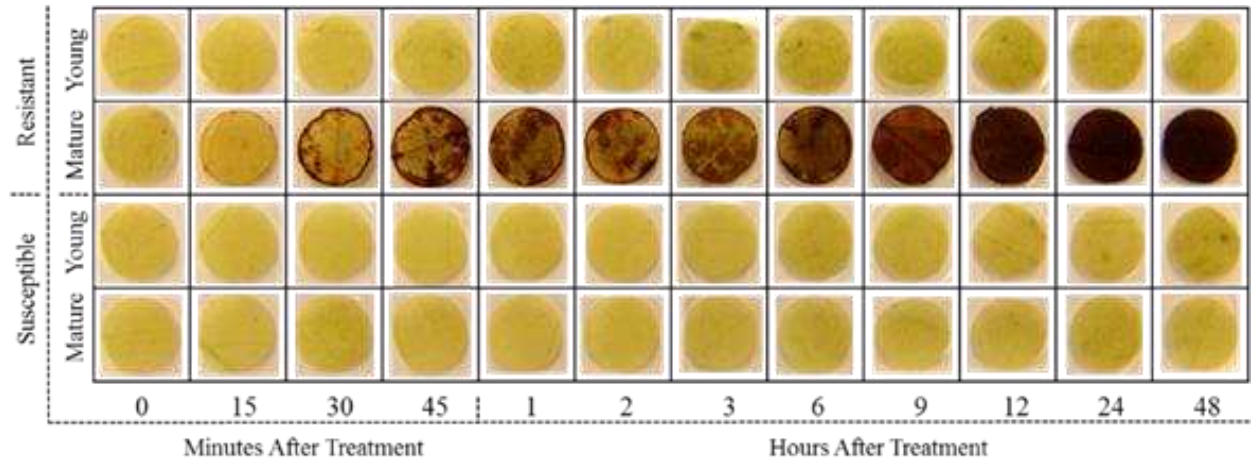

B.

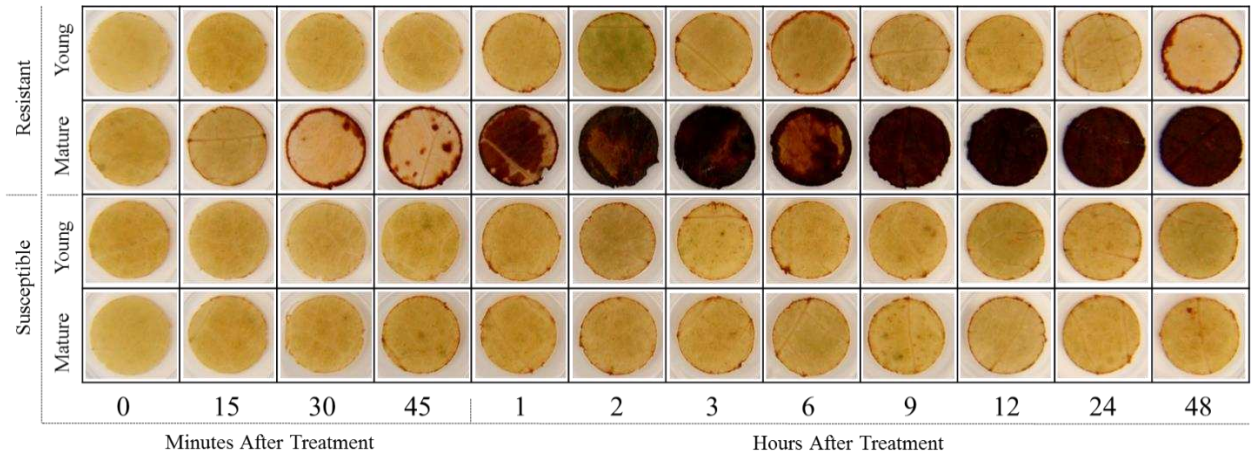

Figure 2.12. A and B represent repeated experiments in time. DAB stained leaf discs for H_2O_2 accumulation after glyphosate treatment. Left column: Leaf discs taken from untreated individuals. Sequential columns to the right: Leaf discs taken at time points from treated individuals ranging from 15 minutes after treatment to 48 hours after treatment. Top two rows: Leaf discs taken from young tissue (top) and mature tissue (bottom) of a single GR rapid response individual. Bottom two rows: Leaf discs taken from young tissue (top) and mature tissue (bottom) of a single GS individual.

CHAPTER 3. TRANSCRIPTOMIC ANALYSIS OF THE GLYPHOSATE-RESISTANT RAPID RESPONSE IN GIANT RAGWEED

3.1 INTRODUCTION

Modern cropping systems rely heavily on chemical control of weeds to protect crop yields, especially with the increasing adoption of genetically engineered crops to be herbicide-resistant (Duke and Powles, 2008; Leslie and Baucom, 2014; Powles, 2008). Glyphosate is a non-selective, broad spectrum herbicide that provides effective control over a range of weeds and has become the most widely used herbicide around the world (Baylis, 2000; Dill, 2005; Duke and Powles, 2008; Powles and Preston, 2006). The widespread adoption of transgenic, glyphosate-resistant (GR) crops has resulted in an increased reliance on this single herbicide in modern-day agriculture (Powles, 2008; Shaner, 2000). There are currently 35 weed species that have evolved resistance to glyphosate and failure to control weeds caused by herbicide resistance is a significant and increasing problem worldwide (Gaines *et al*., 2014; Heap, 2014; Powles, 2008).

Glyphosate resistance mechanisms identified in other weed species include target site mutations (Powles and Preston, 2006; Wakelin and Preston, 2006), target gene amplification (Gaines *et al*., 2010), and altered translocation possibly due to vacuolar sequestration (Feng *et al*., 2004; Ge *et al*., 2010; Shaner, 2009; Wakelin *et al*., 2004). The mechanism of resistance in giant ragweed is unknown. Two giant ragweed studies have shown less glyphosate translocating out of the treated leaf in a resistant population compared to a susceptible population (Green, 2014; Robertson, 2010). This result was seen in the GR rapid response biotype, where a resistant individual will exhibit a unique phenotype involving the rapid tissue death of all mature leaves, while young meristematic tissue is

unaffected and the plant survives through continued growth from these tissues (Robertson, 2010). A recent microscopy study has compared the cellular reorganization in mature tissue after glyphosate treatment to an autophagy-like programmed cell death (PCD) (Lespérance *et al*., 2016). Autophagy can serve both a pro-death and a pro-survival role during plant response to stress and this determination is age dependent as demonstrated by *Arabidopsis* autophagy-defective (*atg*) mutants showing the spreading of hypersensitive-response PCD only in the older leaves of older plants, while younger leaves show increased resistance (Liu and Bassham, 2012). Accumulation of H_2O_2 in the mature leaf tissue of GR individuals was seen as early as 30 minutes after glyphosate treatment, while no H_2O_2 was found to accumulate in the young tissues of GR treated individuals within 48 hours after treatment (Van Horn and Westra, 2015). Hydrogen peroxide levels are known to increase in response to various biotic and abiotic stresses, which may lead to oxidative damage to cells and/or function as a signal during a stress response triggering programmed cell death (Bueso *et al*., 2007). The regulation of stress responses in plants is highly complex and controlled by many different genes and signaling molecules, many of which are unknown (Zurbriggen *et al*., 2010). The data and results to come from this project have the potential to provide further insight to plant responses to stress and may elucidate a novel mechanism leading to a type of programmed cell death.

Giant ragweed is a non-model species with little to no genomic resources available for genetic characterization of glyphosate resistance or the unique rapid response phenotype. Next-generation sequencing technologies have become more robust in recent years and have been adapted for use in non-model species such as weeds (Gaines *et al*., 2014; Leslie and Baucom, 2014). Different platforms of the Illumina technologies can be used to obtain a reference transcriptome through a *de novo* assembly when no previous transcriptome data are available, as well as conduct transcript quantification and detection of lower abundance transcripts in an approach known as RNA-Seq (Gaines *et al*., 2014; Lister *et al*., 2009). Other studies have implemented

RNA-Seq to identify differentially expressed genes in model and non-model plants during developmental processes as well as plant responses to herbicides and weed stress (Gaines *et al*., 2014; Gao *et al*., 2013; Horvath *et al*., 2015; Leslie and Baucom, 2014; Liu *et al*., 2013; O'Rourke *et al*., 2013). A recent study has created a first preliminary reference transcriptome for giant ragweed accompanied by a single-replicate RNA-Seq experiment showing a difference in gene expression patterns between glyphosate-resistant (GR) and -susceptible (GS) individuals (Padmanabhan *et al*., 2016).

Here, we present a second fully annotated reference transcriptome and use this reference to identify and validate differential expression of specific genes between biological replicates of GR and GS giant ragweed under normal, untreated, conditions and at three early time points after glyphosate application. An additional forward genetics validation experiment is conducted on a segregating population for the glyphosate resistance trait using two candidate contigs identified through RNA-Seq. Our RNA-Seq experiment also examines differences between young and mature tissues to address the rapid response phenotype only observed in mature tissues of the GR rapid biotype, with the hypothesis that inhibition of the shikimate pathway caused by glyphosate is rapidly triggering a transcriptionally regulated cascade of events leading to H_2O_2-induced PCD and a resulting upregulation of stress response pathways (Bright *et al*., 2006; Bueso *et al*., 2007; Padmanabhan *et al*., 2016). It is important to note that the RNA-Seq experiment was used to generate hypotheses for candidate genes with rational biological functions in resistance and the rapid response to glyphosate. Results from RNA-Seq do not necessarily indicate a causal relationship between candidate genes and resistance. These hypotheses were tested using a forward genetics approach and will undergo additional functional validation pending successful qRT-PCR validation. This research contributes to the long-term goals to both expand genomic

resources for giant ragweed and elucidate the genetic basis of resistance and the rapid response to glyphosate in this species.

3.2 MATERIALS AND METHODS

Generation of the reference A. trifida transcriptome

To generate the *Ambrosia trifida* (L.) reference transcriptome, a cDNA library was constructed using RNA extracted from tissue collected from a single GR rapid response individual grown from seed in ambient greenhouse conditions at the Colorado State University Weed Research facility located in Fort Collins, CO. This individual came from an accession that went through two generations of inbreeding by single-seed descent from a line originally collected from an agricultural field located in Leamington, Ontario. Seeds collected from field sites were stored at 10 °C until conditioning for experiments. For conditioning, seeds were planted in moist commercial potting media (Fafard Custom Mix, Sun Gro Horticulture, 770 Silver Street, Agawam, MA 01001) in plastic Magenta® boxes where they would undergo cold stratification for 4-8 weeks to break dormancy. Once germinated, seedlings were transplanted to 2 L pots containing the potting mix. Plants were fertilized once with 30 g 14-14-14 (N, P_2O_5, and K_2O) Osmocote® at the time of transplantation and grown in a greenhouse (25/20 °C day/night, 14-h photoperiod). Plants were in-bred through self-pollination for two generations. Plants for seed production were grown to maturity and individually bagged, using micro-perforated bags, once male flower development was observed. Pollination bags were 12 x 34 inches with a pore size of 0.75 millimeters. Self-pollinated individuals would produce seed that was collected and stored dry at 10 °C until needed for experiments.

Plant material used to generate the reference transcriptome was collected from various developmental stages including, cotyledons, meristematic tissue from the first true leaves, mature leaf tissue from the second node of fully expanded leaves, and from individuals at heights of 10 to 15 cm, meristematic and mature leaf tissue immediately prior to glyphosate treatment as well as at the following time points after glyphosate treatment, 15, 60, and 180 minutes after treatment (MAT). Individuals were sprayed with glyphosate at 0.84 $kg \cdot ae \cdot ha^{-1}$ using a commercial chamber track sprayer equipped with an 8002EVS single even flat-fan nozzle (TeeJet, Spraying Systems Co., Wheaton, IL) calibrated to deliver 187 $L \cdot ha^{-1}$ spray solution at the level of the plant canopy. Collected tissue was flash frozen with liquid nitrogen and stored at -80 °C. All tissue was pooled and ground in liquid nitrogen with mortar and pestle. Less than 100 mg of tissue was used for RNA isolation.

Total RNA was extracted using the QIAGEN® RNeasy plant mini kit, following the supplied protocol. Quality control was assessed using a NanoDrop (ND-1000 Spectrophotometer; ThermoScientific, Waltham, MA, USA) for quantification and assurance of minimal carbohydrate and protein contamination, and then on a bioanalyzer (Agilent 2100 Bioanalyzer; Agilent Technologies, Santa Clara, CA, USA) using the RNA setting for size determination and assessment of integrity. Five µg of DNase I-treated total RNA from the reference transcriptome sample was sent to LGC Genomics GmbH, Berlin, Germany. The cDNA library construction, sequencing and transcriptome assembly steps were performed at LGC genomics.

One µg of total RNA was used to purify mRNA on Oligo dT coupled to paramagnetic beads (NEBNext Poly(A) mRNA Magnetic Isolation Module). Purified mRNA was fragmented and eluted from the beads in one step by incubation in 2 x first strand buffer at 94 °C for only 7

min (not 15 min), followed by first strand cDNA synthesis using random primed reverse transcription (NEBNext RNA First Strand Synthesis Module), followed by random primed second strand synthesis using an enzyme mixture of DNA PolI, RnaseH and *E. coli* DNA Ligase (NEBNext Second Strand Synthesis Module). cDNA was purified and concentrated on MinElute Columns (Qiagen) and used to construct an Illumina library using the Ovation Rapid DR Multiplex System 1-96 (NuGEN).

The library was amplified in 5 x 20 µl (parallel) PCR reactions using MyTaq (Bioline) and standard Illumina TrueSeq amplification primers. Cycle number was limited to 10 Cycles. PCR primer and small fragments were removed by Agencourt XP bead purification using 0.6 volume of beads. The PCR enzyme was removed by an additional purification on Qiagen MinElute Columns. The Library was eluted in a final volume of 20 µl water. Normalization was done using Trimmer Kit (Evrogen). 1 µg cDNA library in 12 µl water was mixed with 4 µl 4x hybridization buffer, denatured for 3 min at 98 °C and incubated for 5 hours at 68 °C to allow re-association of DNA fragments. 15 µl of 2x DSN master buffer was added and the samples were incubated for 10 min at 68 °C. One Unit of DSN enzyme (1 U/µl) was added and the reaction was incubated for another 30 min. Reaction was terminated by the addition of 20 µl DSN Stop Solution, purified on a Qiagen MinElute Column and eluted in 10 µl Tris Buffer (5 mM Tris/HCl pH:9). The normalized library was re-amplified in 5 x 20 µl (parallel) PCR reactions using MyTaq (Bioline) and standard Illumina TrueSeq amplification primers. Cycle number was limited to 18 Cycles. The normalized library was finally size selected on a LMP-Agarose gel, removing fragments smaller than 350 bp and those larger than 600 bp.

Sequencing was done on a MiSeq using Illumina V3 Chemistry (2 x 300 bp) reads on one multiplexed lane with twenty other unknown samples. The data analysis completed at LGC

Genomics includes demultiplexing of all samples using Illumina's CASAVA data analysis software, clipping of Illumina TruSeq™ adapters in all reads, filtering rRNA sequences using RiobPicker 0.4.3, clipping of sequence adapters and quality trimming of all reads, combining forward and reverse reads using FLASh 1.2.4, *de novo* assembly with Newbler v 2.8, ORF identification with TransDecoder, and finally creation of FastQC reports for all FASTQ files.

Functional annotation of the reference transcriptome

Open reading frames (ORFs) for the *de novo* assembled transcripts were predicted using TransDecoder (https://transdecoder.github.io). Standard settings were used, and any peptides smaller than 100 amino acids were excluded in the final predicted protein list. Gene function was prescribed based on homology with known proteins from curated databases and by predicting protein domains with Hidden Markov Models (HMM). BlastP was used to align the predicted peptides from TransDecoder against both the uniprot/swissprot and TAIR10 protein data bases (accessed on 07/30/2015) (Dimmer *et al*., 2012). BlastP was run using default criteria for both queried databases (cutoff value $e \leq 1x\ 10^{-10}$). Additionally, only the top hit was taken and used for prescribing gene function for each search. Protein domains were predicted using the Pfam and hmmer3 programs with standard settings (Haas *et al*., 2013). Both BlastP searches and protein domains were taken into consideration for predicting transcript function.

Plant material, tissue collection and sample preparation for RNA-seq

Plant material used for RNA-seq were generated as described above, such that the GR rapid response individuals are siblings to the individual used to generate the reference transcriptome. The GS individuals were generated from a known GS accession originally

collected from a wood-lot in Ridgetown, Ontario. From individuals at heights of 10 to 15 cm, tissue samples were collected from three GR rapid response and three GS individuals immediately prior to glyphosate treatment and at the following time points after glyphosate treatment, 15, 60, and 180 MAT. Glyphosate treatment was the same as described above. Both young meristematic tissue and mature leaf tissue samples were collected from each individual at each time point. The two biotypes, three biological replicates, two tissue types, and four treatment time points including untreated represent a total of 48 samples collected for the RNA-seq experiment (Figure 3.3). Collected tissue was flash frozen with liquid nitrogen and stored at -80 °C. Tissue samples were ground separately in liquid nitrogen with mortar and pestle. Less than 100 mg of tissue was used for RNA isolation.

Total RNA was extracted from experimental individuals using the QIAGEN® RNeasy plant mini kit, following the supplied protocol. RNA quality and concentration was measured on a NanoDrop UV spectrophotometer and an RNA Nano chip on an Agilent Bioanalyzer 2100. All samples had a RNA Integrity Number (RIN) score of ≥6. DNase 1 treated total RNA was then sent to Fasteris SA, Plan-les-Ouates, Switzerland for cDNA library preparation, sequencing and quality filtering. Illumina sequencing for 150-bp paired-end reads was conducted for the 48 samples using bar-coded adapters with six samples multiplexed in each lane of an eight lane chip on an Illumina HiSeq2500.

Mapping of sequence reads and analysis of differentially expressed genes

The RNA-Seq Analysis program of CLC Genomics Workbench ver. 7.0 (CLC Bio-Qiagen, Aarhus, Denmark, http://www.clcbio.com/index.php) was used for mapping and expression computation using default parameters with the exception of paired-end distance (min

distance = 200 and max distance = 400). Forward and reverse reads were interleaved and the matched reads were counted as one paired read hereby referred to as a fragment. Fragments were imported into CLC Genomics Workbench and mapped to the reference transcriptome using CLC Map Reads to Reference tool (similar to bowtie). Mismatch score was set to 1 with a mismatch cost of 2. A linear gap cost model was used with insertion and deletion costs set to 3. The length fraction parameter was set to 0.5 and the similarity fraction parameter set to 0.8. For non-specific match handling, the map randomly setting was selected. Normalized measures of expression intensity, Fragments Per Kilobase per Million mapped fragments (FPKM) were computed from the fragment counts, the length of the targeted region, and total number of mapped fragments. Differential gene expression was investigated using the empirical differential gene expression (EDGE) test in CLC (Robinson and Smyth, 2008), which implements a negative binomial distribution for the modeling of gene expression using for the most parts the default settings in the edgeR package, version 3.4.0. Twelve two-group pairwise comparisons between three biological replicates of one condition and three biological replicates of another condition were made between the untreated, 15, 60, and 180 MAT time points of GR young tissue and GS young tissue, GR mature tissue and GS mature tissue, and GR young tissue and GR mature tissue. These three comparisons were made to investigate differences between resistant and susceptible biotypes as well as differences between young and mature tissue to address the resistant phenotype showing rapid tissue death only in mature tissue after glyphosate treatment.

Identification, primer design and optimization of control and candidate genes

Differentially expressed putative genes, hereby referred to as contigs, across the four time points from each of the three comparisons made above were clustered using R Statistical

Language software (R Development Core Team 2013; R Foundation for Statistical Computing, Wien, Austria). FPKM expression values were z-scaled and clustered using hierarchical clustering (hclust) in R. A dendrogram of the scaled data was made to show how the contigs clustered and a heat map showing the scaled expression data across samples was made using heatmap.2 in gplots library (R Statistical Language software). Differentially expressed contig lists were compiled using Microsoft Access and narrowed by making additional cutoffs of a fold change $\geq \pm 10$ between compared groups and statistical significance at $P \leq 0.05$ FDR (false discovery rate) adjusted p-value at any time point from each of the three comparison groups described above. Only contigs with FPKM >3 in at least one treatment group were analyzed in order to only consider transcriptionally active contigs (Gaines *et al*., 2014; O'Rourke *et al*., 2013). A total of 65,623 contigs were filtered from an original 158,314 contigs generated from the CLC mapping by excluding any contig less than 500 bp. Additionally, the *Arabidopsis* Gene Cloud website was used to generate gene lists associated with a key word. Keywords analyzed include: "abscisic acid", "apoptosis", "carboxylase", "defense", "drought stress", "ethylene", "hypersensitive response", "jasmonic acid", "lipid synthesis", "NADPH", "osmotic stress", "oxidative stress", "pathogen", "peroxidase", "programmed cell death", "reactive oxygen species", "redox", "salicylic acid", "salt stress", "stress response", and "superoxide dismutase" (Krouk *et al*., 2015). Genes from the *Arabidopsis* Gene Cloud lists were combined with contigs from the filtered differentially expressed contig lists in Access to create a list of 185 candidate contigs based on expression profile and gene function as related to the phenotype of interest.

From the list of 185 candidate contigs, 42 contigs shared the same TAIR gene code. A final list of 15 candidate contigs was selected for validation experiments based on the relatedness of the predicted protein function to the observed resistant rapid response phenotype. Control

genes were selected by dividing the average FPKM across all samples by the standard deviation to generate a coefficient of variation score (Levine *et al*., 1999; Vandesompele *et al*., 2002). This measure of gene-stability effectively identifies the top candidate control genes with the most stable expression. Genes with the highest scores and well known to be stably expressed were selected.

Primers for 15 candidate contigs and five control genes were designed in the most conserved regions of the gene. Conserved regions were identified by aligning the gene sequence from the *A. trifida* reference transcriptome with the corresponding gene sequence from TAIR using Clustal Needle (EMBL-EBI, Wellcome Genome Campus, Hinxton, Cambridgeshire, CB10 1SD, UK). Primers were designed to be approximately 20-21 bp in length with a GC content of approximately 50% and a melting temperature of 60 °C having a predicted amplicon of 150-200 bp. Initial testing by PCR was done to exclude any primer sets amplifying multiple products, products of incorrect sizes, or having no amplification. PCR reaction mixtures consisted of 10 μL EconoTaq Master Mix®, cDNA to a final concentration of 50 ng/μL, forward and reverse primers to final concentrations of 0.25 μM each, and water to bring the reaction mixture to 20 μL. Cycle conditions were as follows: 95 °C for 2 min, 40 cycles of 95 °C for 15 s, 60 °C for 15 s, and 72 °C for 30 s, then 72 °C for 5 min. PCR products were separated by gel electrophoresis.

Quantitative real-time reverse transcription polymerase chain reaction (qRT-PCR) was used to generate primer efficiency curves for each primer set, having passed the PCR analysis, using a 1/10x dilution series of cDNA from RNA-Seq samples showing the highest level of expression for each particular candidate contig of interest. Reaction mixtures were set up containing 10 μL of SYBRGreen Master Mix, 1 μL cDNA dilution (1x, 1/10x, 1/100x, 1/1000x), forward and reverse primers to final concentrations of 0.25 μM each, and water to bring the reaction mixture to 20 μL. A no template control (NTC) was also included as part of the dilution series to assess the effect

of the primers on the reaction. Cycle conditions included 15 min incubation at 95 °C, then 50 cycles of 95 °C for 30 s and 60 °C for 1 min, followed by a melt-curve analysis to confirm single PCR product amplification. Threshold-cycle (*C*t) values were calculated for each reaction using the CFX Manager™ Software (BioRad Laboratories, 1000 Alfred Nobel Drive, Hercules, California 94547, USA). Variable slopes for target and internal control genes were observed in amplification plots, so efficiency values were calculated for each primer set using the equation $E = -1+ 10^{(-1/m)}$, where *m* is the slope (http://www.genomics.agilent.com/biocalculators/calcSlopeEfficiency.jsp).

Validation of expression using qRT-PCR

The same six individuals that were submitted to Fasteris for Illumina sequencing were used in the qRT-PCR validation. cDNA was synthesized in 20 µL reaction volumes with 1 µg of DNase I-treated total RNA using the qScript™ cDNA Synthesis Kit (Quanta Biosciences, Inc. 100 Cummings Center Suite 407J Beverly, MA 01915) for first-strand cDNA synthesis with random and oligo(dT) primers, followed by digestion with RNase H. All qRT-PCR reactions were performed in duplicate, and 18 RNA-Seq samples were run for each gene analyzed. The samples used for validation include three biological replicates from susceptible young tissue at untreated and 60 min time points, resistant young tissue at untreated and 60 min time points and resistant mature tissue at untreated and 60 min time points. The cDNA was kept constant across all qRT-PCR samples (1µg), allowing for comparison of mean control gene *C*t values between resistant and susceptible individuals.

Six candidate contigs and two control genes were selected for validation by qRT-PCR based on their calculated efficiencies and melt curves. The calculated efficiency values were

used in the Pfaffl method for calculating relative gene expression (Pfaffl, 2001). The Pfaffl method is only slightly modified from the comparative *C*t method or $2^{-\Delta\Delta Ct}$ (Schmittgen and Livak, 2008), wherein the amplification efficiencies of the candidate and control genes are similar. The following equation was used to determine the expression ratio between the sample and calibrator:

$$\text{Ratio} = ((E_{\text{candidate}})^{\Delta Ct,\ \text{candidate (calibrator – test)}}) / ((E_{\text{control}})^{\Delta Ct,\ \text{control (calibrator – test)}}),$$

where $E_{\text{candidate}}$ and E_{control} are the amplification efficiencies of the candidate and control genes, respectively. Δ*C*t, candidate (calibrator – test) = *C*t of the candidate gene in the calibrator sample minus the *C*t of the candidate gene in the test sample, and Δ*C*t, control (calibrator – test) is the *C*t of the control gene in the calibrator sample minus the *C*t of the control gene in the test sample. The calibrator sample used for validation calculations was GS plant replicate 1, young untreated. The calibrator sample was chosen due to the observed higher raw *C*t values (lower expression), while still in the range of confidence for qRT-PCR (*C*t < 30). The above equation assumes that each gene (candidate and control) has the same amplification efficiency in calibrator and test samples, but it is not necessary that the candidate and control genes have the same amplification efficiency as each other (www.gene-quantification.de/real-time-pcr-guide-bio-rad.pdf). Relative expression values (REV) of each candidate contig were calculated twice, using a single control gene separately rather than averaging the control genes, due to the 100-fold difference in stable expression values between each control gene. The REV from an average of the two technical replicates were determined using the control genes glyceraldehyde 3-phosphate dehydrogenase (GAPDH) and translation elongation factor 1-alpha (EF1A). A linear regression was made showing the correlation between FPKM and REV for final validation of RNA-Seq by qRT-PCR.

Plant material, tissue collection and sample preparation for F_2 segregating individuals

A forward genetics approach was used to assess the linkage between candidate contig expression and resistance phenotype in a F_2 population segregating for glyphosate resistance. For generation of F_2 individuals, untreated GR rapid response and GS giant ragweed individuals were grown to maturity and allowed to cross pollinate. The GR rapid response individual was a sibling to the GR rapid response individuals used for the RNA-seq and reference transcriptome experiments. The GS individual was a sibling to the GS individuals used in the RNA-seq experiment. The GR rapid response individual was emasculated and served as the female in the cross. The GS individual served as the male in the cross. Both individuals were isolated in a large pollination bag together. Seeds produced by the female GR rapid response individual were collected and conditioned for germination as described above. These seeds produced F_1 individuals that were grown to maturity in the greenhouse and inbred by single-seed descent. Only two F_1 individuals reached maturity and produced seed. Seeds from one F_1 individual were collected and conditioned for germination, producing F_2 individuals. A total of 32 F_2 individuals were grown in the greenhouse. At the time of glyphosate treatment, plants were 20 to 30 cm with at least 6 nodes. Glyphosate treatment was the same as described for the RNA-seq experiment. Individuals were classified as glyphosate-resistant (F_2-GR) if they displayed the rapid response phenotype, survived the 1 x treatment and exhibited continued growth from the apical meristem and axillary growing points. Individuals were classified as glyphosate-susceptible (F_2-GS) if no rapid response was seen, the apical meristem was controlled (dead) three weeks after glyphosate treatment and little to no continued growth was observed from axillary growing points.

Tissue samples were collected from all 32 F_2 individuals immediately prior to glyphosate treatment and at the following time points after glyphosate treatment, 15, 60, and 180 MAT.

Both young meristematic tissue and mature leaf tissue samples were collected from each individual at each time point. Collected tissue was flash frozen with liquid nitrogen and stored at -80 °C. Tissue samples were ground separately using a TissueLyser II (QIAGEN, Valencia, CA, USA). Less than 100 mg of tissue was used for RNA isolation. Total RNA was extracted from F_2 individuals using the QIAGEN® RNeasy plant mini kit, following the supplied protocol. RNA quality and concentration was measured on a NanoDrop UV spectrophotometer. cDNA was synthesized in 20 μL reaction volumes with 1 μg of DNase I-treated total RNA using the qScript™ cDNA Synthesis Kit (Quanta Biosciences, Inc. 100 Cummings Center Suite 407J Beverly, MA 01915) for first-strand cDNA synthesis with random and oligo(dT) primers, followed by digestion with RNase H.

qRT-PCR analysis of candidate genes using F_2 segregating individuals

The four most F_2-GR individuals displaying a clear rapid response phenotype and the four F_2-GS individuals were used in the forward genetics validation. cDNA was prepared as described above. All qRT-PCR reactions were performed in duplicate, and 64 F_2 samples were run for each gene analyzed. The 64 samples consist of four time points (untreated, 15, 60, and 180 MAT) and two tissue types (young and mature) for each of the eight F_2 individuals analyzed. Two candidate contigs and two internal control genes were selected for validation by qRT-PCR based on initial F_2 qRT-PCR of a single time point for five candidate contigs. The REVs from an average of the two technical replicates and each biological replicate were determined using both GAPDH and EF1A to normalize expression between samples. These control genes were not averaged due to the 100-fold difference in stable expression values between GAPDH and EF1A.

Differences in REVs between the F_2-GR and F_2-GS groups were evaluated by F-tests for sample variance and T-tests for significant difference in group means using Microsoft Excel.

3.3 RESULTS AND DISCUSSION

Reference transcriptome quality, completeness and functional annotation

Sequencing on the Illumina MiSeq V3 platform generated 8.4 M 300 bp paired-end sequence reads (fragments) for a total of 59.2 Mb of high quality bases (≥Q40). Assembly of these fragments using Newbler (454 Life Sciences) v2.8 returned 158,314 total transcripts or putative genes, hereby referred to as contigs. In total, 58.5% of the assembled contigs were < 500 bp and 41.5%, or 65,623 contigs were ≥500 bp (Table 3.1 and Figure 3.1 A). The average length of contigs greater than or equal to 500 bp was 915 bp with an N50 contig size of 934 bp, whereas the maximum length of contigs was 17,835 bp (Table 3.1). The total number of bases contained in the reference was 60,094,544, and 98.5% had a quality score higher than Q40 (0.01% chance of error). Of the 8.4 M total fragments, a majority of the fragments, 66.1% were mapped back to the assembly. Transcriptome coverage was good with 81,938 contigs, 51.7%, having ≥ 20 fragments mapped and 12.5% of the total contigs having ≥ 200 fragments mapped (Figure 3.1 B).

Annotation using both UniProtKB (Consortium, 2012) and TAIR10 (Swarbreck *et al.*, 2008) databases by BlastP was done on 49,696 contigs, as any peptides shorter than 100 amino acids in length were excluded from the final predicted protein list. A total of 44,247 contigs returned at least one annotation, providing 92% annotation of the reference transcriptome (Table 3.2 and Figure 3.2 A and B). A total of 5,133 contigs returned unique, un-shared UniProt IDs and

38,565 contigs returned UniProt IDs that were shared with two or more contigs (Table 3.2). The large number of contigs containing shared predicted gene annotations suggests multiple contigs may represent different segments of one unigene. In fact, the 65,623 large contigs in our reference transcriptome do not necessarily represent unigenes, as they have been computationally assembled and we do not have genomic sequence for comparison (Gaines *et al*., 2014). This will be important to consider when identifying candidate contigs, as we will need to confirm contig identity using blast as well as look at the FPKM levels for all contigs sharing gene annotations with a particular candidate contig.

RNA-Seq expression quantification

An RNA-Seq experiment was then performed using a GR rapid and GS accession. A total of six individuals, three biological replicates each for the GR and GS accessions, were treated with 0.84 kg·ae·ha^{-1} glyphosate. Samples for RNA-Seq were collected from both young and mature tissue at time untreated, 15, 60, and 180 minutes after treatment (Figure 3.3). The 48 RNA libraries were sequenced using Illumina HiSeq2500 and 150 bp paired-end reads, producing 2.1 billion reads ranging from 33 to 57 million reads per sample. Forward and reverse reads were interleaved and the resulting fragments were aligned to the reference transcriptome using the Map Reads to Reference tool in CLC (similar to bowtie), FPKM (Fragments Per Kilobase per Million mapped fragments) values for each contig were calculated, and differential expression statistical analysis was conducted using the EDGE test in CLC (Robinson and Smyth, 2008). Analysis using EDGE with additional cutoffs of ≥500 bp contig length, ±10 fold change, $P \leq 0.05$ FDR adjusted p-value and ≥3 FPKM detected a total of 27 differentially expressed contigs meeting the criteria above at every treatment time point across the three separate

comparisons of GR young tissue vs GS young tissue, GR mature tissue vs GS mature tissue and GR young tissue vs GR mature tissue (Appendix 7). When comparing glyphosate-untreated samples to each glyphosate-treated sample of the same biotype and tissue type, only 5 differentially expressed contigs meeting the criteria above were detected in the GR mature tissue untreated vs GR mature tissue treated time points, while no significantly differentially expressed contigs were detected in the other comparisons involving GR young tissue, GS young tissue and GS mature tissue (Appendix 8). Eight contigs sharing identical TAIR annotations (AT2G45300) and pfams identified as EPSP synthase exhibited no significant differential expression between GR and GS accessions (average EDGE Fold Change = 0.5, FDR *P*-value = 0.99) indicating that resistance in this accession is not conferred by overexpression of EPSP synthase. Interestingly there was one contig (ID:103424) with a different TAIR annotation (AT1G48860) but identical pfam as the other eight contigs identified as EPSP synthase exhibiting significant differential expression between untreated GR and GS accessions in both young and mature tissue (average EDGE Fold Change = 43, FDR *P*-value = 0.007). Contig103424 does align perfectly with the full length cDNA EPSPS found in contig03694, but is only 322 bp in length. It is possible that contig103424 and the other seven EPSPS annotated contigs are all part of the same unigene or at least an allele of the same gene and failed to assemble at the same locus. This may have led to preferential fragment alignment to a particular contig over the others, creating false results in the EDGE test. Transcriptomic analysis using RNA-Seq is a useful approach to detect and quantify the expression of low abundance transcripts, but it is important to understand the assumptions and inherent errors involved in the analysis of large sequencing datasets.

Candidate contig selection and qRT-PCR validation of RNA-Seq

Based on our observations of the resistant rapid response to glyphosate, we tested the hypothesis that contigs differentially expressed between GR and GS as well as GR young tissue and GR mature tissue with predicted annotations related to programmed cell death, defense response, or response to stress would be predictive transcriptional markers for rapid response resistance to glyphosate. Initial clustering of large gene lists in R Statistical software was not stringent enough to identify a manageable number of candidate contigs based on expression patterns across all four time points, two tissue types and both biotypes. However, the cluster analysis of all six individuals was useful in showing similar expression patterns of all contigs between biological replicates. This shows that the same contig is generally expressed more or less to a similar extent from plant to plant within an accession (Figure 3.4 A and B).

Differentially expressed contigs were compiled in Microsoft Access and selected for further evaluation based on a number of criteria including a variety of stringency filters as well as Pfam and TAIR putative assignment to genes involved in molecular processes related to our hypothesis regarding the resistance phenotype. This selection resulted in 143 unique contigs, from which 15 candidate contigs were selected based on the relatedness of the predicted protein function to the observed resistant rapid response phenotype (Table 3.3 and 3.4). The top 15 candidate contigs showed FPKM expression patterns across treatment time points that provided a clear hypothesis describing the possible connection between candidate gene function and the resistant rapid phenotype (Table 3.3 and 3.4). Through PCR selection, only six of the top 15 candidate contigs were selected for confirmation of RNA-Seq results using qRT-PCR. The other 11 candidate contigs resulted in either no amplification, multiple products or unacceptable calculated efficiencies. Furthermore, the six selected contigs had primer efficiencies in the

acceptable range of 90 to 110%, and were suitable for use in qRT-PCR validation of RNA-Seq. The FPKM expression patterns for these six candidate contigs were clustered using R Statistical software (Figure 3.5).

EF1A and GAPDH were identified in the top 100 out of the total 158,314 contigs as having the most stable expression using the coefficient of variation method (Levine *et al*., 1999; Vandesompele *et al*., 2002). EF1A and GAPDH were selected as internal control genes based on their coefficient of variation score as well as their frequent use as reference genes in published literature (Fernández-Aparicio *et al*., 2013). FPKM and relative expression value (REV) correlation results of each candidate contig for both internal control genes were similar and combined in Figure 3.6 A-F. The qRT-PCR analysis of the expression patterns of six candidate contigs support our RNA-Seq results, with a positive and significant correlation between the two methods (Figure 3.6 A-F). The imperfect match between FPKM and REV for some genes may be due to the qRT-PCR primers amplifying multiple members of a gene family with very similar sequences, but very different differential expression patterns. Thus, the need for sequencing and additional validation of full genes is necessary to confirm a causal relationship between gene function and the resistance trait.

Forward genetics validation

Two of the six validated contigs were next evaluated using a forward genetics approach with an F_2 population segregating for glyphosate resistance derived from a GR by GS cross of siblings to the GR and GS individuals used in the RNA-Seq experiment. Only 32 F_2 individuals were generated from one F_1 self-pollinated individual. Susceptible (F_2-GS) individuals (n = 4) were identified using the criteria that they did not exhibit the rapid response to glyphosate and

the apical growing point did not survive a 1 x glyphosate application with little to no continued growth from lower axillary shoots. Resistant (F_2-GR) individuals (n = 28) were identified on the basis that they exhibited the rapid response to glyphosate, survived a 1 x glyphosate application and showed robust continued growth following treatment. It is important to note the segregation ratio of 7:1, with a bias towards the resistance trait. This ratio does not clearly explain the mode of inheritance for the resistance trait. A Mendelian inheritance pattern would suggest a 3:1 ratio (monohybrid) or 9:3:3:1 (dihybrid) or some permutation (9:4:3 or 12:3:1), which could be possible, but due to the low sample number (n=32) in the F_2 population, we cannot clearly determine if the trait follows a Mendelian inheritance pattern. Because the cross was made with a GR individual serving as the female parent, the possibility of cytoplasmic-controlled inheritance such as a chloroplast-located gene cannot be ruled out. The difference in genetic background should also be considered, as the parental lines are originally from two different field sites. Despite the lagging genetic information, validation of candidate contigs in F_2 plants may prove to be a fast approach to further support the hypothesis that these genes will function as molecular markers for glyphosate resistance or PCD in response to stress.

Both osmotin 34 (OSM34) and S-adenosylmethionine synthetase 3 (SAMS3) were the two candidate contigs selected for the forward genetics validation along with glyceraldehyde 3-phosphate dehydrogenase (GAPDH) and translation elongation factor 1-alpha (EF1A) as internal control genes. These two candidate contigs were chosen based on their FPKM expression pattern in the RNA-Seq experiment, performance and quality as candidate contigs through qRT-PCR validation experiments and from their predicted protein function. Additionally, we wanted to make use of the four GS and four most GR individuals (64 samples) for the initial qRT-PCR analysis. Therefore, only two genes were selected to reduce time and cost. Future testing of

greater numbers of candidate contigs may be done only on selected tissues or treatment time points. Stress responses in plants have been extensively studied and much is known about the downstream signaling molecules and cellular effects during plant abiotic stress, but relatively little is known about the initial perception mechanisms during abiotic stresses (Kaurilind *et al*., 2015). The early steps of plant responses to stress include recognition of a chemical or signal and activation of downstream responses (Kaurilind *et al*., 2015). The rapid response to glyphosate in giant ragweed is of particular interest because no other plant species has shown this rapid of a PCD-type response to the herbicide. Therefore, this study may lead to the identification of a novel stress response pathway or signaling molecule in plants and/or a known pathway previously unknown to interact with herbicides.

Signaling hormones and pathways during defense or response to stress are often overlapping having both synergistic and antagonistic interactions, leading to a number of possible outcomes (Kaurilind *et al*., 2015). Though OSM34 and SAMS3 have known functions acting in pathways known to be involved in defense or stress responses and PCD, they may also be involved in other unknown interactions. Osmotin is a thaumatin-like pathogenesis-related (PR) protein that causes rapid cell death in yeast (*S. cerevisiae*) (Lee *et al*., 2010; Yun *et al*., 1998). First detected in tobacco cultivars displaying a hypersensitive-response (HR) to tobacco mosaic virus (TMV), osmotin has been described as a multifunctional protein also providing salt tolerance and protecting cells from osmotic stress by sequestering Na^+ ions and compartmentalizing them into vacuoles and intercellular spaces (Abdin *et al*., 2011; Kumar *et al*., 2015; Stintzi *et al*., 1991). Osmotin causes apoptosis in yeast by activation of the RAS_2/cAMP pathway leading to the accumulation of reactive oxygen species (ROS) (Kumar *et al*., 2015). In plants, osmotin is regulated by the mitogen-activated protein kinase (MAPK)

phosphorylation cascade, which is activated when exposed to stress conditions like salt, drought, cold, and pathogen attack (Kumar *et al*., 2015). Osmotin induced proline accumulation has been reported to confer tolerance against both biotic and abiotic stress, but the exact mechanism of induction of proline by osmotin is unknown (Abdin *et al*., 2011). Osmotin has been thought to act as both a transcription factor and cell signaling molecule leading to rapid cellular changes in response to a variety of stresses, which makes osmotin a popular candidate for its involvement in the resistant rapid response to glyphosate in giant ragweed (Abdin *et al*., 2011).

SAMS3 synthesis of S-adenosyl-L-methionine (SAM) from methionine and ATP is the first step leading to the synthesis of both polyamine and ethylene (Buchanan *et al*., 2015; Espartero *et al*., 1994; Lim *et al*., 2002). Polyamine is a well-known regulator of plant tolerance to both abiotic and biotic stresses and its synthesis is dependent on SAM levels in plants (Gong *et al*., 2014). It is suggested that an enzyme, possibly SAMS3, is induced and in turn responsible for the increase in ethylene production during water stress (Apelbaum and Yang, 1981; Lim *et al*., 2002). Increased levels of *SAMS3* expression enhances the expression of downstream target genes including polyamine oxidase (PAO), which along with polyamines can increase H_2O_2 and Ca^{2+} concentrations in guard cells to induce stomatal closure during osmotic stress (Gong *et al*., 2014; Guo *et al*., 2014). Hydrogen peroxide derived from polyamine catabolism signals the induction of developmental PCD in maize (Gong *et al*., 2014). SAM is the precursor molecule to both polyamine and ethylene synthesis, which implicates *SAMS3* as having a critical role in plant responses to various abiotic stressors (Buchanan *et al*., 2015; Gong *et al*., 2014; Lim *et al*., 2002).

Expression of OSM34 and SAMS3 were evaluated in young and mature tissues at time points untreated, 15, 60 and 180 minutes after glyphosate treatment in four GR- and four GS-F_2

individuals, for a total of 64 samples (Appendix 9). The expression of OSM34 and SAMS3 seen in the F_2 validation did not co-segregate with the resistance trait, nor did it follow a similar pattern to what was seen in the RNA-Seq experiment (Figure 3.7 A and B; and Figure 3.8 A and B). Differences in relative expression values using a two-tailed distribution between the F_2-GR and F_2-GS groups were not found to be significant at any time point across both tissue types (Student's t-test, $P < 0.05$). Only one sample time point for only one of the control genes resulted in a significant difference between the F_2-GR and F_2-GS groups using a one-tailed distribution. The null hypothesis that group means are equal was rejected for SAMS3 (normalized with EF1A) at the young untreated time point (*t* Statistic (2.4) > *t* Critical one-tail (1.9)). There was no significant difference seen in this sample using the GAPDH normalized calculations. Therefore, we can conclude that the candidate contigs annotated as OSM34 and SAMS3 do not co-segregate with the resistance trait in this experiment. However, these results do not rule out OSM34 or SAMS3 as candidate genes. Further analysis with a larger population of segregating individuals as well as functional validation is necessary to determine their relationship with the resistance trait.

Future directions and continued analysis

The workflow presented above is a first approach to investigate differentially expressed genes related to the resistant rapid response to glyphosate seen in giant ragweed. The sequencing quality of the reference transcriptome as well as the RNA-Seq experiment is excellent. A small portion of the reference transcriptome (11%) failed to return a protein annotation, which would have excluded the identification of candidate contigs based on the AtGeneCloud keyword association, but not based on the RNA-Seq differential expression analysis. The RNA-Seq

analysis using CLC Genomics Workbench returned a large number (12,058) of differentially expressed contigs, which were further filtered by increased stringency for fold change and significance. It is also possible that the resistance trait may be influenced by subtle differences in gene expression that were not statistically significant in the RNA-Seq analysis (Leslie and Baucom, 2014). It would be beneficial to conduct a second analysis of the RNA-Seq data using an alternative approach such as alignment with bowtie followed by differential gene expression analysis using the DEseq2 package in Bioconductor software (Anders *et al*., 2013; Guo *et al*., 2013). This would provide a comparison for validation of our results from CLC as well as identify an alternate set of differentially expressed contigs. For example, CLC aligned fragments to six different contigs sharing identical annotation for SAMS3, only two of which were larger than 500 bp. Three of these contigs, including our chosen candidate, showed interesting differential expression patterns between GR and GS, while two contigs showed relatively equal but low expression between GR and GS and one contig showed zero expression. There is a likely possibility that these six contigs come from two different alleles of a gene and are the results of an imperfect alignment or some contigs could contain sequencing errors leading to preferential fragment alignment to the other contigs. This may also be explained by the presence of gene family members, very similar in sequence, but with very different differential expression patterns. The qRT-PCR primers might be amplifying all gene family members, whereas the RNA-Seq is only quantifying one gene family member. This would need to be overcome by designing primers specific to each isoform to be confident in which gene is being quantified. It is important to consider such caveats when working with a *de novo* assembled transcriptome (Leslie and Baucom, 2014). The results obtained cannot be attributed to a causal relationship

between differentially expressed contigs and resistance, thus the need for candidate selection and functional validation of candidate genes.

In addition, it is important to note that we assessed co-segregation of candidate contigs in an F_2 population with a very small sample size. From the 32 F_2 individuals, we could not report statistically significant results had we found a positive correlation between candidate gene expression and the segregating phenotype, nor can we accurately report the negative results found. Therefore, OSM34 and SAMS3 may still prove to be interesting candidates, as these genes may have complex interactions with other genes contributing to the resistant rapid response, despite the lack of clear evidence for their role in the F_2 validation experiment (Gaines *et al*., 2014). RNA-Seq analyzes transcript levels, but does not provide insight for potentially mechanistic contributions from upstream promoters or intronic regions (Leslie and Baucom, 2014). Candidate gene research will need to be functionally verified by sequencing, cloning, and transforming candidate genes into a testable system, ideally transgenic expression in *A. trifida*. Functional verification will be necessary to identify the causal genetic component underlying resistance in this species. It will also be important to test the expression of candidate genes under different stresses including treatment with alternate herbicides. Tank mixes with alternate modes of action are often used to address resistance issues in modern agriculture and a recent study has shown that an application of glyphosate mixed with other herbicides has an antagonistic effect, reducing the efficacy of the other herbicide due to the rapid decrease in transpiration and photosynthesis in mature leaf tissue caused by glyphosate (Harre *et al*., 2016). Thus far, the rapid response appears to be specific to glyphosate (Van Horn and Westra, 2015), but due to the complexity of stress response pathways in higher plants, candidate genes may be involved in a broader network of responses beyond the response to glyphosate. At this point, the molecular

mechanism triggering the resistant rapid response to glyphosate remains unknown, but this reference transcriptome accompanied by an extensive RNA-Seq experiment of tissue and time course samples provides an invaluable resource for continued genetic research of glyphosate resistance mechanisms in this species.

3.4 TABLES

Table 3.1 Results from *de novo* assembly of *Ambrosia trifida* cDNA reference transcriptome using Illumina MiSeq v3.

	Ambrosia trifida reference transcriptome
Total fragment pairs	8,439,867
Number of aligned fragments	5,585,879
Number of quality bases, >Q40, Mb	59.2 (98.5% of total)
Number of total contigs	158,314
Number of contigs ≥500 bp	65,623
Average contig size, bp, ≥500 bp	915
N50 contig size, bp	934
Maximum contig length, bp, ≥500 bp	17,835

Table 3.2 Results from annotation of *Ambrosia trifida* reference transcriptome using TransDecoder against the uniprot/swissprot and TAIR10 protein data bases.

	Ambrosia trifida reference transcriptome
Total number of contigs	49,696
Contigs without annotation	5449 (11%)
Contigs with Pfam annotation	39,479
Single contigs with non-shared UniProt ID	5,133
Two or more contigs having identical UniProt ID	38,565
Average number of contigs for each UniProt ID	10

Table 3.3 RNA-Seq FPKM values of the top 15 significantly differentially expressed candidate contigs for which primers were designed and tested for use in qRT-PCR validation experiments.

Contig	Pfam Annotation	Biotype	FPKM in Young Tissue at Treatment Time Point (MAT)				FPKM in Mature Tissue at Treatment Time Point (MAT)			
			Unt	15	60	180	Unt	15	60	180
23137	Osmotin 34	R	135.2	130.4	69.5	9.6	614.5	636.6	422.0	146.7
		S	5.6	6.3	3.1	1.3	86.5	55.9	54.9	19.4
44611	S-adenosyl-methionine synthetase protein	R	116.7	110.5	113.0	57.1	588.9	532.5	328.0	87.0
		S	16.3	16.1	16.2	9.8	17.7	9.3	7.1	4.4
18224	Glucose-methanol-choline oxidoreductase	R	9.9	31.0	33.7	11.5	10.7	27.7	312.8	155.4
		S	1.3	0.7	1.9	2.6	0.1	0.5	2.7	4.7
13169	UDP-glucosyltransferase	R	1.1	21.4	24.0	30.9	22.5	130.7	424.9	211.2
		S	0.0	0.2	0.6	2.5	2.1	9.3	75.7	74.4
58166	Jasmonic acid carboxyl methyltransferase	R	6.2	8.2	46.1	7.5	5.0	13.2	100.6	28.7
		S	5.4	4.6	6.7	2.6	3.3	1.7	5.5	4.6
48381	Ethylene-responsive element	R	8.5	7.8	7.7	8.5	3.1	4.5	3.6	9.9
		S	79.0	62.1	86.7	81.0	21.9	28.0	25.7	69.3
36661	Nine-cis-epoxycarotenoid dioxygenase 3	R	1.2	1.0	4.1	3.8	8.8	31.4	59.4	55.1
		S	1.1	0.5	1.4	5.7	7.5	7.5	9.2	2.0
44151	S-adenosyl-L-methionine-dependent methyltransferases	R	148.2	130.1	103.2	44.3	129.7	133.6	113.7	74.4
		S	6.6	6.6	5.2	1.9	8.0	9.3	6.9	5.5
37679	Cytochrome b6f complex subunit (petM), putative	R	46.9	54.0	33.6	19.9	28.6	34.4	34.9	23.1
		S	271.6	306.7	203.9	184.9	364.5	486.0	328.3	305.6
64863	Cinnamyl alcohol dehydrogenase 6	R	2.1	44.8	28.6	93.3	7.5	56.5	824.9	817.0
		S	4.6	5.1	6.5	6.6	4.4	7.1	199.2	192.8
65438	Elicitor-activated gene 3	R	4.7	10.9	10.6	16.4	5.9	17.7	185.8	168.3
		S	8.0	8.2	8.0	4.7	3.6	4.7	35.4	35.2
19285	Allene oxide synthase CYP74A	R	0.4	2.6	4.8	1.9	2.4	7.0	57.9	6.9
		S	0.2	0.5	1.9	0.5	0.8	0.4	7.2	1.6
33193	Allene oxide cyclase 3	R	0.2	14.0	31.5	1.3	0.4	4.4	197.6	36.2
		S	0.4	0.2	8.4	0.2	0.3	0.4	27.5	2.5
12877	Allene oxide cyclase 4	R	5.3	9.1	18.7	4.7	33.6	34.2	401.7	344.3
		S	3.5	2.7	7.1	3.0	18.1	10.2	38.0	18.1
37368	Lipid transfer protein 3	R	2243.3	1907.5	1841.6	1331.4	62.7	62.4	103.6	182.6
		S	2588.3	2532.3	2242.1	1650.0	128.1	588.9	276.7	551.2

Table 3.4 Gene function of the top 15 significantly differentially expressed candidate contigs for which primers were designed and tested for use in qRT-PCR validation experiments.

Contig	Pfam Annotation	Abbreviation	Gene Function
23137	Osmotin 34	OSM34	Response to salt stress. Defense response to fungus. Programmed cell death response.
44611	S-adenosyl-methionine synthetase protein	SAMS3	SAM biosynthesis from methionine. Synthesis of precursor to polyamines and ethylene. Related to plant response to abiotic stress.
18224	Glucose-methanol-choline oxidoreductase	GMC	Cyanide biosynthetic process. Defense response. Oxidation reduction process.
13169	UDP-glucosyltransferase	UGT1	Cell wall biogenesis. Flavonoid biosynthetic process. Flavonoid glucuronidation. Para-aminobenzoic acid metabolic process. Response to salicylic acid.
58166	Jasmonic acid carboxyl methyltransferase	JMT	Jasmonic acid biosynthetic process. Jasmonic acid mediated signaling pathway. Methylation. Oxylipin biosynthetic process. Response to wounding.
48381	Ethylene-responsive element	ERF13	Defense response. Ethylene-activated signaling pathway. Regulation of transcription. Response to chitin.
36661	Nine-cis-epoxycarotenoid dioxygenase 3	NCED3	Abscisic acid biosynthetic process. Hyperosmotic salinity response. Oxidation-reduction process. Response to osmotic stress. Response to water deprivation.
44151	S-adenosyl-L-methionine-dependent methyltransferases	SAMMT	Tocopherol biosynthesis, plastoquinone biosynthesis from methionine. Related to plant response to abiotic stress.
37679	Cytochrome b6f complex subunit (petM), putative	PetM	Plastoquinol--plastocyanin reductase activity.
64863	Cinnamyl alcohol dehydrogenase 6	CAD6	Lignin biosynthetic process. Oxidation-reduction process. Plant type hypersensitive response.
65438	Elicitor-activated gene 3	ELI3	Lignin biosynthetic process. Oxidation-reduction process. Plant type hypersensitive response.
19285	Allene oxide synthase CYP74A	AOS	Cytochrome p450 in jasmonic acid biosynthesis pathway. Defense response to fungus. Redox. Oxylipin biosynthesis. Sterol metabolism.
33193	Allene oxide cyclase 3	AOS3	Jasmonic acid biosynthesis. Response to fungus. Response to salt stress. Leaf senescence.
12877	Allene oxide cyclase 4	AOS4	Jasmonic acid biosynthesis. Response to cold. Expressed during senescence.
37368	Lipid transfer protein 3	LTP3	Lipid transport. Response to abscisic acid. Response to water deprivation.

3.5 FIGURES

A.

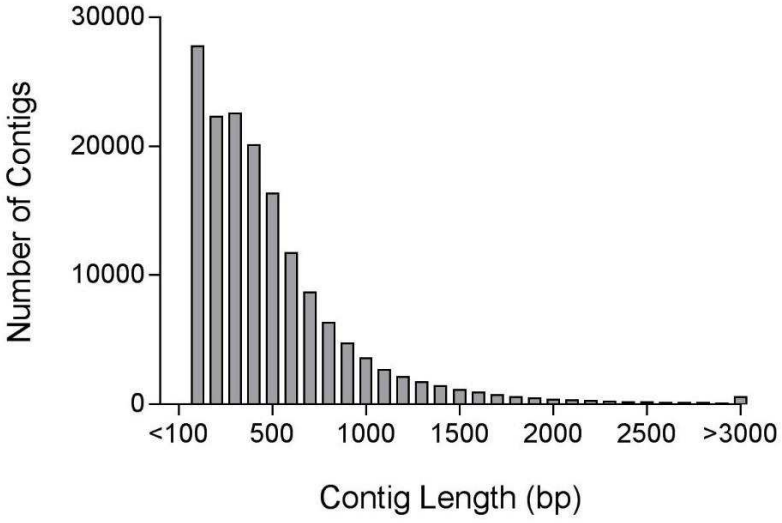

B.

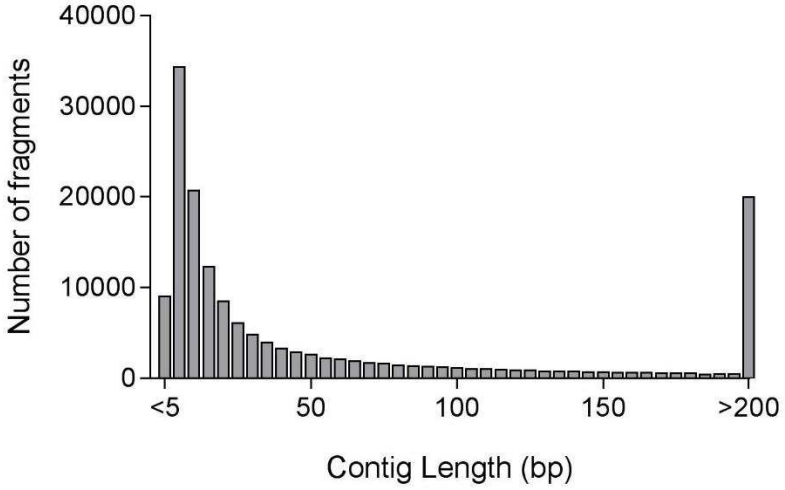

Figure 3.1 Contig size and fragment coverage of the *Ambrosia trifida* reference transcriptome shown by (A) length and distribution of contigs ≥500 bp, and (B) number of fragments mapped by contig length.

A.

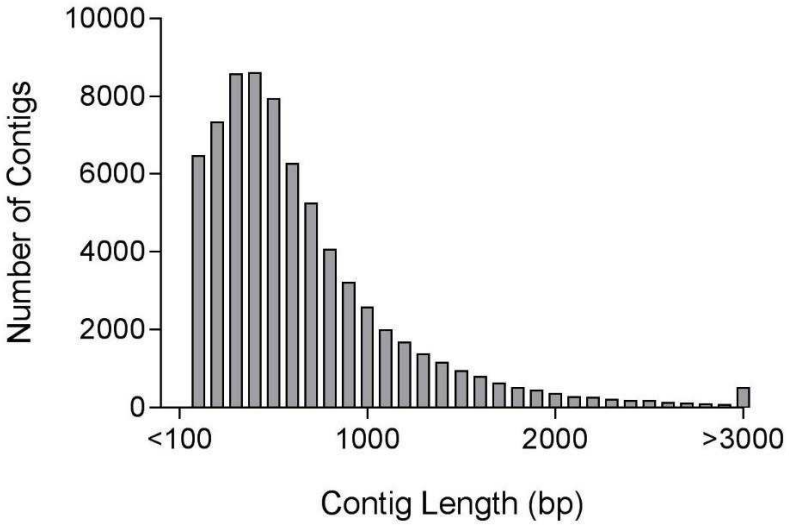

B.

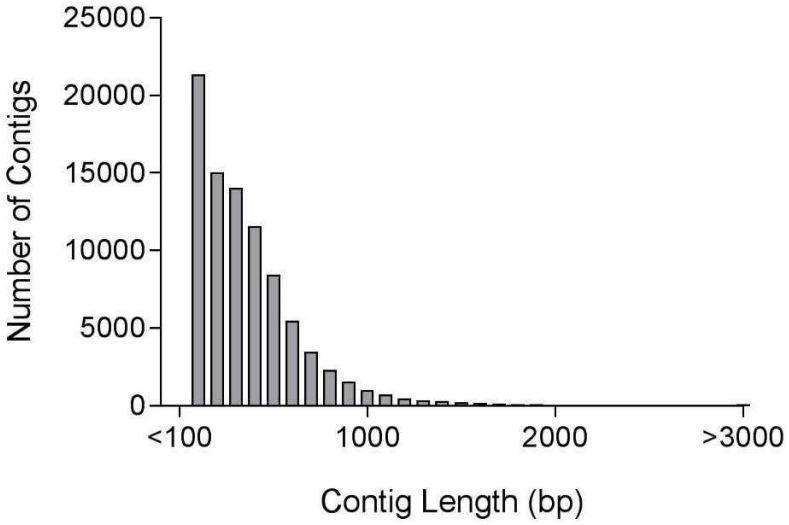

Figure 3.2 Contig size distribution of the *Ambrosia trifida* reference transcriptome shown by (A) contigs that were annotated by blastp to the uniprot/swissprot and TAIR10 protein data bases, and (B) contigs that could not be annotated by blastp.

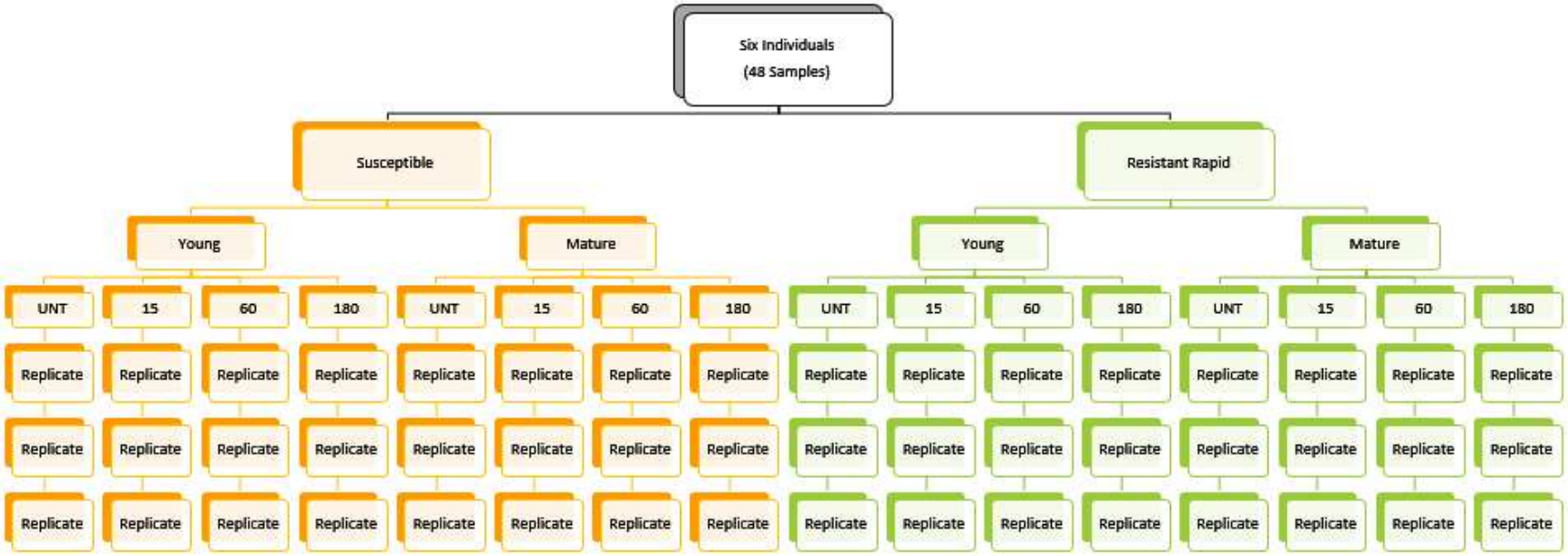

Figure 3.3 Experimental design diagram for the RNA-Seq experiment. Forty-eight total samples were collected from six individuals. Glyphosate-susceptible and -resistant rapid response represent the two biotypes. Young and mature tissue represent the two tissue types. Treatment time points include untreated and 15, 60 and 180 minutes after glyphosate treatment. Three replicate individuals were used from each biotype.

A.

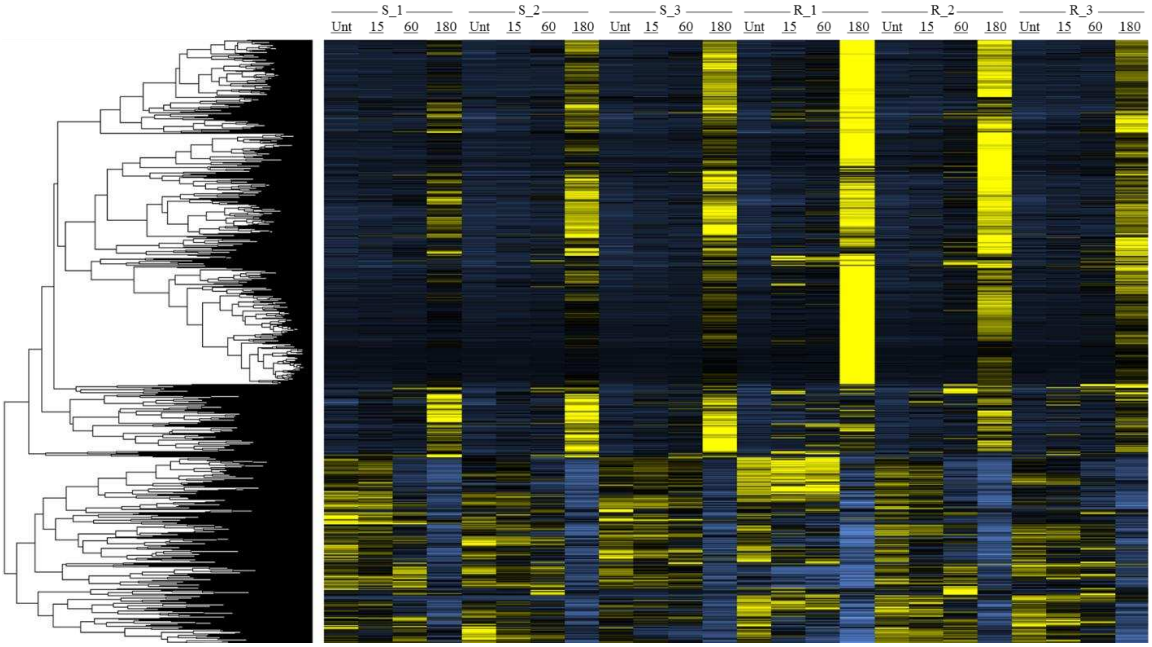

B.

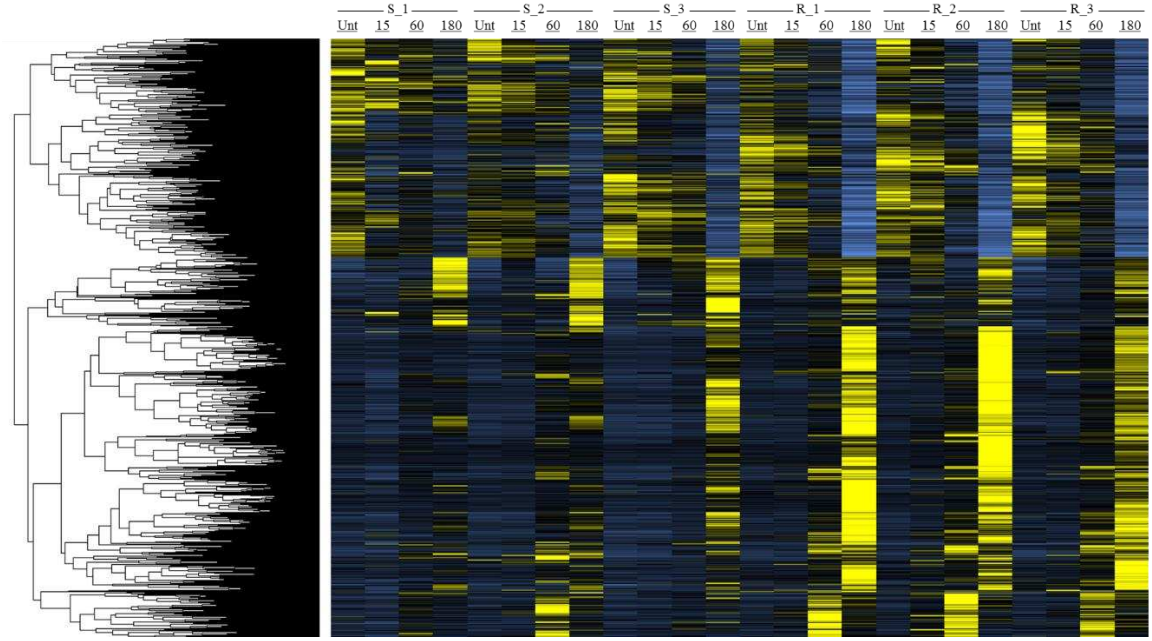

Figure 3.4 Heat map of z-scaled FPKM values from RNA-Seq experiment of 3,596 differentially expressed contigs in young tissue (A) and 8,462 differentially expressed contigs in mature tissue (B) of all six individuals clustered using hclust in R Statistical Language software. Blue color indicates lower expression values (< -2), yellow color indicates higher expression values (> 2).

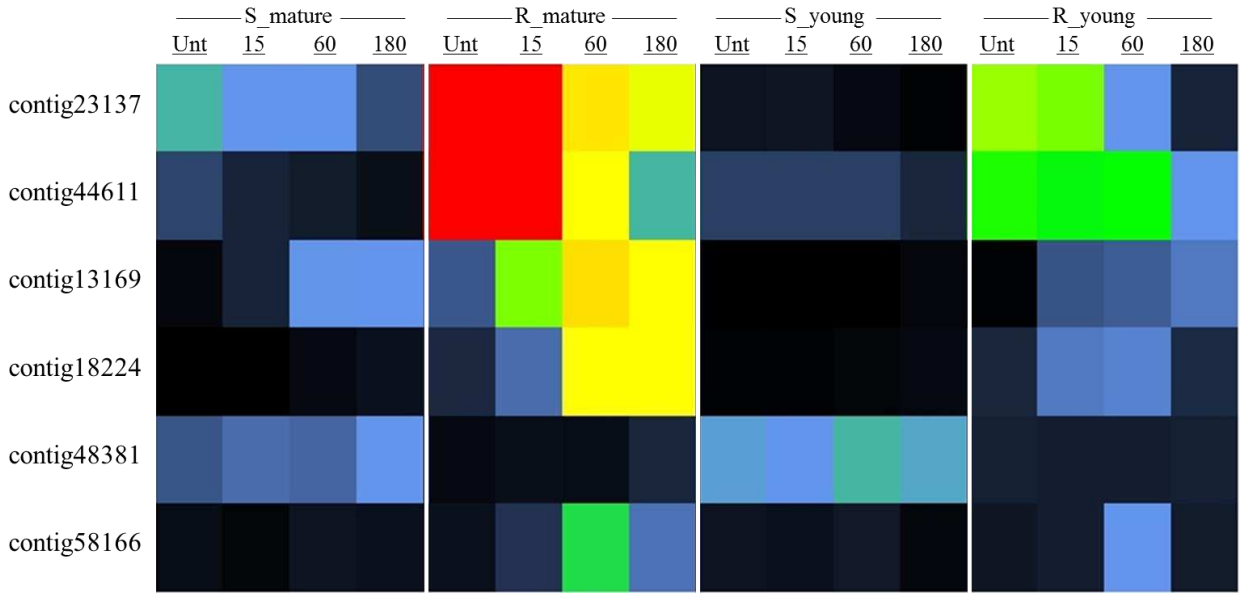

Figure 3.5 Heat map of average FPKM values from RNA-Seq experiment for six contigs selected for qRT-PCR validation. Susceptible (S) and Resistant (R) for both young and mature tissue types at glyphosate-untreated and 15, 60 and 180 minutes after treatment. Warmer colors represent higher expression values. Raw FPKM values range from 0 (black) to ≤ 100 (blue) to ≥ 500 (red).

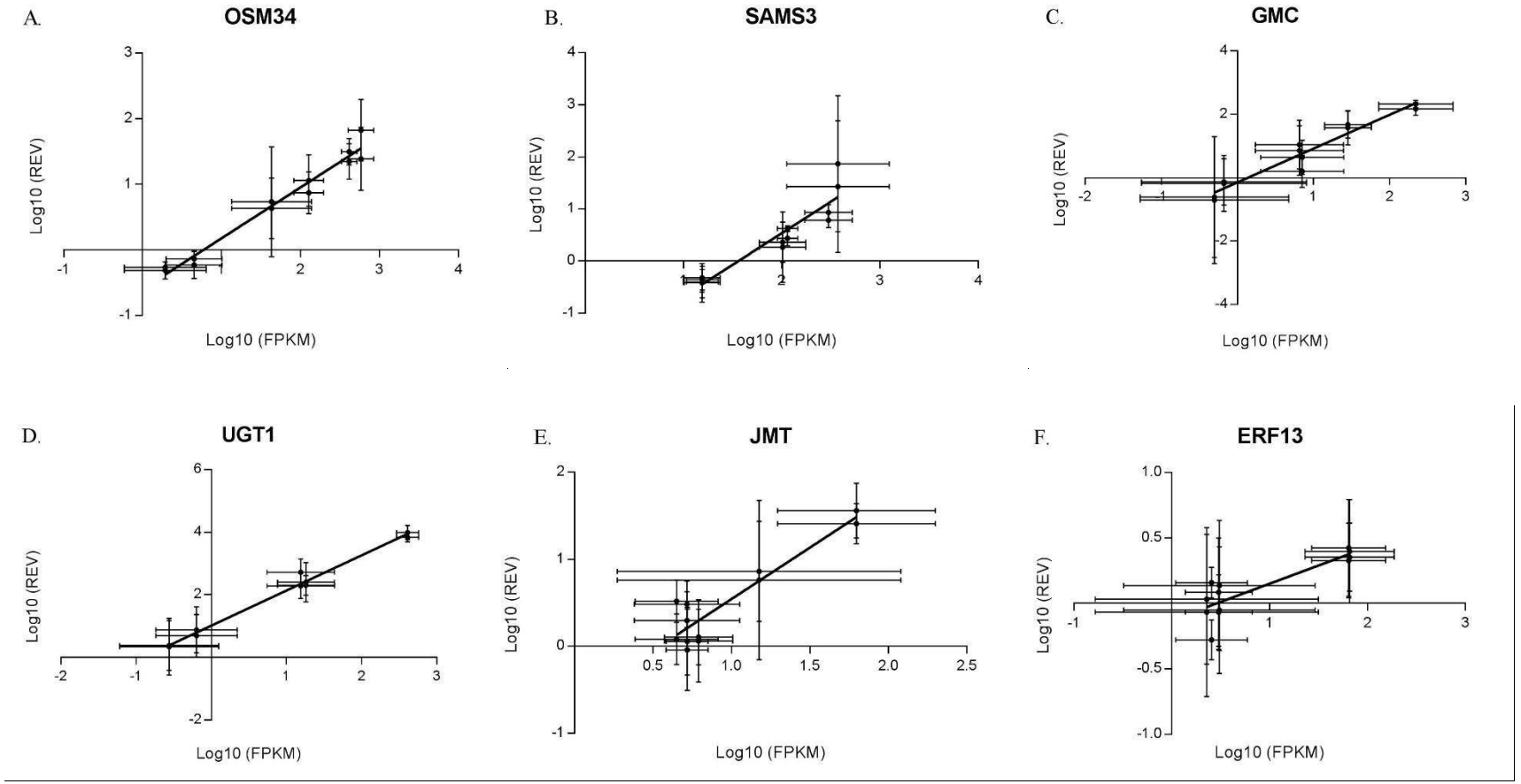

Figure 3.6 Confirmation of six differentially expressed candidate contigs by qRT-PCR on the same RNA samples used for RNA-Seq. Correlation of RNA-Seq (FPKM) to qRT-PCR (REV) by linear regression. Osmotin 34 (OSM34) (A), slope = 0.8, $R^2 = 0.7$, $P < 0.0001$. S-adenosyl-methionine synthetase 3 protein (SAMS3) (B), slope = 1.2, $R^2 = 0.87$, $P < 0.0001$. Glucose-methanol-choline oxidoreductase (GMC) (C), slope = 1, $R^2 = 0.93$, $P < 0.0001$. UDP-glucosyltransferase 1 (UGT1) (D), slope = 1.1, $R^2 = 0.98$, $P < 0.0001$. Jasmonic acid carboxyl methyltransferase (JMT) (E), slope = 1.2, $R^2 = 0.86$, $P < 0.0001$. Ethylene-responsive element 13 (ERF13) (F), slope = 0.3, $R^2 = 0.73$, $P = 0.0004$.

A.

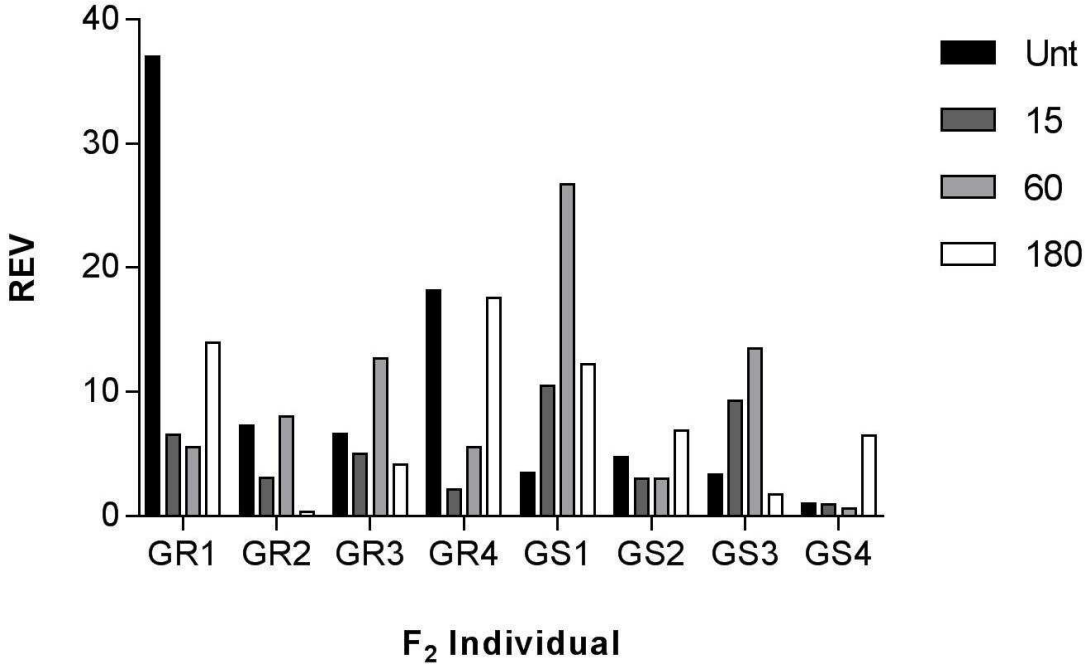

B.

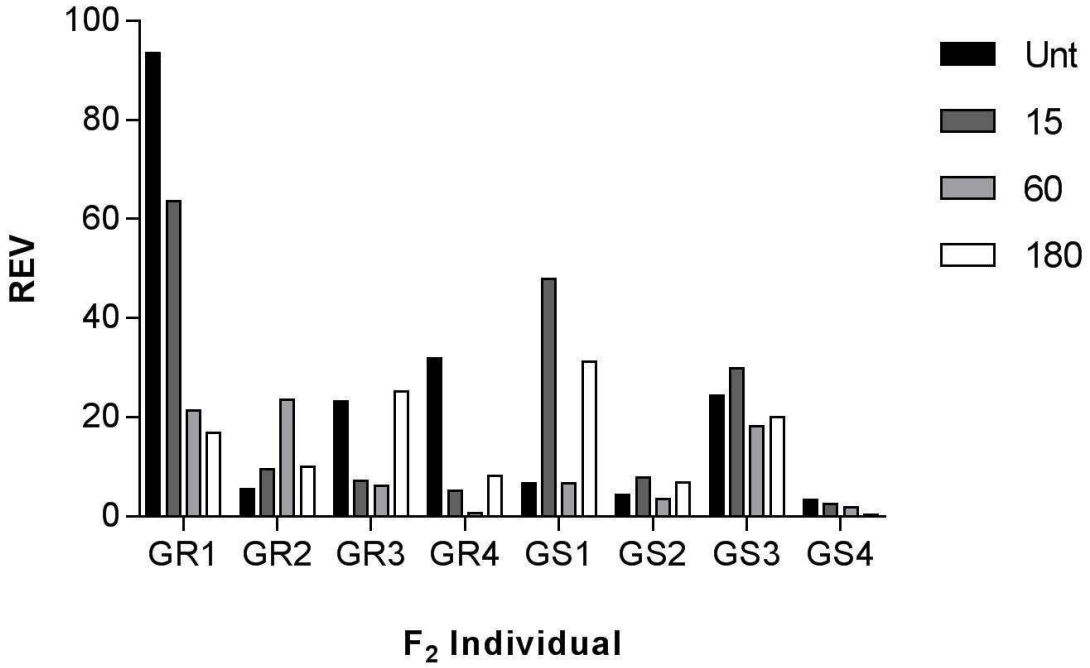

Figure 3.7 Glyphosate-resistant (GR) and -susceptible (GS) expression patterns of OSM34 relative to EF1A in young tissue (A) and mature tissue (B) across untreated and 15, 60 and 180 MAT time points for each individual as relative expression values (REV) from qRT-PCR of F_2 samples.

A.

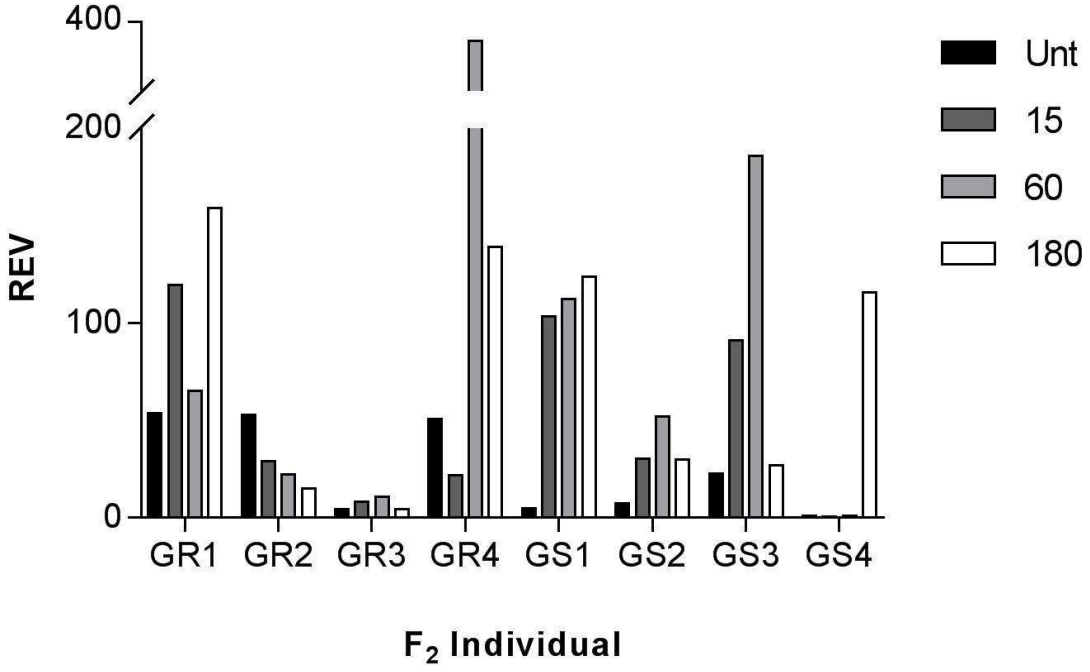

B.

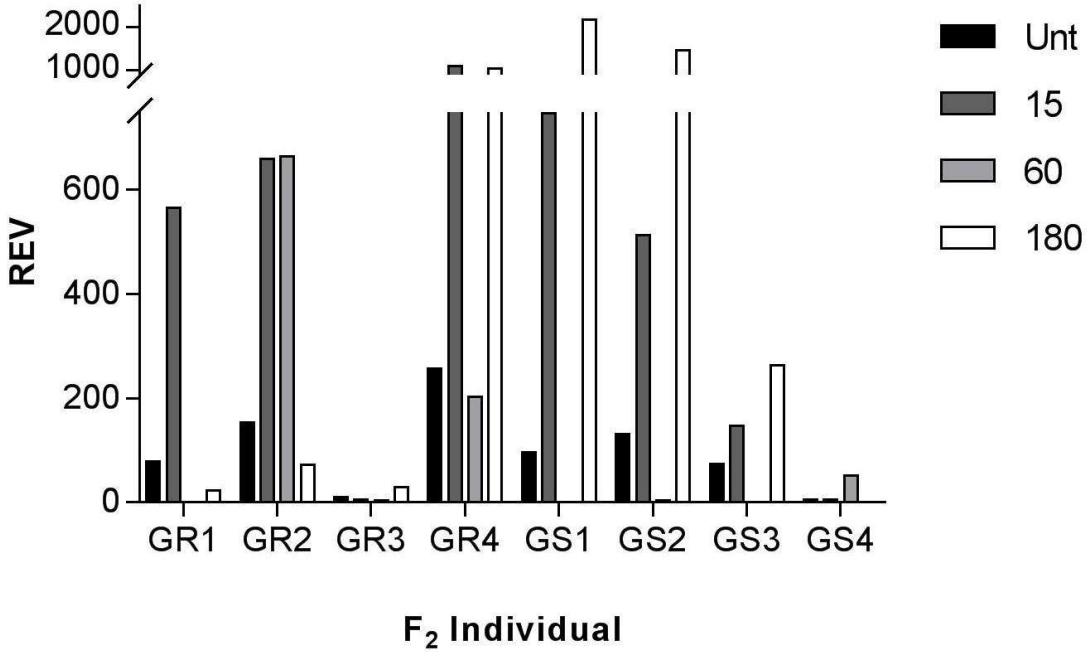

Figure 3.8 Glyphosate-resistant (GR) and -susceptible (GS) expression patterns of SAMS3 relative to EF1A in young tissue (A) and mature tissue (B) across untreated and 15, 60 and 180 MAT time points for each individual as relative expression values (REV) from qRT-PCR of F_2 samples.

CHAPTER 4. CONCLUSIONS

No evidence of a nucleotide mutation was found in a region of the gene encoding the glyphosate target enzyme 5-enolpyruvylshikimate 3-phosphate synthase (EPSPS) across eighteen geographically different giant ragweed accessions, thirteen of which are glyphosate-resistant (GR). Additionally, no evidence for target gene amplification was found in ten GR giant ragweed accessions. Dose response experiments showed differences between GR and glyphosate-susceptible (GS) giant ragweed following glyphosate application. GR biotypes showed a 2.3- to 4.2-fold increase in dry biomass four weeks after glyphosate treatment in comparison to GS biotypes. Levels of resistance between two biotypes of GR giant ragweed exhibiting contrasting phenotypes were similar to each other. Though the level of resistance in both GR biotypes is similar, the drastically different phenotypic response to glyphosate suggests that they have different resistance mechanisms.

Shikimate accumulated in leaf discs excised from young leaves of GS giant ragweed at lower glyphosate doses than GR biotypes. However, similar levels of shikimate accumulated in GS and GR biotypes at higher doses of glyphosate. The leaf disc based shikimate assay provides an indirect measure of glyphosate resistance, as it assumes the accumulation of shikimate is caused by the inhibition of EPSPS by glyphosate. Therefore, the fact that shikimate accumulated in the GR biotypes shows that glyphosate is able to enter the cell and ultimately the chloroplast where it is capable of binding to and inhibiting EPSPS. This result suggests the presence of a mechanism preventing glyphosate from effectively entering the cells or the chloroplasts. The GR slow response biotype has shown no difference in glyphosate absorption or translocation compared to the GS biotype (Glettner, 2013; Norsworthy *et al*., 2011). This could be explained

by the absence or malfunction of a phosphate transporter described to actively transport glyphosate at low concentrations, while at high concentrations, glyphosate moves into the cell through passive diffusion. At the 1 x labeled glyphosate rate, glyphosate may not be at high enough concentrations to move into the cell through passive diffusion allowing the plant to survive, while at higher glyphosate rates, the herbicide is able to reach its target site and the plant is controlled. The GR rapid response biotype has shown differences in glyphosate translocation corresponding with the observed phenotype (Green, 2014; Robertson, 2010). This unique resistance response likely prevents lethal levels of glyphosate to be translocated to the actively growing parts of the plant by rapidly shutting down transpiration and export out of the mature source leaves. Therefore, the remaining glyphosate in living tissues is not present at high enough concentrations to control the plant.

The ability of the GR rapid response biotype to exhibit the same resistance phenotype in the dark with supplemented sucrose as seen under light conditions confirms the rapid response to be a carbon dependent process, not directly reliant on photosynthetic processes taking place under light available conditions. The lack of the rapid response in GR rapid response giant ragweed when high concentrations of Phenylalanine and Tyrosine are supplemented further supports the hypothesis that glyphosate is inhibiting EPSPS and altering the flow of carbon through the shikimate pathway. This result also suggests the rapid response is triggered after EPSPS inhibition, possibly by a secondary signaling molecule associated with a pathway downstream of the shikimate pathway. The rapid accumulation of hydrogen peroxide seen in excised mature leaf discs from GR rapid response treated plants suggests that glyphosate is eliciting a defense or stress response pathway leading to programmed cell death (PCD) of mature tissues in this biotype.

The *de novo* assembled reference transcriptome will provide an invaluable genetic resource for the future of giant ragweed and glyphosate resistance research. Transcriptomics has become a feasible and confident method of quantifying gene expression levels during a variety of plant responses, including herbicide stress. The results of this research provide a significant step in learning more about the way in which plants respond to herbicide stress. RNA-Seq results yielded 27 significant differentially expressed contigs at every treatment time point from the pairwise comparisons of GR young tissue to GS young tissue, GR mature tissue to GS mature tissue and GR young tissue to GR mature tissue. Additionally, 185 contigs showed significant differential expression for at least one treatment time point from the three pairwise comparisons. qRT-PCR used six candidate contigs to positively correlate relative expression values (REV) to FPKM data in validation of RNA-Seq. The forward genetics validation of two candidate contigs using a segregating F_2 population failed to produce significant results correlating candidate contig expression with the segregation of the resistance phenotype. We are working to generate a larger population of F_2 individuals from a reciprocal cross to the first GR X GS cross. We hope to produce a large number of F_1 individuals to screen for resistance as well. This breeding strategy will provide further information about the inheritance of the resistance trait and provide an additional sampling pool for candidate contig testing. We still have a great number of identified candidate contigs that will likely produce an intriguing result. Further analysis of successful candidate genes will require functional validation in a testable system.

In the foreseeable future, herbicides will remain important tools for global weed management as large area farmland continues to rely less on mechanical and cultural weed control methods. In the past 25 years, weed resistance to current herbicides has greatly increased thereby increasing the complexity of weed management decisions. After many years of no

discoveries of new herbicide modes of action, global weed management now relies on a limited number of older herbicides for use in major food crops. The future requires the discovery and development of new herbicide modes of action such as may be uncovered through the research laid out in this PhD thesis on the novel biochemical response of giant ragweed to glyphosate.

REFERENCES

Abdin MZ, Kiran U, Alam A (2011) Analysis of osmotin, a PR protein as metabolic modulator in plants. Bioinformation 5:336-340

Abel A The rotation of weed killers. Pages 249-255

Abul-Faith HA, Bazzaz FA (1979) The biology of *Ambrosia trifida* L. II. Germination, emergence, growth and survival. The New Phytologist 83:817-827

Abul-Fatih H, Bazzaz F, Hunt R (1979) The biology of *Ambrosia trifida* L. New Phytologist 83:829-838

Ali-Rachedi S, Bouinot D, Wagner M-H, Bonnet M, Sotta B, Grappin P, Jullien M (2004) Changes in endogenous abscisic acid levels during dormancy release and maintenance of mature seeds: studies with the Cape Verde Islands ecotype, the dormant model of *Arabidopsis thaliana*. Planta 219:479-488

Amatangelo JR (1974) Infestation of seeds of *Ambrosia trifida*, giant ragweed, by larval insects. Bios:15-18

Amrhein N, Deus B, Gehrke P, Steinrücken HC (1980) The site of the inhibition of the shikimate pathway by glyphosate II. Interference of glyphosate with chorismate formation in vivo and in vitro. Plant Physiol 66:830-834

Anders S, McCarthy DJ, Chen Y, Okoniewski M, Smyth GK, Huber W, Robinson MD (2013) Count-based differential expression analysis of RNA sequencing data using R and Bioconductor. Nature Protocols 8:1765-1786

Apelbaum A, Yang SF (1981) Biosynthesis of stress ethylene induced by water deficit. Plant Physiol 68:594-596

Appleby AP (2005) A history of weed control in the United States and Canada-a sequel. Weed Science 53:762-768

Asada K (2006) Production and scavenging of reactive oxygen species in chloroplasts and their functions. Plant Physiol 141:391-396

Baerson SR, Rodriguez DJ, Tran M, Feng Y, Biest NA, Dill GM (2002) Glyphosate-resistant goosegrass. Identification of a mutation in the target enzyme 5-enolpyruvylshikimate-3-phosphate synthase. Plant Physiol 129:1265-1275

Balagué C, Lin B, Alcon C, Flottes G, Malmström S, Köhler C, Neuhaus G, Pelletier G, Gaymard F, Roby D (2003) HLM1, an essential signaling component in the hypersensitive response, is a member of the cyclic nucleotide–gated channel ion channel family. The Plant Cell Online 15:365-379

Ballard T, Foley M, Bauman T (1996a) Germination, viability, and protein changes during cold stratification of giant ragweed (*Ambrosia trifida* L.) seed. Journal of Plant Physiology 149:229-232

Ballard TO, Foley ME, Bauman TT (1996b) Response of common ragweed (*Ambrosia artemisiifolia*) and giant ragweed (*Ambrosia trifida*) to postemergence imazethapyr. Weed Science:248-251

Barnett KA, Mueller TC, Steckel LE (2013) Glyphosate-resistant giant ragweed (*Ambrosia trifida* L.) control with glufosinate or fomsafen combined with growth regulator herbicides. Weed Technology

Bassett I, Crompton C (1982) The biology of Canadian weeds. *Ambrosia trifida* L. Canadian Journal of Plant Science 62:1003-1010

Bassett IJ, Crompton CW, Parmelee JA (1978) An atlas of airborne pollen grains and common fungus spores of Canada: Printing and Publishing Supply and Services Canada.

Bassham DC (2007) Plant autophagy—more than a starvation response. Current Opinion in Plant Biology 10:587-593

Basu C, Halfhill MD, Mueller TC, Stewart Jr CN (2004) Weed genomics: new tools to understand weed biology. Trends in Plant Science 9:391-398

Baylis AD (2000) Why glyphosate is a global herbicide: strengths, weaknesses and prospects. Pest Management Science 56:299-308

Baysinger JA, Sims BD (1991) Giant ragweed (*Ambrosia trifida*) interference in soybeans (*Glycine max*). Weed Science:358-362

Bell MS, Hager AG, Tranel PJ (2013) Multiple resistance to herbicides from four site-of-action groups in waterhemp (*Amaranthus tuberculatus*). Weed Science 61:460-468

Berg JM, Tymoczko JL, Stryer L (2002) Biochemistry. 5th edn. New York: W H Freeman

Bergelson J, Purrington CB (1996) Surveying patterns in the cost of resistance in plants. American Naturalist:536-558

Boocock MR, Coggins JR (1983) Kinetics of 5-enolpyruvylshikimate-3-phosphate synthase inhibition by glyphosate. FEBS letters 154:127-133

Bostamam Y, Malone JM, Dolman FC, Boutsalis P, Preston C (2012) Rigid ryegrass (*Lolium rigidum*) populations containing a target site mutation in EPSPS and reduced glyphosate translocation are more resistant to glyphosate. Weed Science 60:474-479

Brabham CB, Gerber CK, Johnson WG (2011) Fate of glyphosate-resistant giant ragweed (*Ambrosia trifida*) in the presence and absence of glyphosate. Weed Science 59:506-511

Bradshaw LD, Padgette SR, Kimball SL, Wells BH (1997) Perspectives on glyphosate resistance. Weed Technology:189-198

Bright J, Desikan R, Hancock JT, Weir IS, Neill SJ (2006) ABA-induced NO generation and stomatal closure in *Arabidopsis* are dependent on H2O2 synthesis. The Plant Journal 45:113-122

Bromilow RH, Chamberlain K (2000) The herbicide glyphosate and related molecules: physicochemical and structural factors determining their mobility in phloem. Pest Management Science 56:368-373

Bryson C, DeFelice M (2009) Giant ragweed. Weeds of the South:53

Buchanan B, Gruissen W, Jones R, Malkin R, Niyogi K (2000) Biochemistry and Molecular Biology of Plants. Pp. 568-628

Buchanan BB, Gruissem W, Jones RL (2015) Biochemistry and molecular biology of plants: John Wiley & Sons

Bueso E, Alejandro S, Carbonell P, Perez-Amador MA, Fayos J, Bellés JM, Rodriguez PL, Serrano R (2007) The lithium tolerance of the *Arabidopsis* cat2 mutant reveals a cross-talk between oxidative stress and ethylene. The Plant Journal 52:1052-1065

Caseley JC, Cussans G, Atkin RK (2013) Herbicide resistance in weeds and crops: Elsevier

Chivasa S, Tomé DF, Slabas AR (2013) UDP-glucose pyrophosphorylase is a novel plant cell death regulator. Journal of Proteome Research 12:1743-1753

Comai L, Sen LC, Stalker DM (1983) An altered aroA gene product confers resistance to the herbicide glyphosate. Science 221:370-371

Consortium U (2012) Reorganizing the protein space at the Universal Protein Resource (UniProt). Nucleic Acids Research:D71–D75

Cousens R, Gill G, Speijers EJ (1997) Comment: number of sample populations required to determine the effects of herbicide resistance on plant growth and fitness. Weed Research 37:1-4

Crawford N, Kahn M, Leustek T, Long S, Buchanan B, Gruissem W, Jones R (2000) Biochemistry and Molecular Biology of Plants

Culpepper AS, Grey TL, Vencill WK, Kichler JM, Webster TM, Brown SM, York AC, Davis JW, Hanna WW (2006) Glyphosate-resistant Palmer amaranth (*Amaranthus palmeri*) confirmed in Georgia. Weed Science 54:620-626

Davis AS, Clay S, Cardina J, Dille A, Forcella F, Lindquist J, Sprague C (2013) Seed burial physical environment explains departures from regional hydrothermal model of giant ragweed (*Ambrosia trifida*) seedling emergence in US midwest. Weed Science 61:415-421

Davis VM, Gibson KD, Bauman TT, Weller SC, Johnson WG (2009) Influence of weed management practices and crop rotation on glyphosate-resistant horseweed (*Conyza canadensis*) population dynamics and crop yield-years III and IV. Weed Science 57:417-426

de Carvalho LB, Alves PLdCA, González-Torralva F, Cruz-Hipolito HE, Rojano-Delgado AM, De Prado R, Gil-Humanes J, Barro F, Luque de Castro MaD (2012) Pool of resistance mechanisms to glyphosate in *Digitaria insularis*. J Agric Food Chem 60:615-622

Della-Cioppa G, Bauer SC, Klein BK, Shah DM, Fraley RT, Kishore GM (1986) Translocation of the precursor of 5-enolpyruvylshikimate-3-phosphate synthase into chloroplasts of higher plants in vitro. Proceedings of the National Academy of Sciences 83:6873-6877

della-Cioppa G, Kishore GM (1988) Import of a precursor protein into chloroplasts is inhibited by the herbicide glyphosate. The EMBO Journal 7:1299

Denis MH, Delrot S (1993) Carrier-mediated uptake of glyphosate in broad bean (*Vicia faba*) via a phosphate transporter. Physiologia Plantarum 87:569-575

Dewey SA, Appleby AP (1983) A comparison between glyphosate and assimilate translocation patterns in tall morningglory (*Ipomoea purpurea*). Weed Science:308-314

Dill GM (2005) Glyphosate-resistant crops: history, status and future. Pest Management Science 61:219-224

Dill GM, Sammons RD, Feng PC, Kohn F, Kretzmer K, Mehrsheikh A, Bleeke M, Honegger JL, Farmer D, Wright D (2010) Glyphosate: discovery, development, applications, and properties. Hoboken, NJ, USA: John Wiley and Sons, Inc. Pp. 1-33

Dimmer EC, Huntley RP, Alam-Faruque Y, Sawford T, O'Donovan C, Martin MJ, Bely B, Browne P, Chan WM, Eberhardt R (2012) The UniProt-GO annotation database in 2011. Nucleic Acids Research 40:D565-D570

Dinelli G, Marotti I, Bonetti A, Minelli M, Catizone P, Barnes J (2006) Physiological and molecular insight on the mechanisms of resistance to glyphosate in *Conyza canadensis* (L.) Cronq. biotypes. Pesticide Biochemistry and Physiology 86:30-41

Doke N (1983) Involvement of superoxide anion generation in the hypersensitive response of potato tuber tissues to infection with an incompatible race of *Phytophthora infestans* and to the hyphal wall components. Physiological Plant Pathology 23:345-357

Duke SO (2010) Glyphosate degradation in glyphosate-resistant and-susceptible crops and weeds. J Agric Food Chem 59:5835-5841

Duke SO, Powles SB (2008) Glyphosate: a once-in-a-century herbicide. Pest Management Science 64:319-325

Duke SO, Rimando AM, Pace PF, Reddy KN, Smeda RJ (2003) Isoflavone, glyphosate, and aminomethylphosphonic acid levels in seeds of glyphosate-treated, glyphosate-resistant soybean. J Agric Food Chem 51:340-344

Espartero J, Pintor-Toro JA, Pardo JM (1994) Differential accumulation of S-adenosylmethionine synthetase transcripts in response to salt stress. Plant Molecular Biology 25:217-227

Feng PC, CaJacob CA, Martino-Catt SJ, Cerny RE, Elmore GA, Heck GR, Huang J, Kruger WM, Malven M, Miklos JA (2010) Glyphosate-resistant crops: developing the next generation products. Hoboken, NJ, USA: Wiley

Feng PC, Tran M, Chiu T, Douglas Sammons R, Heck GR, CaJacob CA (2004) Investigations into glyphosate-resistant horseweed (*Conyza canadensis*): retention, uptake, translocation, and metabolism. Weed Science 52:498-505

Fernández-Aparicio M, Huang K, Wafula EK, Honaas LA, Wickett NJ, Timko MP, Yoder J, Westwood JH (2013) Application of qRT-PCR and RNA-Seq analysis for the identification of housekeeping genes useful for normalization of gene expression values during *Striga hermonthica* development. Molecular Biology Reports 40:3395-3407

Fickett ND, Boerboom CM, Stoltenberg DE (2013a) Predicted corn yield loss due to weed competition prior to postemergence herbicide application on Wisconsin farms. Weed Technology 27:54-62

Fickett ND, Boerboom CM, Stoltenberg DE (2013b) Soybean yield loss potential associated with early-season weed competition across 64 site-years. Weed Science 61:500-507

Finch-Savage WE, Leubner-Metzger G (2006) Seed dormancy and the control of germination. New Phytologist 171:501-523

Frankton C (1970) Weeds of Canada. Canadian Department of Agriculture 948:217

Franz JE, Mao MK, Sikorski JA (1997) Glyphosate: a unique global herbicide: American Chemical Society

Fu YM, Lin H, Liu X, Fang W, Meadows GG (2010) Cell death of prostate cancer cells by specific amino acid restriction depends on alterations of glucose metabolism. Journal of Cellular Physiology 224:491-500

Gaines C, Byng G, Whitaker R, Jensen R (1982) L-Tyrosine regulation and biosynthesis via arogenate dehydrogenase in suspension-cultured cells of *Nicotiana silvestris* Speg. et Comes. Planta 156:233-240

Gaines TA, Lorentz L, Figge A, Herrmann J, Maiwald F, Ott MC, Han H, Busi R, Yu Q, Powles SB (2014) RNA-Seq transcriptome analysis to identify genes involved in metabolism-based diclofop resistance in *Lolium rigidum*. The Plant Journal 78:865-876

Gaines TA, Shaner DL, Ward SM, Leach JE, Preston C, Westra P (2011) Mechanism of resistance of evolved glyphosate-resistant Palmer amaranth (*Amaranthus palmeri*). J Agric Food Chem 59:5886-5889

Gaines TA, Zhang W, Wang D, Bukun B, Chisholm ST, Shaner DL, Nissen SJ, Patzoldt WL, Tranel PJ, Culpepper AS, Grey TL, Webster TM, Vencill WK, Sammons RD, Jiang J, Preston C, Leach JE, Westra P (2010) Gene amplification confers glyphosate resistance in *Amaranthus palmeri*. Proceedings of the National Academy of Sciences 107:1029-1034

Gao Y, Xu H, Shen Y, Wang J (2013) Transcriptomic analysis of rice (*Oryza sativa*) endosperm using the RNA-Seq technique. Plant Molecular Biology 81:363-378

Ge X, d'Avignon DA, Ackerman JJ, Duncan B, Spaur MB, Sammons RD (2011) Glyphosate-resistant horseweed made sensitive to glyphosate: low-temperature suppression of glyphosate vacuolar sequestration revealed by 31P NMR. Pest Management Science 67:1215-1221

Ge X, d'Avignon DA, Ackerman JJ, Sammons RD (2010) Rapid vacuolar sequestration: the horseweed glyphosate resistance mechanism. Pest Management Science 66:345-348

Ge X, d'Avignon DA, Ackerman JJ, Collavo A, Sattin M, Ostrander EL, Hall EL, Sammons RD, Preston C (2012) Vacuolar glyphosate-sequestration correlates with glyphosate resistance in ryegrass (*Lolium spp.*) from Australia, South America, and Europe: a 31P NMR investigation. J Agric Food Chem 60:1243-1250

Geiger DR, Kapitan SW, Tucci MA (1986) Glyphosate inhibits photosynthesis and allocation of carbon to starch in sugar beet leaves. Plant Physiol 82:468-472

Ghosh B, Perry MP, Marsh DG (1991) Cloning the cDNA encoding the AmbtV allergen from giant ragweed (*Ambrosia trifida*) pollen. Gene 101:231-238

Giacomini D, Westra P, Ward SM (2014) Impact of genetic background in fitness cost studies: an example from glyphosate-resistant Palmer amaranth. Weed Science 62:29-37

Giacomini DA (2015) EPSPS Gene Duplication in Palmer Amaranth: Relative Fitness, Inheritance, and Duplication Mechanism of the Glyphosate Resistance Trait: Colorado State University. Libraries

Gibson KD, Johnson WG, Hillger DE (2005) Farmer Perceptions of Problematic Corn and Soybean Weeds in Indiana. Weed Technology 19:1065-1070

Giesy JP, Dobson S, Solomon KR (2000) Ecotoxicological risk assessment for Roundup® herbicide: Springer

Glettner CE (2013) Physiology, growth, and fecundity of glyphosate-resistant giant ragweed (*Ambrosia trifida* L.) in Wisconsin

Glettner CE, Stoltenberg DE (2015) Noncompetitive growth and fecundity of Wisconsin giant ragweed resistant to glyphosate. Weed Science 63:273-281

Gong B, Li X, VandenLangenberg KM, Wen D, Sun S, Wei M, Li Y, Yang F, Shi Q, Wang X (2014) Overexpression of S-adenosyl-l-methionine synthetase increased tomato tolerance to alkali stress through polyamine metabolism. Plant Biotechnology Journal 12:694-708

Gottrup O, O'sullivan P, Schraa R, Vanden W (1976) Uptake, translocation, metabolism and selectivity of glyphosate in Canada thistle and leafy spurge. Weed Research 16:197-201

Gougler JA, Geiger DR (1981) Uptake and distribution of N-phosphonomethylglycine in sugar beet plants. Plant Physiol 68:668-672

Gramig GG, Stoltenberg DE (2007) Leaf appearance base temperature and phyllochron for common grass and broadleaf weed species. Weed Technology 21: 249-254

Green AC (2014) Confirmation and mechanism of resistance to glyphosate in giant ragweed (*Ambrosia trifida*) in Ontario. Master of Science. Guelph, Ontario, Canada: The University of Guelph. 81 p

Green AC, Tardif FJ, Sikkema PH Mechanisms of resistance to glyphosate in giant ragweed (*Ambrosia trifida* L.) in Ontario. Pages 30. Niagara Falls, ON, CA

Green JM (2009) Evolution of glyphosate-resistant crop technology. Weed Science 57:108-117

Gresshoff P (1979) Growth inhibition by glyphosate and reversal of its action by phenylalanine and tyrosine. Functional Plant Biology 6:177-185

Grossbard E, Atkinson D (1985) The Herbicide Glyphosate: Butterworths

Grün S, Lindermayr C, Sell S, Durner J (2006) Nitric oxide and gene regulation in plants. J Exp Bot 57:507-516

Guimarães A, Ferreira E, Vargas L, Silva A, Viana R, Demuner A, Concenço G, Aspiazu I, Galon L, Reis M (2009) Chemical composition of the epicuticular wax of Italian ryegrass biotypes resistant and susceptible to glyphosate. Planta Daninha 27:149-154

Guo Y, Li C-I, Ye F, Shyr Y (2013) Evaluation of read count based RNAseq analysis methods. BMC Genomics 14:1

Guo Z, Tan J, Zhuo C, Wang C, Xiang B, Wang Z (2014) Abscisic acid, H2O2 and nitric oxide interactions mediated cold-induced S-adenosylmethionine synthetase in *Medicago sativa* subsp. *falcata* that confers cold tolerance through up-regulating polyamine oxidation. Plant Biotechnology Journal 12:601-612

Haas BJ, Papanicolaou A, Yassour M, Grabherr M, Blood PD, Bowden J, Couger MB, Eccles D, Li B, Lieber M (2013) De novo transcript sequence reconstruction from RNA-seq using the Trinity platform for reference generation and analysis. Nature Protocols 8:1494-1512

Halfhill MD, Good LL, Basu C, Burris J, Main CL, Mueller TC, Stewart Jr CN (2007) Transformation and segregation of GFP fluorescence and glyphosate resistance in horseweed (*Conyza canadensis*) hybrids. Plant Cell Reports 26:303-311

Hall MR, Swanton CJ, Anderson GW (1992) The critical period of weed control in grain corn (*Zea mays*). Weed Science:441-447

Hansen A (1976) *Ambrosia* L. Flora Europaea 4:142-143

Harre NT, Johnson WG, Young BG Does the rapid necrosis response in glyphosate-resistant giant ragweed reduce efficacy of glyphosate tank-mixtures? Pages 410. San Juan, Puerto Rico

Harrison S, Regnier E, Schmoll J, Harrison J (2007) Seed size and burial effects on giant ragweed (*Ambrosia trifida*) emergence and seed demise. Weed Science 55:16-22

Harrison SK, Regnier EE, Schmoll JT (2003) Postdispersal predation of giant ragweed (*Ambrosia trifida*) seed in no-tillage corn. Weed Science 51:955-964

Harrison SK, Regnier EE, Schmoll JT, Webb JE (2001) Competition and fecundity of giant ragweed in corn. Weed Science

Hartnett DC, Hartnett BB, Bazzaz FA (1987) Persistence of *Ambrosia trifida* populations in old fields and responses to successional changes. American Journal of Botany:1239-1248

Harvey B, Spence L, Crothers S (1985) Pre-harvest retting of flax with glyphosate: effect of growth stage at application on uptake, translocation and efficacy of glyphosate. Annals of Applied Biology 107:263-270

Hay J (1974) Gains to the grower from weed science. Weed Science:439-442

Heap I (2005) Criteria for Confirmation of Herbicide-Resistant Weeds - with specific emphasis on confirming low level resistance. http://weedscience.org/documents/resistancecriterion.pdf.

Heap I (2014) Herbicide Resistant Weeds. Pages 281-301 Integrated Pest Management: Springer

Heap I (2016) The International Survey of Herbicide Resistant Weeds. www.weedscience.org. Accessed February 23, 2016

Heath MC (2000) Hypersensitive response-related death. Pages 77-90 Programmed Cell Death in Higher Plants: Springer

Herrmann KM (1995) The shikimate pathway: early steps in the biosynthesis of aromatic compounds. Plant Cell 7:907

Herrmann KM, Weaver LM (1999) The shikimate pathway. Annual Review of Plant Biology 50:473-503

Hetherington P, Marshall G, Kirkwood R, Warner J (1998) Absorption and efflux of glyphosate by cell suspensions. J Exp Bot 49:527-533

Holländer H, Amrhein N (1980) The site of the inhibition of the shikimate pathway by glyphosate I. Inhibition by glyphosate of phenylpropanoid synthesis in buckwheat (*Fagopyrum esculentum* Moench). Plant Physiol 66:823-829

Holt JS, Lebaron HM (1990) Significance and distribution of herbicide resistance. Weed Technology:141-149

Holt JS, Powles SB, Holtum JA (1993) Mechanisms and agronomic aspects of herbicide resistance. Annual Review of Plant Biology 44:203-229

Horvath DP, Hansen SA, Moriles-Miller JP, Pierik R, Yan C, Clay DE, Scheffler B, Clay SA (2015) RNAseq reveals weed-induced PIF3-like as a candidate target to manipulate weed stress response in soybean. New Phytologist 207:196-210

Hoss NE, Al-Khatib K, Peterson DE, Loughin TM (2003) Efficacy of glyphosate, glufosinate, and imazethapyr on selected weed species. Weed Science 51:110-117

Jachetta JJ, Appleby AP, Boersma L (1986) Apoplastic and symplastic pathways of atrazine and glyphosate transport in shoots of seedling sunflower. Plant Physiol 82:1000-1007

Jalaludin A, Han H, Yu Q, Powles S Evolution in action: a double amino acid substitution in the EPSPS gene endows high-level glyphosate resistance. Perth

Jasieniuk M, Ahmad R, Sherwood AM, Firestone JL, Perez-Jones A, Lanini WT, Mallory-Smith C, Stednick Z (2008) Glyphosate-resistant Italian ryegrass (*Lolium multiflorum*) in California: distribution, response to glyphosate, and molecular evidence for an altered target enzyme. Weed Science 56:496-502

Jasieniuk M, Brûlé-Babel AL, Morrison IN (1996) The evolution and genetics of herbicide resistance in weeds. Weed Science:176-193

Jensen RA (1986) The shikimate/arogenate pathway: link between carbohydrate metabolism and secondary metabolism. Physiologia Plantarum 66:164-168

Johnson B, Loux M, Nordby D, Sprague C, Nice G, Westhoven A, Stachler J (2006) Biology and management of giant ragweed. Purdue Extension Publication GWC-12

Johnson KA, Goody RS (2011) The original Michaelis constant: translation of the 1913 Michaelis–Menten paper. Biochemistry 50:8264-8269

Johnson W, Ott E, Gibson K, Nielsen R, Bauman T (2007) Influence of nitrogen application timing on low density giant ragweed (*Ambrosia trifida*) interference in corn. Weed Technology 21:763-767

Katoh A, Uenohara K, Akita M, Hashimoto T (2006) Early steps in the biosynthesis of NAD in *Arabidopsis* start with aspartate and occur in the plastid. Plant Physiol 141:851-857

Kaundun SS, Dale RP, Zelaya IA, Dinelli G, Marotti I, McIndoe E, Cairns A (2011) A novel P106L mutation in EPSPS and an unknown mechanism (s) act additively to confer resistance to glyphosate in a South African *Lolium rigidum* population. J Agric Food Chem 59:3227-3233

Kaurilind E, Xu E, Brosché M (2015) A genetic framework for H2O2 induced cell death in *Arabidopsis thaliana*. BMC Genomics 16:837

Knezevic SZ, Streibig JC, Ritz C (2007) Utilizing R software package for dose-response studies: the concept and data analysis. Weed Technology 21:840-848

Koger CH, Shaner DL, Henry WB, Nadler-Hassar T, Thomas WE, Wilcut JW (2005) Assessment of two nondestructive assays for detecting glyphosate resistance in horseweed (*Conyza canadensis*). Weed Science 53:559-566

Kong C-H, Wang P, Xu X-H (2007) Allelopathic interference of *Ambrosia trifida* with wheat (*Triticum aestivum*). Agriculture, Ecosystems & Environment 119:416-420

Kong CH (2010) Ecological pest management and control by using allelopathic weeds (*Ageratum conyzoides*, *Ambrosia trifida*, and *Lantana camara*) and their allelochemicals in China. Weed Biology and Management 10:73-80

Kovach J, Petzoldt C, Degni J, Tette J (1992) A method to measure the environmental impact of pesticides. New York's Food and Life Sciences Bulletin

Krouk G, Carré C, Fizames C, Gojon A, Ruffel S, Lacombe B (2015) GeneCloud reveals semantic enrichment in lists of gene descriptions. Molecular Plant 8:971-973

Kumar SA, Kumari PH, Kumar GS, Mohanalatha C, Kishor PK (2015) Osmotin: a plant sentinel and a possible agonist of mammalian adiponectin. Frontiers in Plant Science 6

Lai Z, Wang F, Zheng Z, Fan B, Chen Z (2011) A critical role of autophagy in plant resistance to necrotrophic fungal pathogens. The Plant Journal 66:953-968

Lam E, Kato N, Lawton M (2001) Programmed cell death, mitochondria and the plant hypersensitive response. Nature 411:848-853

LeBaron HM (1991) Herbicide Resistance in Weeds and Crops. Oxford: Butterworth-Heinemann. Pp. 27-43

Lee H, Damsz B, Woloshuk CP, Bressan RA, Narasimhan ML (2010) Use of the plant defense protein osmotin to identify *Fusarium oxysporum* genes that control cell wall properties. Eukaryotic Cell 9:558-568

Lee LJ, Ngim J (2000) A first report of glyphosate-resistant goosegrass (*Eleusine indica* (L) Gaertn) in Malaysia. Pest Management Science 56:336-339

Lenz HD, Haller E, Melzer E, Kober K, Wurster K, Stahl M, Bassham DC, Vierstra RD, Parker JE, Bautor J (2011) Autophagy differentially controls plant basal immunity to biotrophic and necrotrophic pathogens. The Plant Journal 66:818-830

Leslie T, Baucom RS (2014) De novo assembly and annotation of the transcriptome of the agricultural weed *Ipomoea purpurea* uncovers gene expression changes associated with herbicide resistance. G3: Genes| Genomes| Genetics 4:2035-2047

Lespérance M, Costea M, Sikkema PH, Tardif FJ Subcellular effects of glyphosate in glyphosate resistant giant ragweed. Pages 434. San Juan, PR

Levine DM, Berenson ML, Stephan D (1999) Statistics for managers using Microsoft Excel: Prentice Hall Upper Saddle River, NJ

Lim CC, Liu JZ, Pua EC (2002) Characterization of S-adenosylmethionine synthetase genes and its expression is associated with ethylene synthesis in mustard (*Brassica juncea*). Physiologia Plantarum 116:522-530

Lister R, Gregory BD, Ecker JR (2009) Next is now: new technologies for sequencing of genomes, transcriptomes, and beyond. Current Opinion in Plant Biology 12:107-118

Liu W-Y, Chang Y-M, Chen SC-C, Lu C-H, Wu Y-H, Lu M-YJ, Chen D-R, Shih AC-C, Sheue C-R, Huang H-C (2013) Anatomical and transcriptional dynamics of maize embryonic leaves during seed germination. Proceedings of the National Academy of Sciences 110:3979-3984

Liu Y, Bassham DC (2012) Autophagy: pathways for self-eating in plant cells. Annual Review of Plant Biology 63:215-237

Liu Y, Ren D, Pike S, Pallardy S, Gassmann W, Zhang S (2007) Chloroplast-generated reactive oxygen species are involved in hypersensitive response-like cell death mediated by a mitogen-activated protein kinase cascade. The Plant Journal 51:941-954

Livak KJ, Schmittgen TD (2001) Analysis of relative gene expression data using real-time quantitative PCR and the $2^{-\Delta\Delta CT}$ method. Methods 25:402-408

Lorraine-Colwill D, Powles S, Hawkes T, Hollinshead P, Warner S, Preston C (2002) Investigations into the mechanism of glyphosate resistance in *Lolium rigidum*. Pesticide Biochemistry and Physiology 74:62-72

Loux MM, Berry MA (1991) Use of a grower survey for estimating weed problems. Weed Technology:460-466

McAllister R, Haderlie L (1985) Translocation of 14C-glyphosate and 14CO2-labeled photoassimilates in Canada thistle (*Cirsium arvense*). Weed Science

Michaeli S, Galili G, Genschik P, Fernie AR, Avin-Wittenberg T (2015) Autophagy in plants–what's new on the menu? Trends in Plant Science

Michaelis L, Menten ML (1913) Die kinetik der invertinwirkung. Biochemistry 49:352

Michitte P, De Prado R, Espinoza N, Pedro Ruiz-Santaella J, Gauvrit C (2007) Mechanisms of resistance to glyphosate in a ryegrass (*Lolium multiflorum*) biotype from Chile. Weed Science 55:435-440

Michitte P, Gauvrit C, Heredia A, De Prado R Resistance to glyphosate in *Lolium multiflorum*: involvement of epicuticular waxes. Pages 597-602

Mittler R (2002) Oxidative stress, antioxidants and stress tolerance. Trends in Plant Science 7:405-410

Mittler R, Lam E, Shulaev V, Cohen M (1999) Signals controlling the expression of cytosolic ascorbate peroxidase during pathogen-induced programmed cell death in tobacco. Plant Molecular Biology 39:1025-1035

Monaco TJ, Weller SC, Ashton FM (2002) Weed Science: Principles and Practices: John Wiley & Sons

Morin F, Vera V, Nurit F, Tissut M, Marigo G (1997) Glyphosate uptake in *Catharanthus roseuscells* Role of a phosphate transporter. Pesticide Biochemistry and Physiology 58:13-22

Mueller TC, Massey JH, Hayes RM, Main CL, Stewart CN (2003) Shikimate accumulates in both glyphosate-sensitive and glyphosate-resistant horseweed (*Conyza canadensis* L. Cronq.). J Agric Food Chem 51:680-684

Mur LA (2007) Hypersensitive response in plants. Encyclopedia of Life Sciences

Mur LA, Kenton P, Lloyd AJ, Ougham H, Prats E (2008) The hypersensitive response; the centenary is upon us but how much do we know? J Exp Bot 59:501-520

Nafziger ED, Widholm JM, Steinrücken HC, Killmer JL (1984) Selection and characterization of a carrot cell line tolerant to glyphosate. Plant Physiol 76:571-574

Nandula VK (2010) Glyphosate Resistance in Crops and Weeds: History, Development, and Management: John Wiley & Sons

Nandula VK, Ray JD, Ribeiro DN, Pan Z, Reddy KN (2013) Glyphosate resistance in tall waterhemp (*Amaranthus tuberculatus*) from Mississippi is due to both altered target-site and nontarget-site mechanisms. Weed Science 61:374-383

Nandula VK, Reddy KN, Poston DH, Rimando AM, Duke SO (2008) Glyphosate tolerance mechanism in Italian ryegrass (*Lolium multiflorum*) from Mississippi. Weed Science 56:344-349

Nandula VK, Wright AA, Van Horn CR, Molin WT, Westra P, Reddy KN (2015) Glyphosate resistance in giant ragweed (*Ambrosia trifida* L.) from mississippi is partly due to reduced translocation. American Journal of Plant Sciences 6:2104

Ng C, Wickneswari R, Salmijah S, Teng Y, Ismail B (2003) Gene polymorphisms in glyphosate-resistant and-susceptible biotypes of *Eleusine indica* from Malaysia. Weed Research 43:108-115

Ng C, Wickneswary R, Salmijah S, Teng Y, Ismail B (2004) Glyphosate resistance in *Eleusine indica* (L.) Gaertn. from different origins and polymerase chain reaction amplification of specific alleles. Crop and Pasture Science 55:407-414

Norsworthy JK, Jha P, Steckel LE, Scott RC (2010) Confirmation and control of glyphosate-resistant giant ragweed (*Ambrosia trifida*) in Tennessee. Weed Technology 24:64-70

Norsworthy JK, Riar D, Jha P, Scott RC (2011) Confirmation, control, and physiology of glyphosate-resistant giant ragweed (*Ambrosia trifida*) in Arkansas. Weed Technology 25:430-435

O'Rourke JA, Yang SS, Miller SS, Bucciarelli B, Liu J, Rydeen A, Bozsoki Z, Uhde-Stone C, Tu ZJ, Allan D (2013) An RNA-Seq transcriptome analysis of orthophosphate-deficient white lupin reveals novel insights into phosphorus acclimation in plants. Plant Physiol 161:705-724

Owen MD, Zelaya IA (2005) Herbicide-resistant crops and weed resistance to herbicides. Pest Management Science 61:301-311

Padgette S, Re DB, Gasser C, Eichholtz DA, Frazier R, Hironaka CM, Levine EB, Shah DM, Fraley RT, Kishore GM (1991) Site-directed mutagenesis of a conserved region of the 5-enolpyruvylshikimate-3-phosphate synthase active site. Journal of Biological Chemistry 266:22364-22369

Padmanabhan KR, Segobye K, Weller SC, Schulz B, Gribskov M (2016) Preliminary investigation of glyphosate resistance mechanism in giant ragweed using transcriptome analysis. F1000Research

Patel S, Dinesh-Kumar SP (2008) Arabidopsis ATG6 is required to limit the pathogen-associated cell death response. Autophagy 4:20-27

Pedersen BP, Neve P, Andreasen C, Powles SB (2007) Ecological fitness of a glyphosate-resistant *Lolium rigidum* population: growth and seed production along a competition gradient. Basic and Applied Ecology 8:258-268

Perez-Jones A, Park KW, Colquhoun J, Mallory-Smith C, Shaner D (2005) Identification of glyphosate-resistant Italian ryegrass (*Lolium multiflorum*) in Oregon. Weed Science 53:775-779

Pérez-Pérez ME, Lemaire SD, Crespo JL (2012) Reactive oxygen species and autophagy in plants and algae. Plant Physiol 160:156-164

Peterson GE (1967) The discovery and development of 2, 4-D. Agricultural History:243-254

Pfaffl MW (2001) A new mathematical model for relative quantification in real-time RT–PCR. Nucleic Acids Research 29:e45-e45

Pline-Srnic W (2006) Physiological mechanisms of glyphosate resistance Weed Technology 20:290-300

Potter TL, Truman CC, Bosch DD, Bednarz C (2004) Fluometuron and pendimethalin runoff from strip and conventionally tilled cotton in the southern Atlantic Coastal Plain. Journal of Environmental Quality 33:2122-2131

Powles SB (2008) Evolved glyphosate-resistant weeds around the world: lessons to be learnt. Pest Management Science 64:360-365

Powles SB, Lorraine-Colwill DF, Dellow JJ, Preston C (1998) Evolved resistance to glyphosate in rigid ryegrass (*Lolium rigidum*) in Australia. Weed Science:604-607

Powles SB, Preston C (2006) Evolved glyphosate resistance in plants: biochemical and genetic basis of resistance Weed Technology 20:282-289

Powles SB, Yu Q (2010) Evolution in action: plants resistant to herbicides. Annual Review of Plant Biology 61:317-347

Powles SO, Duke SB (2010) Glyphosate-resistant crops and weeds: now and in the future. AgBioForum 12:346-357

Preston C, Powles S (2002) Evolution of herbicide resistance in weeds: initial frequency of target site-based resistance to acetolactate synthase-inhibiting herbicides in *Lolium rigidum*. Heredity 88:8-13

Preston C, Wakelin AM, Dolman FC, Bostamam Y, Boutsalis P (2009) A decade of glyphosate-resistant *Lolium* around the world: Mechanisms, genes, fitness, and agronomic management. Weed Science 57:435-441

Price WJ, Shafii B, Seefeldt SS (2012) Estimation of dose-response models for discrete and continuous data in weed science. Weed Technology 26:587-601

Purrington CB (2000) Costs of resistance. Current Opinion in Plant Biology 3:305-308

Putnam A (1976) Fate of glyphosate in deciduous fruit trees. Weed Science:425-430

Rao VS (2000) Principles of Weed Science: CRC Press

Raynor GS, Ogden EC, Hayes JV (1970) Dispersion and deposition of ragweed pollen from experimental sources. Journal of Applied Meteorology 9:885-895

Reddy KN, Norsworthy JK, Nandula V (2010) Glyphosate Resistance in Crops and Weeds: History, Development, and Management: John Wiley & Sons. Pp. 165-184

Reggiori F, Klionsky DJ (2013) Autophagic processes in yeast: mechanism, machinery and regulation. Genetics 194:341-361

Regnier E, Harrison S, Liu J, Schmoll J, Edwards C, Arancon N, Holloman C (2008) Impact of an exotic earthworm on seed dispersal of an indigenous US weed. Journal of Applied Ecology 45:1621-1629

Ritz C, Streibig JC (2005) Bioassay analysis using R. Journal of Statistical Software 12:1-22

Robertson RR (2010) Physiological and biochemical characterization of glyphosate resistant *Ambrosia trifida* L: Purdue University. 87 p

Robins W, Graft A, Raynor R (1952) Weed control. Weed Control

Robinson MD, Smyth GK (2008) Small-sample estimation of negative binomial dispersion, with applications to SAGE data. Biostatistics 9:321-332

Rojas CM, Senthil-Kumar M, Tzin V, Mysore KS (2014) Regulation of primary plant metabolism during plant-pathogen interactions and its contribution to plant defense. Frontiers in Plant Science 5

Roush ML, Radosevich SR, Maxwell BD (1990) Future outlook for herbicide-resistance research. Weed Technology:208-214

Rubin JL, Gaines CG, Jensen RA (1982) Enzymological basis for herbicidal action of glyphosate. Plant Physiol 70:833-839

Ryals JA, Neuenschwander UH, Willits MG, Molina A, Steiner H-Y, Hunt MD (1996) Systemic acquired resistance. Plant Cell 8:1809

Ryan G (1970) Resistance of common groundsel to simazine and atrazine. Weed Science:614-616

Salas RA, Dayan FE, Pan Z, Watson SB, Dickson JW, Scott RC, Burgos NR (2012) EPSPS gene amplification in glyphosate-resistant Italian ryegrass (*Lolium perenne ssp*. multiflorum) from Arkansas. Pest Management Science 68:1223-1230

Salzmann D, Handley RJ, Müller-Schärer H (2008) Functional significance of triazine-herbicide resistance in defence of *Senecio vulgaris* against a rust fungus. Basic and Applied Ecology 9:577-587

Sammons RD, Gaines TA (2014) Glyphosate resistance: state of knowledge. Pest Management Science

Sandberg C, Meggitt W, Penner D (1980) Absorption, translocation and metabolism of 14C-glyphosate in several weed species. Weed Research 20:195-200

Schmittgen TD, Livak KJ (2008) Analyzing real-time PCR data by the comparative CT method. Nature Protocols 3:1101-1108

Schönbrunn E, Eschenburg S, Shuttleworth WA, Schloss JV, Amrhein N, Evans JN, Kabsch W (2001) Interaction of the herbicide glyphosate with its target enzyme 5-enolpyruvylshikimate 3-phosphate synthase in atomic detail. Proceedings of the National Academy of Sciences 98:1376-1380

Schutte BJ, Regnier EE, Harrison SK (2012) Seed dormancy and adaptive seedling emergence timing in giant ragweed (*Ambrosia trifida*). Weed Science 60:19-26

Schutte BJ, Regnier EE, Harrison SK, Schmoll JT, Spokas K, Forcella F (2008) A hydrothermal seedling emergence model for giant ragweed (*Ambrosia trifida*). Weed Science 56:555-560

Segobye K (2013) Biology and ecology of glyphosate-resistant giant ragweed (*Ambrosia trifida* L.): Purdue University

Servaites JC, Tucci MA, Geiger DR (1987) Glyphosate effects on carbon assimilation, ribulose bisphosphate carboxylase activity, and metabolite levels in sugar beet leaves. Plant Physiol 85:370-374

Shaner D, Caseley J, Cussans G, Atkin R (2013) Herbicide Resistance in Weeds and Crops: Elsevier

Shaner DL (2000) The impact of glyphosate-tolerant crops on the use of other herbicides and on resistance management. Pest Management Science 56:320-326

Shaner DL (2009) Role of translocation as a mechanism of resistance to glyphosate. Weed Science 57:118-123

Shaner DL, Lindenmeyer RB, Ostlie MH (2012) What have the mechanisms of resistance to glyphosate taught us? Pest Management Science 68:3-9

Shaner DL, Nadler-Hassar T, Henry WB, Koger CH (2005) A rapid in vivo shikimate accumulation assay with excised leaf discs. Weed Science 53:769-774

Shrestha A, Hanson BD, Fidelibus MW, Alcorta M (2010) Growth, phenology, and intraspecific competition between glyphosate-resistant and glyphosate-susceptible horseweeds (*Conyza canadensis*) in the San Joaquin Valley of California. Weed Science 58:147-153

Siehl D (1997) Inhibitors of EPSP synthase, glutamine synthetase and histidine synthesis. Reviews in Toxicology 1:37-68

Siehl DL, Castle LA, Gorton R, Keenan RJ (2007) The molecular basis of glyphosate resistance by an optimized microbial acetyltransferase. Journal of Biological Chemistry 282:11446-11455

Sikkema P, Soltani N, Shropshire C, Smith P, Lawton M, Tardif F Suspected glyphosate-resistant giant ragweed in Ontario. Pages 167

Simarmata M, Kaufmann JE, Penner D (2003) Potential basis of glyphosate resistance in California rigid ryegrass (*Lolium rigidum*). Weed Science 51:678-682

Singh BK, Shaner DL (1998) Rapid determination of glyphosate injury to plants and identification of glyphosate-resistant plants. Weed Technology:527-530

Smart CC, Johänning D, Müller G, Amrhein N (1985) Selective overproduction of 5-enol-pyruvylshikimic acid 3-phosphate synthase in a plant cell culture which tolerates high doses of the herbicide glyphosate. Journal of Biological Chemistry 260:16338-16346

Stachler J, Loux M, Johnson W, Westhoven A Management of giant ragweed populations that are difficult to control with glyphosate. Pages 226

Stachler JM (2008) Characterization and management of glyphosate-resistant giant ragweed (*Ambrosia trifida* L.) and horseweed [*Conyza canadensis* (L.) Cronq.]: The Ohio State University. 124 p

Stakman E (1915) Relation between *Puccinia graminis* and plants highly resistant to its attack. Journal of Agricultural Research:193-200

Stalker DM, Hiatt WR, Comai L (1985) A single amino acid substitution in the enzyme 5-enolpyruvylshikimate-3-phosphate synthase confers resistance to the herbicide glyphosate. Journal of Biological Chemistry 260:4724-4728

Stallings WC, Abdel-Meguid SS, Lim LW, Shieh H-S, Dayringer HE, Leimgruber NK, Stegeman RA, Anderson KS, Sikorski JA, Padgette SR (1991) Structure and topological symmetry of the glyphosate target 5-enolpyruvylshikimate-3-phosphate synthase: a distinctive protein fold. Proceedings of the National Academy of Sciences 88:5046-5050

Steinrücken H, Amrhein N (1980) The herbicide glyphosate is a potent inhibitor of 5-enolpyruvylshikimic acid-3-phosphate synthase. Biochemical and Biophysical Research Communications 94:1207-1212

Steinrucken HC, Schulz A, Amrhein N, Porter CA, Fraley RT (1986) Overproduction of 5-enolpyruvylshikimate-3-phosphate synthase in a glyphosate-tolerant Petunia hybrida cell line. Archives of biochemistry and biophysics 244:169-78

Stintzi A, Heitz T, Kauffmann S, Legrand M, Fritig B (1991) Identification of a basic pathogenesis-related, thaumatin-like protein of virus-infected tobacco as osmotin. Physiological and Molecular Plant Pathology 38:137-146

Stoller E, Wax L (1974) Dormancy changes and fate of some annual weed seeds in the soil. Weed Science:151-155

Stoltenberg D, Sivesind E, Jeschke M Cropping system effects on giant ragweed. Pages 162

Suh H, Hepburn AG, Kriz AL, Widholm JM (1993) Structure of the amplified 5-enolpyruvylshikimate-3-phosphate synthase gene in glyphosate-resistant carrot cells. Plant Molecular Biology 22:195-205

Swanton CJ, Weise SF (1991) Integrated weed management: the rationale and approach. Weed Technology:657-663

Swarbreck D, Wilks C, Lamesch P, Berardini TZ, Garcia-Hernandez M, Foerster H, Li D, Meyer T, Muller R, Ploetz L (2008) The *Arabidopsis* Information Resource (TAIR): gene structure and function annotation. Nucleic Acids Research 36:D1009-D1014

TAIR (2016) The *Arabidopsis* Information Resource. www.arabidopsis.org. Accessed June, 20, 2016

Thompson JA (2012) The influence of environment and spray dose on the growth and fitness of glyphosate-resistant and-susceptible giant ragweed (*Ambrosia trifida* L.) biotypes: The University of Western Ontario London. 99 p

Thordal-Christensen H, Zhang Z, Wei Y, Collinge DB (1997) Subcellular localization of H2O2 in plants. H2O2 accumulation in papillae and hypersensitive response during the barley—powdery mildew interaction. The Plant Journal 11:1187-1194

Troyer JR (2001) In the beginning: the multiple discovery of the first hormone herbicides. Weed Science 49:290-297

Tsukada M, Ohsumi Y (1993) Isolation and characterization of autophagy-defective mutants of *Saccharomyces cerevisiae*. FEBS Letters 333:169-174

USDA (2016) Crop Values 2015 Summary: United States Department of Agriculture.

van Doorn WG, Woltering EJ (2005) Many ways to exit? Cell death categories in plants. Trends in Plant Science 10:117-122

Van Horn CR, Westra P Updates on molecular response of glyphosate resistant giant ragweed (*Ambrosia tifida*). Pages 99. Colorado Springs, CO

Van Horn CR, Westra P Molecular basis of glyphosate resistance and the rapid necrosis response in giant ragweed. Pages 91. Portland, Oregon

Vandesompele J, De Preter K, Pattyn F, Poppe B, Van Roy N, De Paepe A, Speleman F (2002) Accurate normalization of real-time quantitative RT-PCR data by geometric averaging of multiple internal control genes. Genome Biology 3:1

VanGessel MJ (2001) Glyphosate-resistant horseweed from Delaware. Weed Science 49:703-705

Vanhee C, Guillon S, Masquelier D, Degand H, Deleu M, Morsomme P, Batoko H (2010) A TSPO-related protein localizes to the early secretory pathway in *Arabidopsis*, but is targeted to mitochondria when expressed in yeast. J Exp Bot:erq283

Vila-Aiub MM, Neve P, Powles SB (2009) Fitness costs associated with evolved herbicide resistance alleles in plants. New Phytologist 184:751-767

Vink JP, Soltani N, Robinson DE, Tardif FJ, Lawton MB, Sikkema PH (2012a) Glyphosate-resistant giant ragweed (*Ambrosia trifida* L.) in Ontario: Dose response and control with postemergence herbicides. American Journal of Plant Sciences 3:608-617

Vink JP, Soltani N, Robinson DE, Tardif FJ, Lawton MB, Sikkema PH (2012b) Occurrence and distribution of glyphosate-resistant giant ragweed (*Ambrosia trifida* L.) in southwestern Ontario. Canadian Journal of Plant Science 92:533-539

Vollenberg A, Rayburn L, Zheng D, Tranel P Natural hybridization between giant and common ragweed. Pages 144

Wakelin A, Preston C (2006) A target-site mutation is present in a glyphosate-resistant *Lolium rigidum* population. Weed Research 46:432-440

Wakelin AM, Lorraine-Colwill D, Preston C (2004) Glyphosate resistance in four different populations of *Lolium rigidum* is associated with reduced translocation of glyphosate to meristematic zones. Weed Research 44:453-459

Wang P, Liang W, Kong C, Jiang Y (2005) Allelopathic potential of volatile allelochemicals of *Ambrosia trifida* L. on other plants. Allelopathy Journal 15:131-136

Washitani I, Nishiyama S (1992) Effects of seed size and seedling emergence time on the fitness components of *Ambrosia trifida* and *A. artemisiaefolia* var. elatior in competition with grass perennials. Plant Species Biology 7:11-19

Weaver LM, Herrmann KM (1997) Dynamics of the shikimate pathway in plants. Trends in Plant Science 2:346-351

Webster TM, Loux MM, Regnier EE, Harrison SK (1994) Giant ragweed (*Ambrosia trifida*) canopy architecture and interference studies in soybean (*Glycine max*). Weed Technology:559-564

Webster TM, Sosnoskie LM (2010) Loss of glyphosate efficacy: a changing weed spectrum in Georgia cotton. Weed Science 58:73-79

Westhoven AM, Kruger GR, Gerber CK, Stachler JM, Loux MM, Johnson WG (2008) Characterization of selected common lambsquarters (*Chenopodium album*) biotypes with tolerance to glyphosate. Weed Science 56:685-691

Wiersma AT, Gaines TA, Preston C, Hamilton JP, Giacomini D, Buell CR, Leach JE, Westra P (2014) Gene amplification of 5-enol-pyruvylshikimate-3-phosphate synthase in glyphosate-resistant *Kochia scoparia*. Planta:1-12

Wilcut J, York A, Jordan D (1993) Weed management for reduced-tillage southeastern cotton. 29-35 p

Williams GM, Kroes R, Munro IC (2000) Safety evaluation and risk assessment of the herbicide Roundup and its active ingredient, glyphosate, for humans. Regulatory Toxicology and Pharmacology 31:117-165

Wilson RG, Miller SD, Westra P, Kniss AR, Stahlman PW, Wicks GW, Kachman SD (2007) Glyphosate-induced weed shifts in glyphosate-resistant corn or a rotation of glyphosate-resistant corn, sugarbeet, and spring wheat. Weed Technology 21:900-909

Wyrill III J, Burnside O (1976) Absorption, translocation, and metabolism of 2, 4-D and glyphosate in common milkweed and hemp dogbane. Weed Science:557-566

Xie Z, Chen Z (2000) Harpin-induced hypersensitive cell death is associated with altered mitochondrial functions in tobacco cells. Molecular Plant-Microbe Interactions 13:183-190

Xiong Y, Contento AL, Bassham DC (2007a) Disruption of autophagy results in constitutive oxidative stress in *Arabidopsis*. Autophagy 3:257-258

Xiong Y, Contento AL, Nguyen PQ, Bassham DC (2007b) Degradation of oxidized proteins by autophagy during oxidative stress in *Arabidopsis*. Plant Physiol 143:291-299

Yoshimoto K, Jikumaru Y, Kamiya Y, Kusano M, Consonni C, Panstruga R, Ohsumi Y, Shirasu K (2009) Autophagy negatively regulates cell death by controlling NPR1-dependent salicylic acid signaling during senescence and the innate immune response in *Arabidopsis*. Plant Cell 21:2914-2927

Yu Q, Cairns A, Powles S (2007) Glyphosate, paraquat and ACCase multiple herbicide resistance evolved in a *Lolium rigidum* biotype. Planta 225:499-513

Yu Q, Jalaludin A, Han H, Chen M, Sammons RD, Powles SB (2015) Evolution of a double amino acid substitution in the EPSP synthase in *Eleusine indica* conferring high level glyphosate resistance. Plant Physiol:pp. 00146.2015

Yuan JS, Tranel PJ, Stewart Jr CN (2007) Non-target-site herbicide resistance: a family business. Trends in Plant Science 12:6-13

Yun D-J, Ibeas JI, Lee H, Coca MA, Narasimhan ML, Uesono Y, Hasegawa PM, Pardo JM, Bressan RA (1998) Osmotin, a plant antifungal protein, subverts signal transduction to enhance fungal cell susceptibility. Molecular Cell 1:807-817

Zhou M, Xu H, Wei X, Ye Z, Wei L, Gong W, Wang Y, Zhu Z (2006) Identification of a glyphosate-resistant mutant of rice 5-enolpyruvylshikimate 3-phosphate synthase using a directed evolution strategy. Plant Physiol 140:184-195

Ziska L, Knowlton K, Rogers C, Dalan D, Tierney N, Elder MA, Filley W, Shropshire J, Ford LB, Hedberg C (2011) Recent warming by latitude associated with increased length of ragweed pollen season in central North America. Proceedings of the National Academy of Sciences 108:4248-4251

Zurbriggen MD, Carrillo N, Hajirezaei M-R (2010) ROS signaling in the hypersensitive response: When, where and what for? Plant Signaling & Behavior 5:393-396

APPENDICES

Appendix 1. Dissection of a giant ragweed seed. Left to right: embryo, seed coat, pericarp, involucre.

Appendix 2. Seedlings germinating in Magenta® boxes after 4 to 8 weeks of cold stratification.

Appendix 3. Plants isolated with micro-perforated bags for self-pollination.

Appendix 4. Collected seeds stored in glass vials.

Appendix 5. Example of a cut shoot from a GR rapid response plant placed in 13.2 mM glyphosate immediately after (A) and 24 hours after (B) shoot glyphosate treatment.

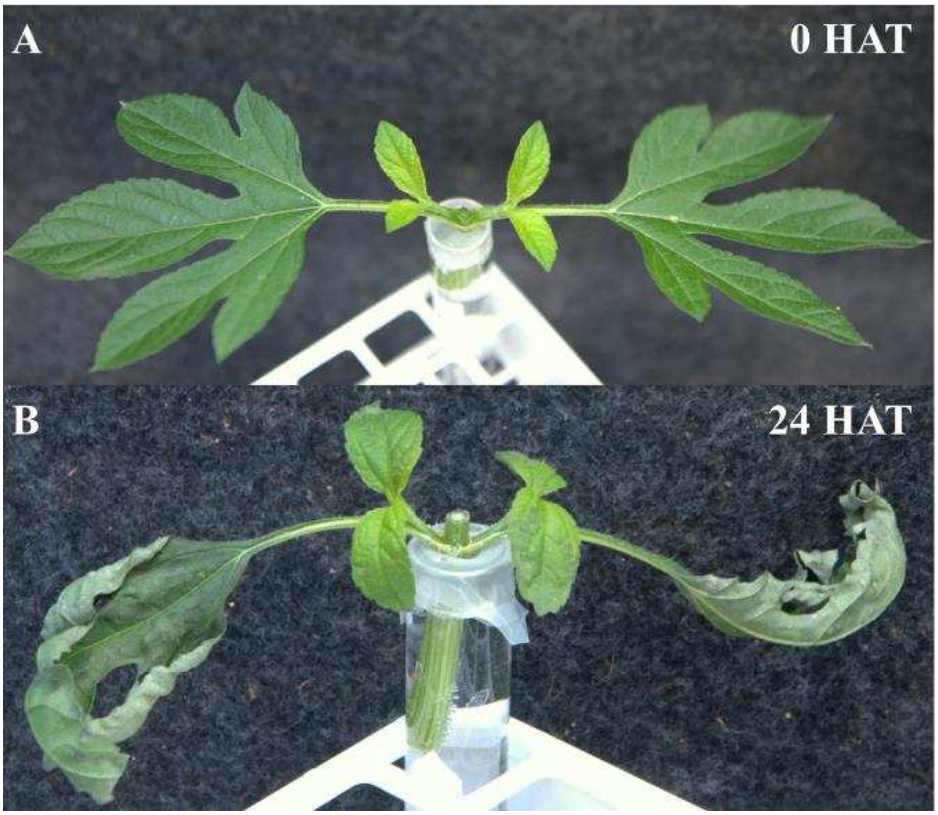

Appendix 6. Percent tissue necrosis at 24 HAT. GR rapid and GS individuals were subjected to light or dark environments after glyphosate application at 0.84 kg·ae·ha^{-1}. Vertical bars represent standard error of the mean. Significance code of '****' represents a P value of ≤ 0.0001. Significance represents comparison to untreated controls of each treatment group (not shown). Data were pooled from repeat experiments (n = 9).

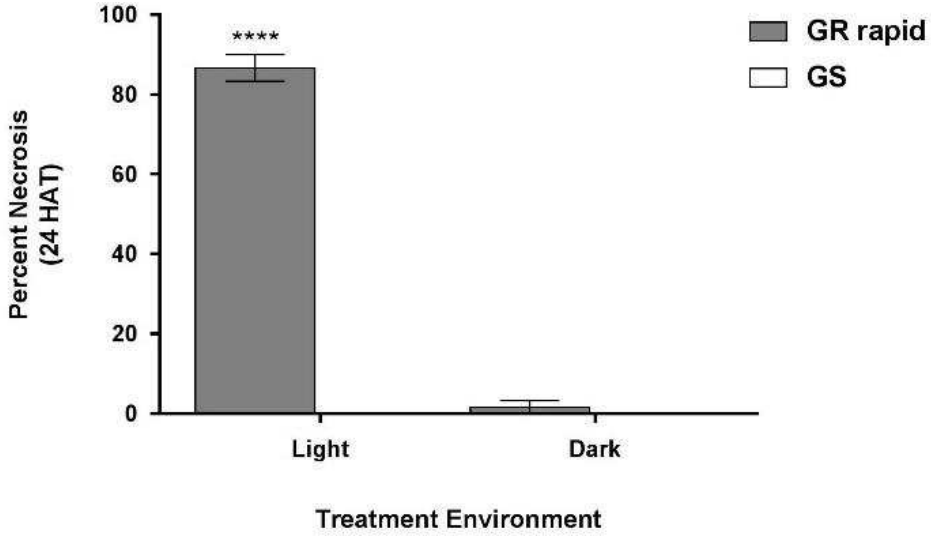

Appendix 7. Fold change values of twenty-seven differentially expressed contigs with filters including ≥500 bp contig length, ±10 fold change, $P \leq 0.05$ FDR adjusted p-value and ≥3 FPKM at every treatment time point. Lists separated by the three pairwise comparisons of GR young tissue vs GS young tissue, GR mature tissue vs GS mature tissue and GR young tissue vs GR mature tissue. Fold change represented by R/S.

Contig	Pfam Annotation	FPKM Fold Change at minutes after treatment			
		Unt	15	60	180
GR young tissue / GS young tissue					
38721	N/A	-17.7	-15.2	-15.5	-20.4
61120	Ubiquitin extension protein 1	-30.3	-34.6	-39.6	-45.1
64504	Histone superfamily protein	37.3	28.1	25.8	33.0
GR old tissue / GS old tissue					
37519	Heavy metal transport/detoxification protein	10.1	11.0	15.0	16.6
37679	Cytochrome B6f complex subunit (petM)	-14.4	-16.5	-10.2	-12.5
44151	S-adenosyl-L-methionine methyltransferase	13.9	12.6	14.9	13.6
44611	S-adenosylmethionine synthetase	29.4	48.1	41	20.1
57846	Ribosomal protein L12	14.4	15.9	17	15
GR young tissue / GR old tissue					
9679	Lipid-transfer protein	30.2	11.6	10.1	14.7
10806	Lipid-transfer protein	270.0	154.7	88.4	95.1
14186	Jojoba acyl CoA reductase	23.4	25.1	17.3	12.1
18068	Germin 3	169.2	44.2	26.9	23.9
19357	Alpha-xylosidase 1	22.2	15.4	29.5	26.4
22365	Histone superfamily protein	10.3	17.9	42.3	20.1
27037	Winged-helix DNA-binding transcription factor	26.9	78.9	96.8	54.9
35759	Alpha-xylosidase 1	12.0	10.1	22.9	21.8
36804	Histone superfamily protein	12.6	12.5	17.4	15.1
39197	Glycosyl hydrolase 9C2	32.9	23.7	19.7	16.0
44834	Ribonuclease 2	64.4	36.3	84.3	101.7
45640	Lipid-transfer protein	-52.4	-14.9	-26.1	-40.7
45759	Histone H2A 12	34.8	28.5	43.8	43.8
46668	Histone superfamily protein	39.9	27.9	38.3	37.7
51028	Pollen Ole e 1 allergen and extension protein	30.0	15.8	12.0	10.5
58880	Glycosyl hydrolase 9C2	23.8	17.1	15.6	12.6
58889	Cellulose synthase-like A02	19.7	16.5	11.4	13.6
62164	Histone superfamily protein	80.2	54.5	86.5	50.3
64387	Histone superfamily protein	33.6	53.7	57.8	22.9

Appendix 8. Fold change values of five differentially expressed contigs with filters including ≥500 bp contig length, ±10 fold change, $P \leq 0.05$ FDR adjusted p-value and ≥3 FPKM at every treatment time point comparing GR untreated mature tissue to GR treated mature tissue. Fold change represented by R/S.

Contig	Pfam annotation	FPKM Fold Change at minutes after treatment		
		15	60	180
31846	NAC domain transcriptional regulator protein	15.8	41.1	17.4
50824	Protein of unknown function (DUF1645)	12.5	23.7	18.9
51054	NAC domain transcriptional regulator protein	14.6	40	16.4
52780	A20/ AN1-like zinc finger family protein	14.1	16.1	51.7
58803	NAC domain transcriptional regulator protein	10.9	29.6	12.4

Appendix 9. Relative expression values (REV) from qRT-PCR analysis of OSM34 and SAMS3 in the forward genetics validation using a segregating F_2 population. UNT is glyphosate-untreated and 15, 60 and 180 represent time points in minutes after glyphosate treatment. Young and Mature represent sampled tissue type.

	F_2 Individual	OSM34								SAMS3							
		Young				Mature				Young				Mature			
		UNT	15	60	180	UNT	15	60	180	UNT	15	60	180	UNT	15	60	180
Normalized to GAPDH	R1	0.6	0.1	0.1	0.5	0.8	1.2	0.6	0.2	0.9	1.5	0.8	5.7	0.7	10.8	0.0	0.2
	R2	0.2	0.2	0.3	0.0	0.1	0.2	0.4	0.3	1.5	2.0	0.8	0.5	3.9	15.1	10.7	2.3
	R3	0.4	0.1	0.9	0.1	0.2	0.1	0.2	0.6	0.2	0.2	0.8	0.1	0.1	0.1	0.1	0.7
	R4	0.3	0.1	0.0	0.1	0.0	0.0	0.0	0.0	0.7	0.7	0.7	1.1	0.2	3.0	12.5	3.0
	S1	2.3	0.5	0.5	0.1	0.2	2.3	0.2	0.2	3.1	4.9	2.3	0.9	3.3	35.1	0.0	12.9
	S2	3.8	0.3	0.1	1.2	0.1	0.3	0.0	0.1	5.8	2.9	2.2	5.2	1.9	18.5	0.0	20.2
	S3	0.1	0.8	0.3	0.1	1.0	2.2	1.1	0.5	1.0	8.2	4.6	1.8	3.0	10.8	N/A	6.5
	S4	1.0	2.4	0.0	0.5	0.2	0.5	0.1	0.0	1.0	1.6	0.0	9.5	0.4	1.3	2.8	0.0
Normalized to EF1A	R1	37.0	6.6	5.6	13.9	93.6	63.7	21.4	16.9	53.7	119.4	65.2	158.9	78.4	566.0	0.6	22.7
	R2	7.3	3.1	8.1	0.4	5.7	9.5	23.6	10.1	53.0	29.2	22.2	14.9	154.3	660.1	665.0	71.8
	R3	6.6	5.1	12.7	4.2	23.2	7.2	6.2	25.2	4.3	8.2	10.8	4.4	10.3	5.1	4.0	29.4
	R4	18.2	2.2	5.6	17.5	31.9	5.2	0.7	8.2	50.5	21.8	372.9	138.7	256.6	1094.2	203.0	1051.0
	S1	3.5	10.5	26.7	12.3	6.8	48.0	6.7	31.3	4.7	103.1	112.2	123.8	96.5	747.7	0.2	2178.1
	S2	4.8	3.0	3.1	6.9	4.3	7.9	3.5	6.9	7.2	30.1	52.0	29.9	130.8	512.7	3.5	1466.6
	S3	3.3	9.3	13.5	1.8	24.3	30.0	18.3	20.1	22.7	91.0	185.9	26.9	73.6	147.1	N/A	263.3
	S4	1.0	0.9	0.6	6.5	3.5	2.6	2.0	0.4	1.0	0.6	1.2	115.5	6.1	6.4	51.6	0.6